BBA - Bioenergetics 1860 (2019) 233–258

Contents lists available at ScienceDirect

BBA - Bioenergetics

journal homepage: www.elsevier.com/locate/bbabio

Molecular mechanism of metabolic NAD(P)H-dependent electron-transfer systems: The role of redox cofactors

Takashi Iyanagi

Department of Life Science, Graduate School of Life Science, University of Hyogo, Koto 3-2-1, Kamighori, Ako, Hyogo 678-1297, Japan

ARTICLE INFO

Keywords:
NAD(P)H-dependent electron-transfer systems
Flavoenzymes
Redox potentials
Catalytic cycle
Cytochrome P450 reductase
Nitric oxide synthase

ABSTRACT

NAD(P)H-dependent electron-transfer (ET) systems require three functional components: a flavin-containing NAD(P)H-dehydrogenase, one-electron carrier and metal-containing redox center. In principle, these ET systems consist of one-, two- and three-components, and the electron flux from pyridine nucleotide cofactors, NADPH or NADH to final electron acceptor follows a linear pathway: NAD(P)H → flavin → one-electron carrier → metal containing redox center. In each step ET is primarily controlled by one- and two-electron midpoint reduction potentials of protein-bound redox cofactors in which the redox-linked conformational changes during the catalytic cycle are required for the domain-domain interactions. These interactions play an effective ET reactions in the multi-component ET systems. The microsomal and mitochondrial cytochrome P450 (cyt P450) ET systems, nitric oxide synthase (NOS) isozymes, cytochrome b_5 (cyt b_5) ET systems and methionine synthase (MS) ET system include a combination of multi-domain, and their organizations display similarities as well as differences in their components. However, these ET systems are sharing of a similar mechanism. More recent structural information obtained by X-ray and cryo-electron microscopy (cryo-EM) analysis provides more detail for the mechanisms associated with multi-domain ET systems. Therefore, this review summarizes the roles of redox cofactors in the metabolic ET systems on the basis of one-electron redox potentials. In final Section, evolutionary aspects of NAD(P)H-dependent multi-domain ET systems will be discussed.

1. Introduction

Biological electron-transfer (ET) systems can be functionary divided into two types. A metabolic ET system catalyses a complex network of biotransformations of organic compounds, while an energetic ET system is linked to the energy conservation. In their first step, metabolic NAD(P)H-dependent ET systems require a flavin as a redox-active cofactor: the protein-bound oxidized flavin (Fl_{ox}) accepts the two electrons and one proton as a hydride ion ($H^- \rightleftharpoons H^+ + 2e^-$) from NAD(P)H, and then the reduced flavin transfers electrons to a one-electron protein carrier, one at a time (Scheme 1). In 1930s, Michaelis. [1,2] proposed that the oxidation-reduction reactions of the flavin that requires the transfer of two electrons take place in two reversible steps, in which the one-electron reduced semiquinone is the intermediate form. The semiquinone form of flavin participates as a reversible converter between two electron donors, NAD(P)H and a one-electron protein carrier [3–6]. The final electron acceptor includes a metal-containing redox center and accepts electrons from the one-electron protein carrier by sequential one-electron transfer. In principle, the metabolic ET systems include three steps: (i), (ii), and (iii) (Scheme 1). These steps are regulated by several factors, including hydride ion transfer, one-electron reduction potentials of protein-bound flavin and one-electron protein carrier, proton-coupled ET, dynamic conformational changes and distance between the redox centers of each components.

The NAD(P)H-dependent metabolic ET systems are typically classified as one-, two- and three-components, in which ET reactions involve specific interactions between these components (Figs. 1 and 2). The mitochondrial cyt P450 ET system contains three-components, which include the flavin-containing NADPH-dehydrogenase, [2Fe-2S] cluster containing non-heme iron protein as a one-electron carrier and heme-containing cyt P450s [7,8]. In contrast, the microsomal cyt P450 ET system has two components, and includes diflavin cyt P450

Abbreviations: ET, electron-transfer; Fl, oxidized flavin; FlH^-, anionic fully reduced flavin; FlH_2, neutral fully reduced flavin; $Fl^{\bullet -}$, anionic flavin semiquinone; $FlH^{\bullet}$, neutral flavin semiquinone; H^-T, hydride ion transfer; Fdx, ferredoxin; Adx, adrenodoxin; Fldx, flavodoxin; $E_{ox/sq}$, oxidized (ox)-semiquinone (sq) couple one-electron reduction potential; $E_{sq/red}$, semiquinone (sq)-fully reduced (red) couple one-electron reduction potential; FNR, ferredoxin-$NADP^+$oxidoreductase, NADPH-cytochrome P450 reductase, cyt P450 reductase; CYP, cytochrome P450; cyt b_5 reductase, NADH-cytochrome b_5 reductase; MS reductase, methione synthase reductase; NOS, nitric oxide synthase; nNOS, neuronal NOS; eNOS, endothelial NOS; iNOS, inducible NOS; P450BM3, bacteria cytochrome P450BM3; cryo-EM, cryo electron microscopy; CaM, calmodulin; HGT, horizontal gene transfer; ER, endoplasmic reticulum; EPR, electron paramagnetic resonance

https://doi.org/10.1016/j.bbabio.2018.11.014
Received 16 April 2018; Received in revised form 30 October 2018; Accepted 7 November 2018
Available online 09 November 2018

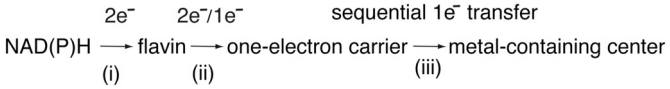

Scheme 1. ET processes from NAD(P)H to metal-containing center.

reductase (FAD and FMN-containing) and cyt P450s [9,10], the former is a fusion enzyme that has evolved from the genes encoding a FAD-binding ferredoxin-$NADP^+$ reductase (FNR) and an FMN-containing flavodoxin (Fldx) [11–13]. The equilibrium one-electron reduction potentials of two flavin redox cofactors have been measured from potentiometric titration curves [5,14]. Meanwhile, the nitric oxide synthase (NOS) isozymes are a single-component system, which includes a cyt P450 reductase-like and heme-containing oxygenase domains [15–17]. In addition, the active form is a dimer of identical subunits. The cyt P450 ET system is not strictly regulated, but the reductase domain of NOS isozymes is regulated by calmodulin (CaM) [18–20]. The similarities and differences between microsomal cyt P450 ET system and NOS isozymes have been reviewed extensively [21–27]. At present, the mechanism of differential regulation between cyt P450 ET system and NOS isozymes has been focused on the role of the FMN domain [28–34]. The structural analysis by X-ray [12,17,20], and cryo-electron microscopy (cryo-EM) [35–38] provide more detailed informations for the multi-components and multi-domain ET systems. In this review, the roles of the flavin cofactors in the catalytic cycle of NAD(P)H-dependent ET systems, including the microsomal and mitochondrial cyt P450 ET systems, NOS isozymes, cytochrome b_5 (cyt b_5) ET systems and methionine synthase reductase (MS reductase) are mainly summarized, and similarities and differences will be discussed based on the redox potentials, and redox-linked conformational changes. In the final Section, evolutionary aspects of the each component in the metabolic NAD(P)H-dependent ET systems will be discussed.

2. NAD(P)H-dependent electron transfer systems

NAD(P)H-dependent ET systems play an important physiological role in the transfer of electrons from NAD(P)H to many single electron accepting-metal proteins or other cofactors (Scheme 1). As shown in Figs. 1 and 2, eukaryotic cyt P450-containing ET systems are mainly divided into mitochondrial and microsomal types. The former ET system is composed of three-components, including a FAD-containing adrenodoxin reductase (Adx reductase), a [2Fe-2S] cluster-containing adrenodoxin (Adx) and heme-containing cyt P450, in which the FAD-[2Fe-2S] pair donates electrons to cyt P450s [7,39,40]. In contrast, the microsomal cyt P450 ET system is composed of two-components, in which the FAD-FMN pair of cyt P450 reductase donates electrons to cyt P450s [4,9,10]. In both cyt P450 ET systems, the FAD accepts two electrons and one proton as a hydride ion from NADPH, and Adx (for the mitochondrial system) or FMN domain (for the microsomal system) acts as a one-electron carrier proteins (Figs. 1 and 2), in which the FAD act as a converter from 2 electron, NAD(P)H to a one electron carrier. More recently, a novel soluble NADPH-dependent diflavin reductase member was isolated from *Bacillus megaterium* [41]. The sequence analysis showed that this reductase contains the FAD and FMN binding motifs as well as NADPH and cyt P450 interaction domains. Additionally, an air-stable semiquinone, FAD-$FMNH^{\bullet}$ state that is characteristic in the cyt P450 reductase is observed [9]. This soluble *Bacillus megaterium* cyt P450 reductase (BM cyt P450 reductase) can donate electrons to a bacterial CYP106A1 and a microsomal CYP21A2. Thus, this report strongly indicates that this reductase is a member of the diflavin family, which corresponds to the truncated cyt P450 reductase lacking the N-terminal membrane-binding anchor. The microsomal desaturase system is composed of three-components, including NADH-cytochrome b_5 reductase (cyt b_5 reductase), cytochrome b_5 (cyt b_5) and desaturase [42,43], while a novel flavoheme protein (Ncb5or) is composed of two-components (Fig. 1) [44], resulting from the fusion enzyme of cyt b_5 reductase and cyt b_5. However, eukaryotic nitric oxide synthase (NOS) isozymes [45,46] are composed of a single component, which shares the cyt P450 reductase-like domain as an electron-donating reductase, and a dimer is the active form (Fig. 1). The prokaryotic flavocytochrome P450BM3 (P450BM3) from *Bacillus megaterium* contains a cyt P450 reductase-like domain, and is a single polypeptide system in which a dimer form is also the active form [47,48]. Therefore, in the metabolic ET systems, a flavin-one-electron carrier pair links from a two-electron donor (NAD(P)H) to a final one-electron acceptor (Figs. 1, 2).

3. Mechanism of electron transfer

NAD(P)H-dependent ET pathways require three functions (Scheme 1): (i) a dehydrogenase to accept a two electrons from NAD(P)H, (ii) one-electron carrier, and (iii) final metal-containing electron acceptor, which contains a heme or non-heme iron prothetic cofactor. In the first step (i), the direct transfer of a hydride ion from NAD(P)H to flavin molecule is generally accepted. This reaction proceeds through the intermediates ($NAD(P)^+$–H^-–Fl_{ox}) (Eq. 1) [49], and the reduced flavin is stabilized by the binding of $NAD(P)^+$. Thus, a redox potential of $NAD(P)^+$-bound reduced flavin, $NAD(P)^+$-FlH^- is more positive, compared with $NAD(P)^+$-free form, and provides a driving force for hydride ion transfer from NAD(P)H to flavin (Eq. (1)) [3].

$$\mathrm{NAD(P)H} + \mathrm{Fl_{ox}} \rightleftharpoons \mathrm{NAD(P)H - Fl_{ox}} \rightleftharpoons [\mathrm{NAD(P)^{+}{-}{-}H^{-}{-}{-}Fl_{ox}}] \rightleftharpoons \mathrm{NAD(P)^{+} - FlH^{-}} \quad (1)$$

In the step (ii), reduced flavin donates electrons to the non-heme iron, cytochrome and flavin cofactors that function as a one-electron carrier, in where the flavin cofactors play a pivotal role in the step-down reaction from a two-electron donor to a one-electron acceptor. In the final step (iii), a one-electron carrier donates electrons to an electron-acceptor by way of sequential one-electron transfer (Scheme 1). For example, the heme containing cyt P450 accepts two electrons during two sequential one-electron transfer steps in which the molecular oxygen is activated in a stepwise reaction [4]. The one- and two-electron transfer reactions within and between proteins are modulated by several factors; one- and two-electron midpoint potential differences between donor and acceptor, the proton-coupled ET, the stability of the flavin semiquinone radical and/or its reactivity, and a small-scale motion within the active site or a large-scale motion of cofactor-binding domains, which cause an alteration of distance and orientation between redox cofactors. In addition, the interactions between these components are required for rapid and specific ET in multiprotein and multidomain redox enzyme systems. Thus, the exquisite control of association and dissociation between the domains or proteins is a key factor for rapid and controlled ET (see Fig. 2 and Ref. [50]).

3.1. One- and two-electron reduction potentials

$NAD(P)^+$/NADPH couple acts as a two-electron/hydride donor or acceptor in the biological systems (Fig. 1). Flavin cofactors play a key role in ET systems because of their ability to participate in either one-electron or two-electron oxidation-reductions. Thus, the one- and two-electron midpoint reduction potentials regulate each steps in the ET from NAD(P)H to a final one-electron acceptor. To understand the redox properties of enzyme-bound redox centers, indirect mediated potentiometry and direct kinetic methods have used.

The flavin (Fl) cofactors possess an isoalloxazine ring, and they can exist in three redox states: fully oxidized Fl (Fl_{ox}) and one-electron reduced semiquinone (Fl_{sq}), in either the anionic ($Fl^{\bullet -}$) or neutral ($FlH^{\bullet}$) form ($Fl^{\bullet -} + H^+ \rightleftharpoons FlH^{\bullet}$), and two-electron fully reduced forms (Fl_{red}) ($FlH^- + H^+ \rightleftharpoons FH_2$) [51,52]. The oxidized Fl is reduced or oxidized by two one-electron way (Fig. 3). Thus, the two-electron midpoint reduction potential, E_m is divided into one-electron midpoint potentials, $E_{ox/}$

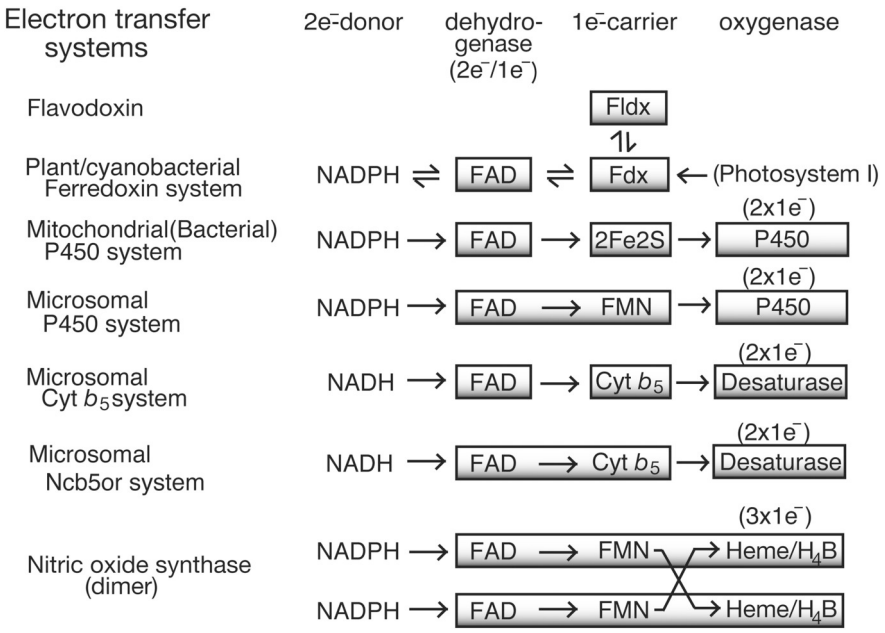

Fig. 1. Typical NAD(P)H-dependent metabolic ET systems.

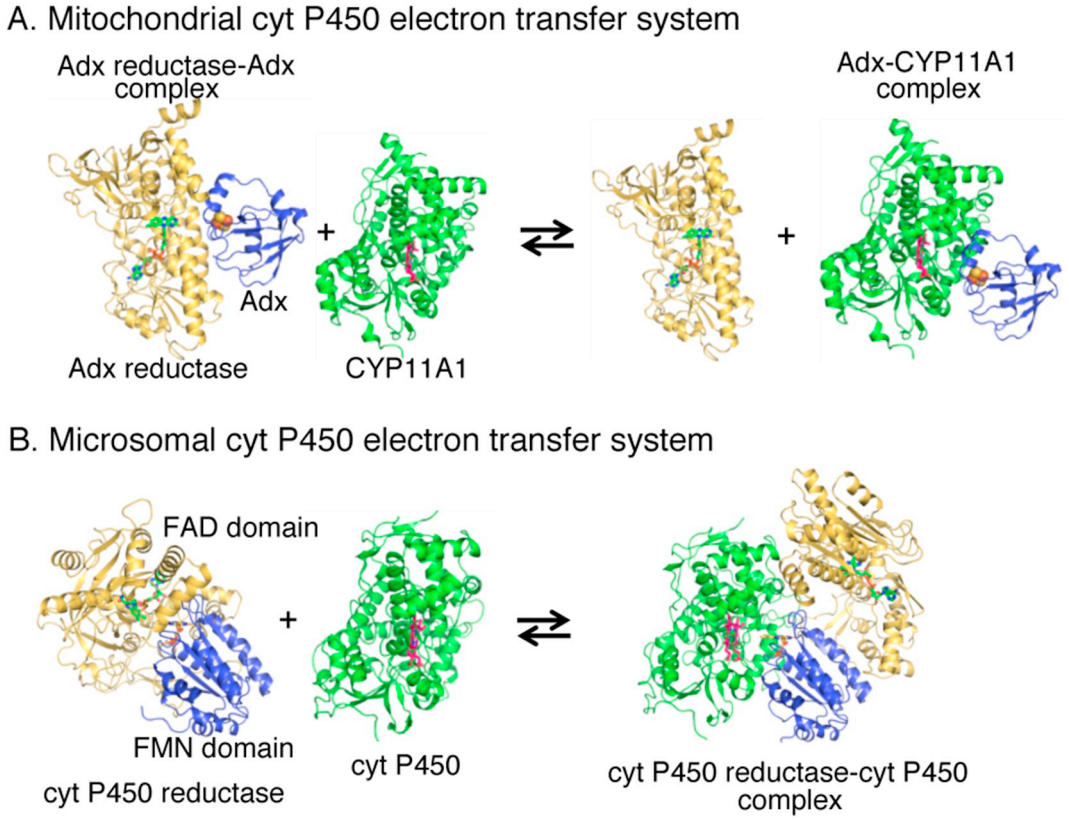

Fig. 2. Docked model of a complex between cyt P450 and electron transfer partners. Figure was adapted from Refs. [4,205] with some modifications.

$_{sq}$ and $E_{sq/red}$, respectively. For two-step oxidation-reduction reactions (red⇌sq ⇌ ox) of organic molecules, such as flavins and quinones, Michaelis proposed the following equations (Eqs. (2) and (3)) [1].

$$E = E_{sq/red} + (RT/F) \ln [sq]/[red] \quad (2)$$

$$E = E_{ox/sq} + (RT/F) \ln [ox]/[sq] \quad (3)$$

where R is the gas constant, T is the absolute temperature, F is the Faraday constant, and [red], [sq] and [ox] are the concentrations of the reduced, semiquinone and oxidized species at each point in the titration.

The E_m value for the overall two-electron transfer reaction lies halfway between $E_{ox/sq}$ and $E_{sq/red}$.

$$E_m = (E_{ox/sq} + E_{sq/red})/2 \quad (4)$$

A semiquinone formation or stabilization constant Ks (ox + red ⇌ 2sq) is:

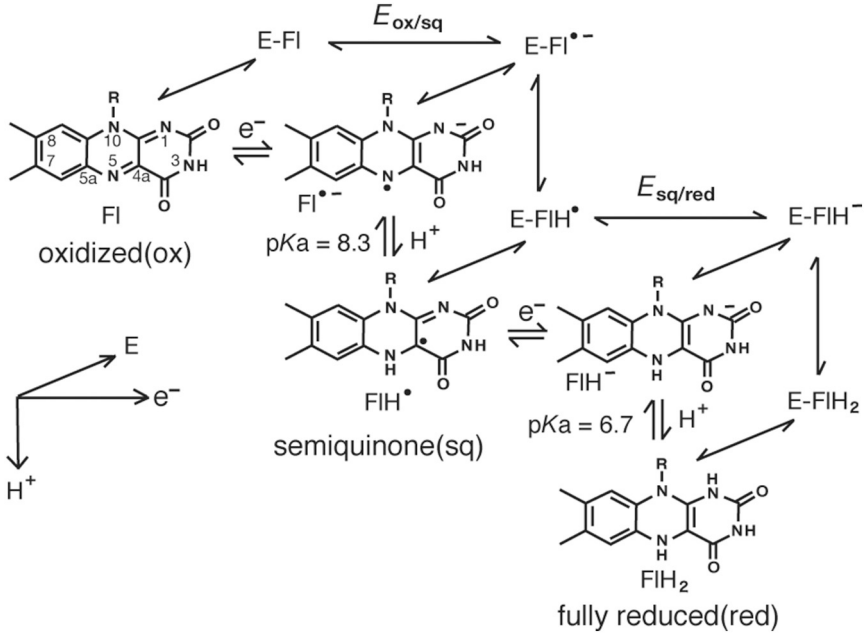

Fig. 3. Redox and ionic states of flavin cofactor. *E*-Fl indicates enzyme bound flavin. $E_{ox/sq}$ (oxidized-semiquinone couple) and $E_{sq/red}$ (semiquinone-fully reduced couple) indicate one-electron reduction potentials, respectively.

$$K_s = (sq)^2/(ox)(red) \quad (5)$$

Thus, the difference in the $E_{ox/sq}$ (ox/sq. couple) and $E_{sq/red}$ (sq/red couple) is related to the semiquinone formation constant K_s.

$$E_{ox/sq} - E_{sq/red} = (RT/F) \ln K_s \quad (6)$$

where, when K_s is larger than unity ($K_s > 1$), the value of $E_{sq/red}$ (sq/red) is more negative than that of $E_{ox/sq}$ (ox/sq), in which semiquinone state is stabilized. Thereby, the reduced state is a stronger reactant than semiquinone state (sq/red). When K_s is less than unity and greater than zero ($1 > K_s > 0$), the value of $E_{sq/red}$ (sq/red) is more positive than that of $E_{ox/sq}$ (ox/sq), and the semiquinone is a stronger reactant than its reduced form (red). When $K_s = 1$, the values of $E_{ox/sq}$ and $E_{sq/red}$ coincide. The values of $E_{ox/sq}$ and $E_{sq/red}$ cross at this point. When $K_s = 0$, no semiquinone is formed, and the oxidation-reduction process is ox $+ 2e^- \rightleftharpoons$red.

The NAD(P)H-dependent flavin enzymes can catalyse a one-electron reduction of electron acceptor, A, where the reduced flavin is oxidized by A in a sequential one-electron reaction.

$$NAD(P)H + 2A \rightarrow NAD(P)^+ + 2A^{\cdot -} + H^+ \quad (7)$$

The net free energy change for Eq. (7) is given below:

$$\Delta G^\circ = -nF\Delta E \quad (8)$$

Hence, the ET reaction is more efficient, as the Gibbs free energy of activation, ΔG^o becomes more negative in which ΔE is the redox potential difference between the donor and acceptor, and n is the number of electrons involved in the reaction.

Flavin cofactors function as a donor/or acceptor in the biological ET systems. The one-electron reduction potentials, $E_{ox/sq}$ (−313 mV) for oxidized (ox)-semiquinone (sq) couple, Fl/FlH$^\bullet$ of free flavins (FAD and FMN) is more negative than that of $E_{sq/red}$ (−101 mV) for semiquinone (sq)-fully reduced (red) couple, FlH$^\bullet$/FlH$^-$(FH_2) at pH 7.0 [52]. Thus, the E_m value is −207 mV. The one-electron midpoint reduction potentials for the $E_{ox/sq}$ and $E_{sq/red}$ of enzyme-bound flavin are altered by the local pH, polarity of the environment, and interactions with protein amino acid residues and ligand such as a NAD(P)$^+$ [53].

As an enzymatic example for Michaelis theory, the FAD-containing NADH-cytochrome b_5 reductase (cyt b_5 reductase) is considered (Fig. 4) [3]. The two-electron reduction potential, $E_{m,7}$, is −258 mV for FAD/FADH$^-$ couple (Fig. 4A, curve a), but NAD$^+$-bound two-electron reduction potential for FAD/NAD$^+$-FADH$^-$ couple is −194 mV (Fig. 4A, curve b), indicating that the anionic reduced FAD form is stabilized by binding of NAD$^+$. However, the two-electron reduction potential in the presence of NAD$^+$ deviates from the typical two-electron titration curves (Fig. 4A, curve c). This is because of the formation of the anionic semiquinone species, indicating the stabilization of anionic semiquinone in the presence of NAD$^+$. The one-electron reduction potentials for $E_{ox/sq}$ and for $E_{sq/red}$ are – 88 mV and −147 mV at pH 7 (see curve c of Fig. 4A and Ref. [3]), respectively. This separation corresponds to a semiquinone formation constant of 8 at pH 7. These values deviate from the typical one-electron reduction potential in the pH 6–9 range (see Fig. 4B, curve c). This is due to the pH dependency of semiquinone formation constant in the following reaction: NAD$^+$-FADH$^-$ + NAD$^+$-FAD ⇌2NAD$^+$-FAD$^{\bullet -}$ + H$^+$, in which NAD$^+$ binding to the oxidized FAD promotes the formation of the anionic semiquinone form. In fact, such a semiquinone intermediate is observed when oxidized enzyme (FAD) was mixed with equimolar NADH plus cyt b_5 (Fe^{3+}) in the stopped-flow apparatus: NADH + FAD + cyt b_5 (Fe^{3+}) → NAD$^+$-FAD$^{\bullet -}$ + cyt b_5 (Fe^{2+}) + H$^+$, in which the neutral semiquinone intermediate, FADH$^\bullet$ that is formed in the ET reaction from NAD$^+$-FADH$^-$ to cyt b_5 (Fe^{3+}) is rapidly converts to anionic semiquinone FAD$^{\bullet -}$ (see Section 7 and Fig. 12) [3,54,55]. It should be noted that the EPR signal shape and power saturation curve of anionic semiquinone, FAD$^{\bullet -}$ are significantly different (Fig. 4C) from those of the neutral semiquinones, FADH$^\bullet$ and FMNH$^\bullet$ of cyt P450 reductase [9,56].

It is interesting to note the physiological relevance of the shift of the redox potential induced by NAD$^+$ binding. A large redox potential gap between NAD$^+$/NADH (−320 mV) and cyt b_5 (Fe^{3+})/cyt b_5 (Fe^{2+}) (~0 mV) is divided into smaller steps by several redox states of the enzyme bound-flavin, and the high activation energy would be decreased by each oxidation-reduction reaction of the enzyme-bound flavin and each electron of NADH is transferred from the relatively constant redox potentials of enzyme-bound flavin to cyt b_5 (see Fig. 8B and Ref. [3]). In addition, the redox potential of cyt b_5 reductase decreases approx. 30 mV by the binding of cyt b_5, and its FAD group increases the solvent accessibility [57], indicating a strong interaction between both proteins. In contrast, an interaction of cyt b_5 with cyt

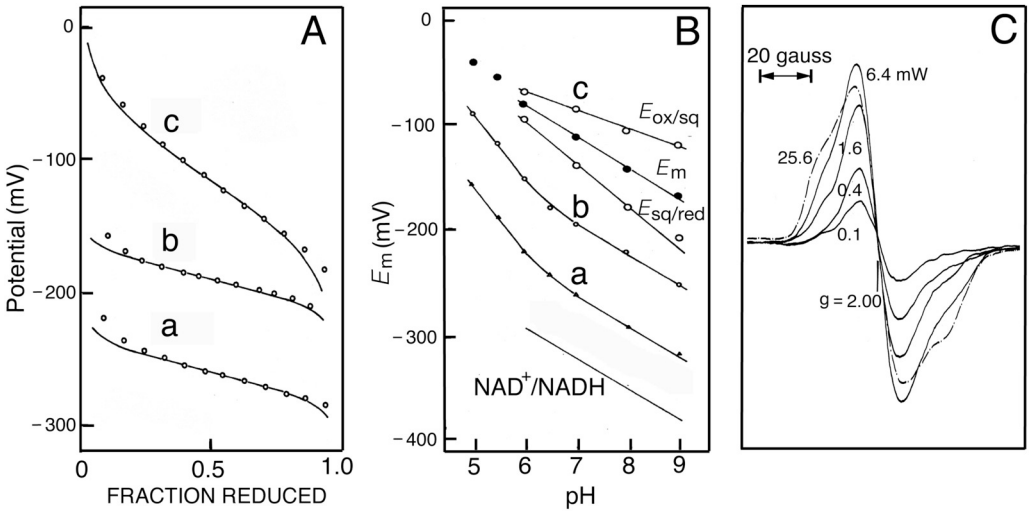

Fig. 4. The reduction potential of the cyt b_5 reductase. A, Potentiometric titration curves, (a) dithionite titration, (b) NADH titration, (c) dithionite titration in the presence of 2 mM NAD^+. B, pH dependence of (a) dithionite titration, (b) NADH titration, and (c) $E_{ox/sq}$, $E_{sq/red}$ and E_m values obtained from dithionite titration in the presence of 2 mM NAD^+. C, Room temperature EPR signals at varying different microwave powers. See Ref. [3] for more detail.

P450 causes a low-to-high spin conversion of cyt P450 [58], in which the reduction potential of cyt P450 could shift to a positive value (see Section 4.2.5). Thus, ET from NADH to cyt P450 is also modulated by the interactions between the redox partners.

3.2. Kinetic method for redox potential measurement

In addition to electrochemical methods, one-electron reduction potentials can also be measured using the kinetic methods, which are based on the determination of rate constants of ET reactions between the electron donor ($D \rightarrow D^+ + e^-$) and acceptor ($A + e^- \rightarrow A^-$) (Eq. (9)). Thermodynamics generally do not influence kinetics, but this is not the case for ET reactions between electron donor and acceptor [59]. Hence, the equilibrium constant, K_{DA} is expressed by the ratio of k_r/k_o in terms of rate constants (Eq. (10)). In 1966, using the rapid mixing technique Yamazaki and Ohnishi [59] confirmed experimentally Eq. (11), in which the rate constants and the equilibrium constant are related to the redox potential difference for the redox partner.

$$D + A \underset{k_o}{\overset{k_r}{\rightleftharpoons}} D^+ + A^- \tag{9}$$

$$K_{DA} = [D^+][A^-]/[D][A] = k_r/k_o \tag{10}$$

$$E_{(D^+/D)} - E_{(A/A^-)} = -(RT/F)\ln k_r/k_o = -(RT/F)\ln K_{DA} \tag{11}$$

where k_r and k_o are rate constants for the forward and reverse in Eq. (9), respectively.

The biological short-lived redox cofactors, such as flavins have been studied by kinetic methods (Eq. 11) using the pulse radiolysis technique [60]. The value of one-electron reduction potential, $E_{(D+/D)}$ is known, it is possible to measure the value of $E_{(A/A^-)}$ [61,62].

4. Redox properties of NAD(P)H-dependent ET components

4.1. Ferredoxin-$NADP^+$ oxidoreductase

The ferredoxin-$NADP^+$oxidoreductase (FNR) is an FAD-containing flavoprotein [63–65]. The FNR family is a prototypic member of the NAD(P)H/FAD-dependent dehydrogenases, which are classified into three groups: the plant-, the glutathione reductase-, and NADPH-thioredoxin reductase types [66]. The plant enzymes are divided into plastidic and bacterial types. These proteins consist of two distinct subdomains: the NADPH-binding domain at the C terminus and FAD-binding domain at the N terminus; these domains are connected by a linker. The NAD(P)H/FAD domain as the NAD(P)H dehydrogenase belongs to the plastid FNR family, including cyt P450 reductase, NOS isozymes, cyt b_5 reductase and MS reductase, whereas adrenodoxin (Adx) reductase belongs to the glutathione reductase family. These proteins comprise the dinucleotide binding fold in the binding of NAD(P)H and FAD cofactors [67]. The redox properties of enzyme bound FAD are modulated by the interactions between the isoalloxazine ring of FAD and NAD(P) cofactors and their partners.

In photosystem I, FNR catalyses the reduction of $NADP^+$ to NADPH, using electrons supplied by ferredoxin (Fdx) that has a low redox potential (−420 mV) (Scheme 2). The reduced Fdx donates electrons to FAD cofactor in two successive one-electron steps: $FAD \rightleftharpoons FADH^{\bullet} \rightleftharpoons FADH^-$, while a hydride ion is directly transferred from $FADH^-$ to $NADP^+$ [68]. Thus, one- and two-electron midpoint potentials are important factors in controlling ET. The redox potential of spinach FNR, E_m values for the overall two-electron reduction potential is −342 mV, and one-electron reduction potentials are −350 mV for $E_{ox/sq}$ and −335 mV for $E_{sq/red}$ at pH 7 [69]. These values correspond to a semiquinone formation constant, K_s of 0.55. The effects of pH on the potentials indicate that the FAD cofactor cycles between the oxidized (FAD_{ox}), neutral semiquinone ($FADH^{\bullet}$) and fully reduced anionic ($FADH^-$) forms at the physiological pH range. In contrast, the redox potential of Fdx is affected by the binding with photosystem I or FNR. A negative shift of 60 mV for photosystem I [70] and 90 mV for FNR [71] are reported, respectively. Thus, the formation of complex between Fdx and FNR could cause a favorable reduction of FNR by Fdx, whereas, the redox potential of FNR is approxi. 20 mV more positive. These results show that the oxidation-reduction state of Fdx strongly affects its association with FNR.

The FAD isoalloxazine ring in the FNR is stacking by two aromatic residues, Tyr314 and Tyr95 [64], in where Tyr314 that is positioned in the C-terminus must move away for a productive hydride anion transfer from the reduced FAD to $NADP^+$. Thus, the nicotinamide moiety of $NADP^+$ stacked against the isoalloxazine ring allows for the hydride ion transfer between the N5 atom of the isoalloxazine ring and C4 atom of the nicotinamide. Ser96 may stabilize a neutral FAD semiquinone,

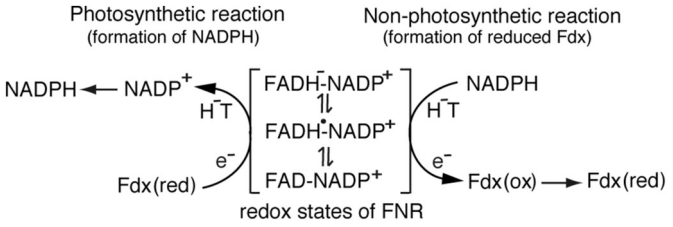

Scheme 2. Switching between one-electron and two-electron transfer reactions in FNR -Fdx system. H^-T, hydride ion transfer.

which interacts with the N5 atom of the isoalloxazine ring. Therefore, Tyr314 and Ser96 could be involved in modulating the flavin redox properties. Additionally, the C-terminal Tyr modulates the affinity for $NADP^+$, the stabilization of the FAD semiquinone and the rate of ET [72,73]. In the ET process from Fdx to $NADP^+$, the $NADP^+$-$FADH^-$ complex is a key intermediate, which has long-wavelength charge transfer (CT) bands at 500–750 nm [74]. In the presence of excess NADPH (> 10-fold), therefore, bound $NADP^+$ is replaced by the NADPH: $NADP^+$-$FADH^-$ + NADPH ⇌ NADPH-$FADH^-$ + $NADP^+$, where the NADPH-$FADH^-$ complex does not reveal significant charge transfer (CT) bands, indicating a decrease of π-π electron staking interactions between the reduced FAD and NADPH. Meanwhile, the E_m for the two-electron reduction of $NADP^+$-FAD_{ox} complex is approx. 40 mV more positive than the E_m of NADPH/$NADP^+$ couple [74]. Thus, the complex formation promotes electrons transfer from the reduced FAD to $NADP^+$. The Fdx can also function in the reverse direction, using NADPH to reduce Fdx, which functions as a one-electron carrier in the metabolic pathway (Scheme 2). Meanwhile, the photosynthetic reaction (Photosystem I → Fdx → $NADP^+$) is thermodynamically favorable, its reverse reaction is unfavorable. The non-photosynthetic reactions function in many metabolic processes such as sulfur and nitrogen assimilation in which distinct FNRs act as an electron source. The difference between $E_{ox/sq}$ and $E_{sq/red}$ values of FNR is relatively small (see Fig. 5), which might enable a reversible reaction in the photosynthetic and non-photosynthetic systems (Scheme 2).

In cyanobacteria and certain algae, Fdx can be a substitute for the low-potential flavodoxin (Fldx) during growth under low-iron conditions [63,65] (Fig. 1). The FMN-containing Fldx(s) are small electron carriers that participate in low-redox potential ET pathway. The FMN is strongly bound via hydrogen bonds on one side of the protein with the isoalloxazine moiety exposed to the solvent. The FMN cofactor of *Desulfovibrio vulgaris* fldx is stacking by two aromatic residues of Trp60 and Tyr98, which are bound with two 60 s and 90 s loops [75]. In all Fldx, the *K*s values are larger than unity, indicating that $E_{ox/sq}$ value is always more positive than $E_{sq/red}$ and that $E_{sq/red}$ value is more sensitive in the protein environments in the proximity of FMN than is $E_{ox/sq}$ [76]. The $E_{ox/sq}$ value is associated with a proton-coupled one-electron reduction at the physiological pH range: $FMN + e^- + H^+ \rightleftharpoons FMNH^{\bullet}$, whereas $E_{sq/red}$ is associated with a one-electron reduction; $FMNH^{\bullet} + e^- \rightleftharpoons FMNH^-$. In the Fldx(s), $E_{ox/sq}$ is shifted from −240 mV to less-negative values, and $E_{sq/red}$ is shifted from −170 mV to ~ −540 mV, depending on the pH and Fldx species. The neutral semiquinone of Fldx, $FMNH^{\bullet}$ is stabilized by the interaction of the carbonyl and amide groups of the protein backbone with N5 atom of isoalloxazine ring of the flavins [34,76]. The anionic fully reduced $FMNH^-$ is destabilized by the hydrogen bond between N(3)H and the primary chain acceptor groups such as the nonionizable carbonyl group of the peptide bond [77,78], where their anionic states have a low redox potential. Thus, the $FMNH^{\bullet}$/$FMNH^-$ couple ($FMNH^- \rightleftharpoons FMNH^{\bullet} + e^-$) acts as a one-electron carrier.

As shown in Scheme 2, the FNR/Fdx system participates in the photosynthetic and non-photosynthetic (metabolic) reactions. FNR can transfer electrons to both Fdx and Fldx, and its interactions with Fdx or Fldx occur at the same structural region in the FAD-binding domain [65,79]. In the metabolic pathway, ET sequence is NAD(P)H → FNR (FAD) → Fdx/or Fldx → metal containing proteins. In the FNR-Fdx complex, the distance between the dimethylbenzene edge of FAD cofactor and the [2Fe-2S] cluster of Fdx is ~6 Å [65,80,81], suggesting that the ET proceeds through a bridge-mediated mechanism in a specific protein–protein complex. In the FNR-Fdx complex, the ET is facilitated by Fdx loop-residues 40–49 [65]. On the other hand, the modeling analysis of the FNR-Fldx complexes indicates the distance between two flavin rings being ~4 Å, with no intervening residues are present between the two cofactors [81]. This model is structurally similar to the relative orientation of the FAD and FMN binding domains reported in the cyt P450 reductase [12,81], suggesting that a direct electron transfer between FNR and Fldx is more efficient than that of a bridge-mediated ET [128]. However, it is reported that the rate of ET from FNR to Fdx is ~9-fold higher than that of FNR/Fldx system, which is based on the NADPH-dependent cyt *c* reductase activity (NADPH → Fdx/or Fldx → cyt *c*) [79]. On the other hand, Saen-oon et al. [65] investigated the ET process between FNR and its partners using a theoretical approach, which is based on a multiscale modeling approach including all-atom protein–protein docking, the quantum mechanical/molecular mechanical (QM/MM) e-Pathway analysis and electronic coupling calculations. In FNR/Fldx complex, they confirmed a direct ET between redox cofactors and less complex specificity than in Fdx. Hence, they proposed the working hypothesis: more than one orientation in the encounter complex that is initially formed by electrostatic interactions between FNR and its redox partners can be efficient in ET. The rate of ET arises from the dynamic nature of the weak binding process, which leads to the formation of an optimal protein-protein complex [50,65]. Although the similarities and differences in the complexes between FNR and its redox partners have been studied extensively [65,81], the overall ET rate between FNR/Fdx or FNR/Fldx and its physiological redox partners remains to be explained in the

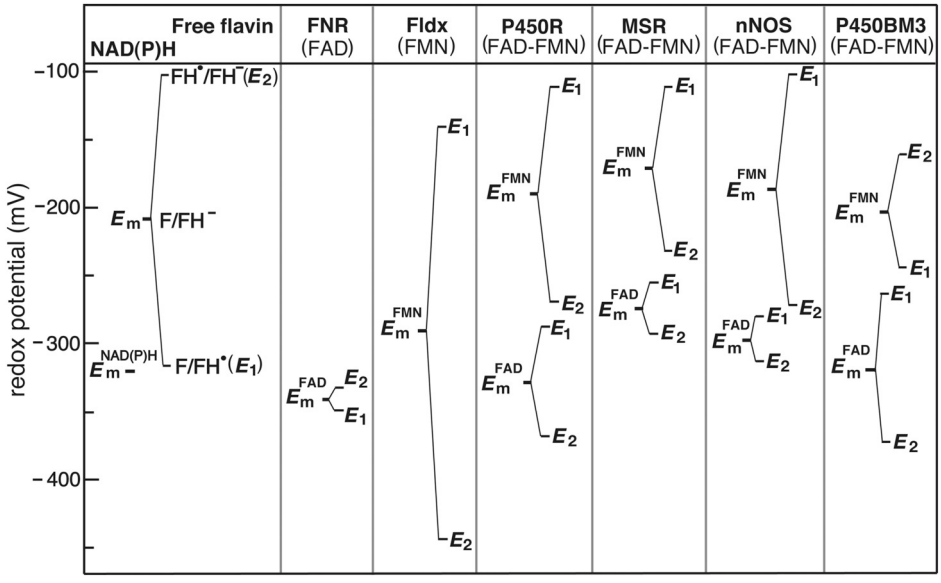

Fig. 5. One-electron midpoint reduction potentials of diflavin reductase family members. FNR, Ferredoxin-$NADP^+$oxidoreductase; Fldx, -*Desulfovibrio vulgaris* flavodoxin; P450R, cyt P450 reductase; MSR, methione synthase (MS) reductase; nNOS, neuronal NOS reductase domain; P450BM3, reductase domain from *Bacillus megaterium* P450BM3.

structural and mechanistic terms.

4.2. Cyt P450 reductase and nitric oxide synthase

In 1973, a new NADPH-dependent flavoprotein which contains the FAD and FMN cofactors per single polypeptide was isolated from rabbit liver microsomes [9]. The protein has similar properties to microsomal NADPH-cytochrome *c* reductase [82]. In addition, air stable semiquinone state derived from enzyme was compared with that of bacterial Fldx. The role of each flavin was proposed: one flavin accepts two reducing equivalents from NADPH at a time, and then donates to the other flavin one reducing equivalent at a time at two different stages of the catalytic cycle [6,9]. This proposal suggested a new microsomal cyt P450 ET system, which is different from mitochondrial cyt P450 ET system (see Fig. 2 and Ref. [7]). In 1973, Ichihara et al. [83] isolated two fractions from the detergent solubilized liver microsomes, in which fraction II involves NADPH-cyt *c* reductase activity; however, this fraction did not contain any significant amount of iron, while fraction I contains cyt P450. The reconstituted system of both fractions exhibited fatty-acid ω-hydroxylation activities. They proposed that fraction II contains a novel type of electron carrier. At present, this unique flavoprotein is known as NADPH-cytochrome P450 reductase (CPR) or NADPH-cytochrome P450 oxidoreductase (CYPOR) [4,6,9]. Thus, this enzyme is the first member of the diflavin reductase family. The structure of the FAD/NADPH-binding C-terminal subdomain of the diflavin reductase family is structurally homologous to that of plant-type FNR, whereas the FMN-binding N-terminal subdomain is similar to bacterial FMN-containing flavodoxin (Fldx) [11,12]. The distinct FAD and FMN domains of diflavin reductase family are connected by an additional connecting domain (CD) and a flexible hinge (H) [12]. Cyt P450 reductase donates electrons to multiple cyt P450s (Figs. 1 and 13A). Thus, cyt P450 reductase functions as an electron donating system (known as reductase) to heme-containing cyt P450 (known as oxygenase).

The NOS isozymes are homodimeric flavocytochromes, and each monomer contains an N-terminal heme-containing oxygenase subdomain and a C-terminal reductase subdomain, both of which are connected by a CaM-binding motif [15–20]. In addition to heme iron, the N-terminal half of the oxygenase subdomain contains tetrahydrobiopterin (H_4B) that acts as a one-electron donor or acceptor, and the substrates L-arginine. On the other hand, the C-terminal half, reductase domain of the NOS isozymes resembles cyt P450 reductase [15]. These electron donating systems to heme oxygenase domain require sequential one-electron transfer reactions for the activation of molecular oxygen in which the air-stable semiquinone, FAD-FMNH$^{\bullet}$ is an important catalytic intermediate (see Scheme 5B and Refs. [9,16]). The heme prosthetic group of cyt P450 accepts two electrons sequentially from cyt P450 reductase and oxidized products, including drugs and xenobiotics [4,23]. Eukaryotic NOS isozymes accept three electrons from the reductase domain in which L-arginine is converted into L-citrulline and nitric oxide (NO) via two consecutive mono-oxygenation reactions. The neuronal (nNOS) and endotherial (eNOS) isozymes are differentially controlled by Ca^{2+}-CaM, whereas the inducible NOS (iNOS) activity is independent of intracellular Ca^{2+} concentration.

4.2.1. Redox potentials of diflavin reductase family

The redox potentials of diflavin reductase family that couple to metal-containing centers are the driving force in the reactions between the donor and acceptor, and the redox states of the protein-bound flavins are modulated by their interactions with the protein. First I will discuss the redox states of semiquinones and fully reduced form of the FAD and FMN, respectively. The enzyme bound FAD and FMN cofactors have very similar absorption peaks, in which it is difficult to distinguish between the redox states of the two flavins. As intermediates of the reactions, neutral semiquinone forms of both FAD and FMN cofactors have a broad band in the 500–700 nm, with a broad shoulder at 580–600 nm [9], while an anionic semiquinone is characterized by a pronounced peak at about 380 nm and a low absorbance at 500–700 nm, for example, cyt b_5 reductase exhibits absorbance peak at 375 nm [3]. On the other hand, both semiquinones are distinguished by a line width in the electron paramagnetic resonance (EPR), in which an anionic semiquinone and a neutral semiquinone exhibits ~16 and ~20 Gauss, respectively. For cyt P450 reductase, the FMN neutral semiquinone reveals a shoulder at 630 nm, but its shoulder is not observed in neutral FAD semiquinones [6,9]. A neutral FAD semiquinone of NOS isozymes has an additional broad peak at 520–530 nm [84–87], but this peak is not observed in the cyt P450 reductase [6,9]. These peaks are also observed in the plant FNR (see Fig. 5D of Ref. [64]). In contrast, the FAD semiquinone of NADH-cyt b_5 reductase which is a FNR member is converted from a neutral to an anionic form (see Section 7), and its fully reduced form is anionic (Fig. 4), but the T66 V mutant stabilizes a neutral semiquinone, and its semiquinone has an additional a peak at 515 nm (Fig. 3, panel d of Ref. [54]). The neutral FAD semiquinone of bacteria P450BM3 exhibits an additional peak at ~500 nm, whereas the FMN is the anionic form, FMN$^{\bullet -}$ [88,89]. Thus, both semiquinones can be distinguished by their spectral differences. In contrast, the anionic and neutral states of fully reduced form are spectrally indistinguishable. The p*K*a of the fully reduced flavin is ~6.7 (Fig. 3) and therefore at pH 7, the anionic hydroquinone is mainly formed, which has a net negative charge. However, their redox states are dependent on the p*K*a in the protein. It is interesting to note that the $E_{ox/sq}$ values for both the FMN and FAD cofactors of cyt P450 reductase exhibit linear pattern at a pH 7.0–8.5 range, although the slopes deviate from the predicted value of −59 mV/pH for one-electron reduction associated with one proton [90,91], whereas the $E_{sq/red}$ values for both the FMN and FAD are a relatively constant at a pH 7.0–8.0 range, indicating the unusual redox properties. It is probable that semiquinone formation constant for one-electron redox potentials, $E_{ox/sq}$ and $E_{sq/red}$ for FAD and FMN is dependent on the pH, as indicated in Fig. 4B, curve c. On the other hand, Shukla et al. (2006) reported that a pH dependence of ~ −59 mV/pH unit is consistent with proton-coupled ET for the redox potentials of both the FAD and FMN [92]. In this report, they used the voltammetric method in where the redox potentials of the FAD and FMN cofactors have been identified using both cyclic and square wave voltammetry.

In contrast, the FAD directly accepts hydride ion from NADPH (Eq. (1)), resulting in the fully reduced anionic form, $FADH^-$, while the formation of the neutral form, $FADH_2$ involves the proton-coupled hydride ion transfer in which a proton may be transferred from a solvent. However, a mechanism of detailed proton-coupled hydride ion transfer has not been clarified. The FMN domain of cyt P450 reductase functions as a one-electron carrier, and hence the proton-couple ET is not necessary. The FMN-containing fldx which has similar structure to that of cyt P450 reductase shuttles between the $FMNH^-$ and the FMNH$^{\bullet}$ as a one-electron carrier. Taken together, the structure of FMN domain in the diflavin reductases shares the two loops in the FMN binding site. In this review, I will assume that the fully reduced forms are in both anionic $FADH^-$ and $FMNH^-$, to be consistent with the analogous plant FNR [69] and bacterial fldx [76] in the physiological pH range.

In 1974, the $E_{ox/sq}$ and $E_{sq/red}$ values of two flavins for rabbit cyt P450 reductase were determined from potentiometric titration curves by Iyanagi et al. [5,9]. The values of $E_{ox/sq}$ and $E_{sq/red}$ for FAD are −290 mV and −372 mV, and those for FMN are −110 mV and −270 mV, respectively. The K_s values of each flavins are larger than unity (see Fig. 5). The redox properties of human cyt P450 reductase are similar to those reported for rabbit cyt P450 reductase [14]. The redox potentials of cyt P450 reductase have been analysed by using a truncated form, which lacks the N-terminal membrane binding anchor domain. However, the lipid components modulate the redox potentials of the FAD and FMN prosthetic groups of the membrane-bound enzyme [91]. When bound to the positively charged lipids, the redox potentials shift to more positive. On the other hand, in the negatively charged

lipids, the $E_{sq/red}$ value for FMN cofactor shifts ~80 mV to the negative, which could provide a driving force for the reduction of cyt P450.

For the rat nNOS reductase domain, the values of $E_{ox/sq}$ and $E_{sq/red}$ for FAD are −283 mV and −310 mV, while the values of $E_{ox/sq}$ and $E_{sq/red}$ for FMN are −105 mV and −274 mV, respectively [93]. The calmodulin (CaM) does not affect the redox potential of either FAD or FMN prosthetic groups. In contrast, Dunford and coworkers [94] reported the different redox potentials for both the FAD and FMN cofactors of the nNOS reductase domain, where the $E_{sq/red}$ value for FMN shifts ~86 mV to the negative by the binding of CaM. This could provide a driving force for the reduction of the oxygenase domain. However, the differences between these two reports have yet to be resolved in detail.

As described in later Sections, cyt P450 and NOS ET systems include a hydride ion transfer from NADPH to FAD, proton-coupled ET from $FADH^-$ to FMN, and proton coupled internal ET from $FADH^\bullet$ to $FMNH^\bullet$, and in the final step the fully reduced FMN ($FMNH^-$) donates electrons to the oxygenase domain. The stable neutral FMN semiquinone that is formed by a one-electron oxidation of fully reduced FMN is stabilized by a peptide flip of a Gly, in which a new strong hydrogen bond between an FMN-N5 atom and conserved Gly (Gly141 in rat cyt P450 reductase) [34] and Gly810 in rat nNOS [33] is formed. Thus, the FMN cofactor shuttles between the fully reduced and semiquinone forms as a one-electron carrier.

In contrast, the FAD-N5 atom forms a weak hydrogen bond with the side chain hydroxyl of Ser457 [34].

In the bacterial P450BM3, however, the conserved Gly residue is absent in the FMN domain [95]. The values of $E_{ox/sq}$ and $E_{sq/red}$ for FMN are −240 mV and −160 mV at a pH of 7 ($E_{sq/red} > E_{ox/sq}$), respectively [96], indicating that the K_s value of the FMN is less than unity. Thus, the fully reduced form of FMN is thermodynamically more stable than its semiquinone form. In this case, the FMN semiquinone is an anionic form, $FMN^{\bullet-}$, exhibiting a higher reactivity than the neutral semiquinone. In analogy of the cyt P450 reductase, the reduced FMN can sequentially donate electrons to the heme iron: $FMNH^- \rightarrow FMN^{\bullet-} \rightarrow FMN$. However, Murataliev et al. [97] proposed that the three-electron reduced form ($NADP^+$-$FADH^-$-$FMN^{\bullet-}$ ⇌$NADP^+$-$FAD^{\bullet-}$-$FMNH^-$) is an inactive intermediate in the substrate-free form, in which an interaction of bound $NADP^+$ with anionic FAD semiquinone ($NADP^+$-$FAD^{\bullet-}$-$FMNH^-$) causes more positive shift than the reduction potential of heme-ferric ion value. From above proposal, authors considered the catalytic cycle in a 0-2-1-0 sequence, suggesting that a catalytic cycle is significantly different from that of cyt P450 reductase (see Ref. [97] and Fig. 6). Thus, it is likely that the FMN cofactor shuttles between the anionic form, $FMN^{\bullet-}$ and oxidized FMN, in which the FMN acts as a one-electron carrier ($FMN^{\bullet-} \rightleftharpoons FMN + e^-$). However, Dubey and Shaik [98] reported that ET from anionic FMN semiquinone to heme iron is controlled by the substrate-dependent large conformational change in which substrate binding leads to formation of an organized water chain connecting the FMN and heme moieties. The distance between the FMN (anionic FMN semiquinone) donor and acceptor (oxidized heme iron) is reduced from 18.6 Å to as little as 8.8 Å, which enhances the ET rate (by 10^4–10^6 fold) to the oxidized heme ion.

More recently, two studies have reported one-electron reduction potentials of the ΔGly mutants for the FMN of nNOS [33] and cyt P450 reductase [34], respectively. In rat nNOS, the values of $E_{ox/sq}$ and $E_{sq/red}$ are −179 mV and −314 mV at a pH of 7.4 for wild enzymes, respectively; however, their values for the ΔGly mutant (ΔGly810) change to −280 mV and −190 mV, respectively [33] For rat cyt P450 reductase the values of $E_{ox/sq}$ and $E_{sq/red}$ for FMN are −56 mV and −249 mV, respectively [34]. The values for ΔGly mutants of $E_{ox/sq}$ and $E_{sq/red}$ are −229 mV and −53 mV, respectively. The ΔGly mutants of both enzymes cause the reversal of $E_{ox/sq}$ and $E_{sq/red}$ values in which the FMN semiquinones are the anionic forms instead of the neutral semiquinone. ET from anionic FMN semiquinone, $FMN^{\bullet-}$ to cyt P450 heme center does not include proton-coupled ET. Therefore, the activity of anionic

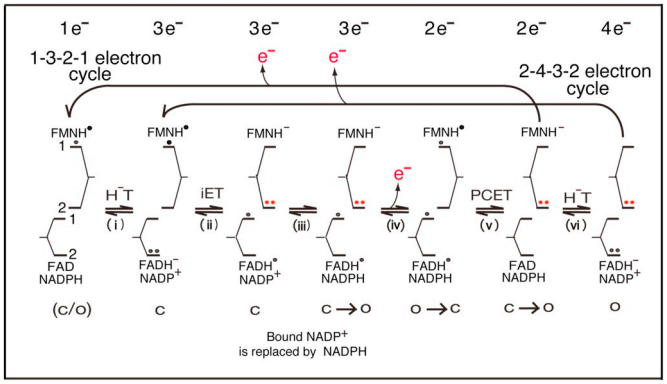

Fig. 6. Redox potentials of the individual redox couples of FAD and FMN cofactors, and the catalytic cycle for the cyt P450 reductase. The cycle starts from one-electron reduced, NADPH-FAD-$FMNH^\bullet$ (1-3-2-1 electron cycle) or two-electron reduced, NADPH-FAD-$FMNH^-$ (2-4-3-2 electron cycle). The bound $NADP^+$ replaced by NADPH in the presence of excess NADPH (step iii), resulting the NADPH-$FADH^\bullet$-$FMNH^-$. The fully reduced $FMNH^-$ that is indicated by the double dot (red) transfers an electron to cyt P450. H^-T, hydride ion transfer (steps i and vi); iET, an internal one-electron transfer between the two flavins (step ii); PCET, a proton-coupled ET (step v): $FADH^\bullet$-$FMNH^\bullet \rightarrow FAD$-$FMNH^- + H^+$; c → o, a conversion from the closed to open forms, and o → c, a conversion from the open to closed forms. 1 and 2 indicate a one-electron reduction potentials for $E_{ox/sq}$ and $E_{sq/red}$, and couples, respectively.

FMN semiquinone could be expected to be higher than that of the neutral FMN semiquinone of the wild type enzymes. However, this is not necessarily the case. In the bacteria P450BM3 system, however, this reversal of the redox potentials suggests an efficient ET from the anionic semiquinone to the heme center, compared to the microsomal cyt P450 system.

Although the structures of diflavin reductase family members are very similar to each other [4], their one-electron midpoint redox potentials are significantly different (Fig. 5). For example, *D. vulgaris* Fldx bears a similar loop structure with the FMN binding sites of cyt P450 reductase and NOS reductase domain, but the value of −440 mV for $E_{sq/red}$ is significantly lower than are those of diflavin reductase family of ~200 mV (Fig. 5). Ishikita [99] suggested that the protein backbone conformation of the 60 s loop modulates the redox potentials of Fldx. A segment of the 60 s loop (59-TWG**D**SIEL-67) of *D. vulgaris* Fldx includes a negative charge residue, Asp 62 (D62). While, this Asp62 corresponds to the neutral charge residue, Gly143(G143) in the segment of loop (139-TYGE**G**DPTD-147) of cyt P450 reductase, and Gly-812(G812) in the segment of loop (808-TFGN**G**DPPE-816) of nNOS, respectively. It is likely that the large negative shift in the redox potential for $E_{sq/red}$ of FMN of the Fldx might be due to the conformational changes of the loop structures in the proximity of the FMN binding site. From the mutant proteins of the 140 s loop of cyt P450 reductase, Rwere and Xia et al. [34] recently proposed that the structure and dynamics are major determinants of redox potential. Thus, the values of $E_{ox/sq}$ and $E_{sq/red}$ of each diflavin enzymes have been optimized for function during evolution.

The diflavin reductase family members share unique sequential one-electron transfer systems. The cyt P450 reductase transfers two-electrons to cyt P450 for substrate oxidation [4]. The cyt P450 reductase-like flavin domain of NOS isozymes transfers three-electrons to the oxygenase domain, in which the NO radical is formed from L-arginine [100]. Seven electrons are transferred to heme oxygenase from cyt P450 reductase in which the enzyme-bound heme cofactor is converted to biliverdin [101]. The bacterial NADPH-sulfite reductase transfers six electrons for the reduction of sulfite to sulfide [102,103]. On the other hand, the methione synthase (MS) reductase donates one electron to the MS-cob(II)alamin center [104]. In these ET systems, the FAD functions as a converter from two-electron donor to a one-electron carrier. The

FMN functions as a one-electron carrier, and its reduced form ($FMNH^-$) donates electrons sequentially in the final metal-containing one-electron acceptors, in which the neutral FMN semiquinone is an inactive intermediate. Thus, the FMN shuttles between the fully reduced and its semiquinone states.

4.2.2. Dynamic conformational changes

In 1997, Wang et al. [12] reported the three-dimensional structure of cyt P450 reductase. Its structure clearly demonstrated that the dimethylbenzene edge of the isoalloxazine ring of FMN, which is exposed to the solvent in Fldx, is covered by NADPH/FAD domain, suggesting direct ET between the dimethylbenzene edges of FAD and FMN cofactors. This closed form cannot explain how electrons are donated to the redox active center such as cyt P450. There are several possible mechanisms for ET from the FAD-FMN pair to the electron acceptor. ET from the FMN to the electron acceptor could occur without an associated conformational change or with a large-scale movement of the FMN domain. In 2005, the redox-linked conformational model during the catalytic cycle for both cyt P450 reductase and NOS reductase domain was proposed by Iyanagi [22]. In 2009, direct evidence for domain movement was demonstrated by Hamdane and Xia et al. [28] by constructing a cyt P450 reductase variant with a four amino acid deletion in the hinge region. The three extended conformations (open states) with varying distances between the FAD and the FMN are found in the same crystal, indicating that a conversion from the closed form to the open form is regulated by a flexible hinge. Additionally, Xia et al. [30] demonstrated that the mutant cyt P450 reductase with an engineered disulfide bond between the FAD/NADPH and FMN domains is incapable of inter-flavin ET from the FAD to FMN cofactors, and is unable to support of cyt P450-dependent monooxygenase activity. At present, several studies supports the idea that cyt P450 reductase adopts thermodynamically closed and open conformations in solution [32,105–112], in which the dynamic equilibrium between closed and open forms is regulated by several factors. The proposed redox-linked conformational changes may be caused by the redox states of protein bound FAD and FMN cofactors. The closed form is stabilized for ET from FAD to FMN in which the reduced FAD domain has a high affinity for the FMN domain. The closed form is converted to the open form for ET from reduced FMN to cyt P450, in which reduced FMN has a high affinity for cyt P450 [4]. This proposed mechanism may depend on the solvation dynamics and protein conformation near the functional sites of the FMN isoalloxazine ring, as is suggested in *D. vulgaris* Fldx [113] in which the positively charged surfaces of cyt P450 can interact with the negatively charged surfaces of the FMN domain. Therefore, the position of the conformational equilibrium between closed (compact) and open (extended) states could be affected by the ionic strength [111,112]. In addition, NADPH/$NADP^+$-binding modulates the conformational equilibrium between the closed and open states. The $NADP^+$-free form of cyt P450 reductase adopts predominantly more open conformations in solution [106,114], but its crystal structure adopts the closed form [12,30]. The $NADP^+$-binding promotes the formation of the closed state. Whereas, when the enzyme is reduced with excess NADPH, an additional opening phase is observed after initial closing triggered by (stoichiometric) NADPH reduction [106]. For these observations, it is probable that the enzyme-bound $NADP^+$ replaces with NADPH and NADPH-bound enzyme could promote further formation of open form (see Fig. 6), in which the K_m for NADPH and K_i for $NADP^+$ have similar values [10]. This opening allows the enzyme to transfer electrons rapidly from the FMN domain of cyt P450 reductase to partner proteins.

However, Kovrigina et al. [115] recently demonstrated that a truncated cyt P450 reductase lacking the N-terminal membrane-binding anchor is closed in both the reduced and oxidized states in the absence of the redox partner. Thus, it is possible to convert to open form by a combination of the ligand- and partner-promoted conformational changes. Additionally, the membranes may also assist the conformational changes by their anchor-anchor interactions (see Section 4.2.7). At present, the redox-linked conformational ET model is the best interpretation for the dynamic closed and open transition, which is linked to individual steps in the catalytic cycles (see Fig. 6). However, more detailed information is needed. While, as described in the Section 5, NOS isozymes are regulated by the CaM-dependent conformational changes (see Section 5) [18–20,116–119].

All diflavin enzymes involve conformational shuttling between closed and open states in which the fully reduced FMN state of open form donates electrons to final electron acceptors. Haque et al [120,121] have directly estimated the rate of conformational switching from rapid kinetics studies of cyt *c* reduction by reduced enzyme, in which the open form of diflavin reductases reacts rapidly with cyt *c*. The rate of conformational switching between closed unreactive and open reactive states is the order of cyt P450 reductase > nNOS > MS reductase > eNOS. Thus, the reductase domain of diflavin reductases is differentially regulated by dynamic conformational changes between the closed and open forms.

4.2.3. Electron transfer from FAD to FMN

On the basis of one-electron midpoint potentials, the reaction mechanisms of diflavin reductases including cyt P450 reductase, MS reductase and NOS reductase domain have been compared, using rat or human enzyme. The overall structures of diflavin reductase family are very similar to each other. In these enzymes, ET from NADPH to the metal-containing center involves the following reactions; (i) NADPH → FAD, (ii) FAD → FMN, (iii) FMN → metal-containing center (Figs. 1 and 2). In particular, the reduction process by NADPH of cyt P450 reductase [6,121] and nNOS reductase domain [29] have been analysed using the oxidized (FAD-FMN) or one-electron reduced (FAD-$FMNH^•$) enzyme. In this Section, the similarities and differences in these ET processes are discussed.

In the reduction of oxidized (FAD-FMN) and one-electron reduced (FAD-$FMNH^•$) of cyt P450 reductase by NADPH, the hydride ion transfer and interflavin ET processes occur without any lag phase [6,122], indicating that the hydride ion transfer is kinetically coupled to internal ET between the two flavins. The rate of hydride ion transfer from NADPH to FAD is slower than that of the one-electron transfer from reduced $FADH^-$ to oxidized FMN, in which the FAD-stacking aromatic residue, Trp676 (rat enzyme numbering) must move away from the isoalloxazine ring of FAD, allowing the nicotinamide ring to interact with the flavin for the hydride ion transfer to FAD to occur [123]. The cyt P450 reductase variants, Trp676Phe and Trp676Tyr are lacking the coupling reactions that cause a decrease in both rate of the FAD reduction and internal ET between the two flavins [124]. In the vicinity of FAD lies His322, which forms a hydrogen-bond with the highly conserved Asp677, but in MS reductase, Ala312 replaces the His322 (see Fig. 1 of Ref. [125]). In cyt P450 reductase, the substitution of His322 to Ala residue does not affect the rate of NADPH hydride ion transfer, but does impede interflavin ET [125]. For MS reductase, swapping Ala312 for a histidine residue results in the kinetic coupling of hydride ion and interflavin ET. From this information, Meints et al. [125] proposed the proton-coupled ET mechanism in which the proximal FAD histidine (His) residue accepts a proton released from the FAD hydroquinone ($FADH_2$), resulting in an anionic form ($FADH^-$), which transfers one-electron to the oxidized FMN. A similar proton-coupled ET mechanism is also proposed for cyt b_5 reductase (see Section 7 and Refs. [54,55]). On the other hand, Xia et al. [126] reported the role of the mobile Gly631-Asn635 loop (Asp632 loop) using mutant enzymes of Asp632. The structure of 4-electron-reduced $NADP^+$-bound wild-type cyt P450 reductase shows the plane of the nicotinamide ring positioned perpendicular to the FAD isoalloxazine ring with its carboxamide group forming hydrogen-bonds with N1 of the methyl groups of the flavin ring and the Thr535 hydroxyl group, and the distance between C8 and C8 of the methyl groups of the isoalloxazine rings of FAD and FMN is ~1 Å closer compared to the fully oxidized and one-

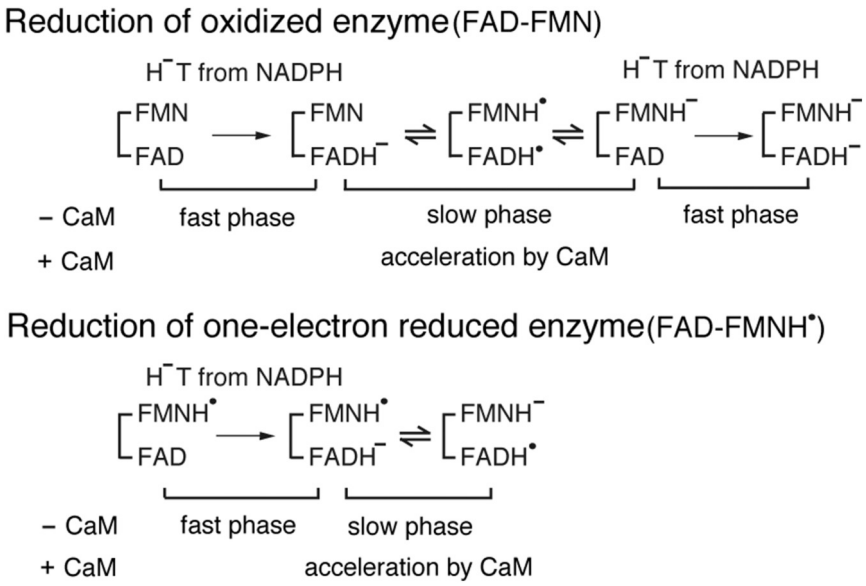

Scheme 3. The reduction of oxidized (FAD-FMN) and one-electron reduced (FAD-FMNH$^{\bullet}$) enzymes by NADPH in the absence (−) and presence (+) of CaM, respectively. The fast phases indicate the hydride ion transfer ($H^{-}T$) from NADPH to FAD. The slow phases include internal ET between the two flavins.

electron-reduced structures, suggesting that the FAD reduction facilitates internal flavin ET.

In the second step, internal ET from FAD_{red} to FMN_{ox} is thermodynamically in a "quasi-equilibrium" of all states [6,90,127]: $FADH^{-}$-FMN ⇌ $FADH^{\bullet}$-$FMNH^{\bullet}$ ⇌FAD-$FMNH^{-}$, and the formation of fully reduced enzyme proceeds via these steps (see Fig. 6 and Schemes 3 and 4). The distance between the FAD and FMN co-factors is ∼4 Å for cyt P450 reductase [12] and ∼5 Å for nNOS [17], suggesting that one-electron transfer reactions occur directly between the dimethylbenzene edges of the flavin isoalloxazine rings, where both FAD and FMN semiquinones are in neutral states. The formation of reduced enzyme proceeds via quasi-equilibrium mixture, in which the spin-spin ($FADH^{\bullet}$(↑)···(↓)$FMNH^{\bullet}$ ⇌$FADH^{\bullet}$ ↑↓ $FMNH^{\bullet}$) interactions between the $FADH^{\bullet}$ and $FMNH^{\bullet}$ radicals could be predictable, but such a data have not been reported [9,94,116]. Thus, it is likely that a one-electron transfer reaction from FAD to FMN could directly occur in the electron hopping mechanism.

The short distance, ∼4 Å for cyt P450 reductase between the two flavins is expected to result in very fast and efficient ET between the neutral semiquinones, according to what is known as Dutton's ruler [128]. However, the rate of ET between the FAD and FMN co-factors is relatively slow (∼50 s^{-1}) [127]. Thus, this rate is not explained by Dutton's ruler. Thereby, the internal ET between the two flavins could be gated by the proton-coupled electron transfer ($FADH^{\bullet}$-$FMNH^{\bullet}$ → FAD-$FMNH^{-}$ + H^{+}) and dynamic distance changes between the FAD and the FMN domains in solution. In contrast, for the CaM-bound nNOS, Haque et al. [120] have estimated the rate constant, ∼200 s^{-1} for internal ET between the two flavins. This value is much faster than that of cyt P450 reductase, although a distance of 5.2 Å between the FAD and FMN in the closed form is longer than that of cyt P450 reductase [12]. When the FAD and FMN domains of cyt P450 reductase are fixed in closed form with a disulfide linkage, the distance between the two flavins is increased to ∼5.2 Å [30], and the relative orientations of FAD and FMN cofactors in the active sites are similar to those of nNOS [17]. This modified cyt P450 reductase keeps a ferricyanide activity of approxi. 30% of the wild type enzyme. However, the rate of internal ET from the FAD to FMN is very slow as compared to that of wild type enzymes [30], suggesting that the relative orientation of the two flavin is necessary for the interflavin ET. In cyt P450 reductase, the plane of the FAD and FMN molecules are inclined relative to each other at an angle of ∼135°. This orientation could favor the orbital overlap between the extended π-orbital systems of the prosthetic groups. Meanwhile, Meints et al. [129] proposed the model on the role of the conserved FAD staking Trp679, in which the binding of NADPH facilitates interflavin ET in the flipped out conformation, by forming a favorable contact with the FMN domain (see Fig. 9 of Ref. [129]). This mechanism could also share in both MS reductase and cyt P450 reductase. It is interesting to note that the methyl groups at C7 and C8 of the isoalloxazine ring are important sites for ET [130]. Martınez et al. [131] reported that the rotation of the methyl groups at C7 and C8 of an isoalloxazine ring that participates in ET is limited at room temperature. Therefore, when a methyl group with a restricted orientation

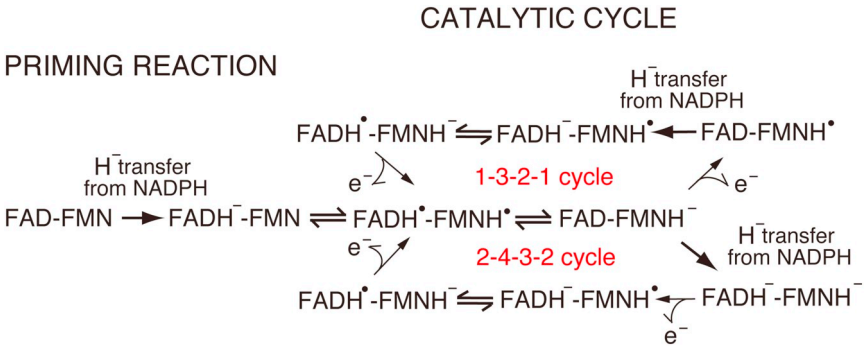

Scheme 4. A catalytic cycle for diflavin reductases. The anionic fully reduced FMN state ($FMNH^{-}$) donates electrons to metal-containing redox center.

functions in electron hopping between the two flavins, the optimal reorientation and distance between the two flavins could be important factors for efficient ET, as compared to a rapidly rotating methyl group.

On the other hand, the ET processes in the NOS reductase domain are summarized in Scheme 3, showing the biphasic kinetics including fast and slow phases in the absence or presence of CaM. Two primary mechanisms have been discussed concerning the role of CaM in the NOS reductase domains. Daff and co-workers [29,93,132] have proposed the conformation-dependent hydride ion transfer mechanism in which the reductase domain exists in an equilibrium between the open and closed conformations in the CaM-free form. This motion is relatively slow in that the FMN domain inhibits hydride ion transfer to FAD from NADPH. Therefore, CaM alters the equilibrium between the open and closed conformations. In contrast, Iyanagi and co-workers [84,87,133] have proposed that the FAD cofactor of NOS isoforms reductase domain is rapidly reduced by NADPH regardless of the absence or presence of CaM. The NOS isoforms have a high ferricyanide reductase activity in the CaM-free form, and its activity exhibits the Michaelis-Menten kinetics [19,85,86,133]. Their activity increases two- or three-fold in the presence of CaM. The values of $> \sim 100\ s^{-1}$ for the reduction of FAD by NADPH are expected from ferricyanide reductase activity [84]. Thereby, the fast phase for hydride ion transfer from NADPH to FAD is difficult to measure accurately, which often is within dead time of stopped flow apparatus. Thus, the internal ET reactions from the $FADH^-$ to $FMNH^\bullet$ have been examined using a special absorption peak for flavins (see Section 4.2.1). In cyt P450 reductase, the decrease of the shoulder at 630 nm indicates the conversion of $FMNH^-$-$FMNH^\bullet$ to $FADH^\bullet$-$FMNH^-$ [6,85], resulting the $FADH^\bullet$-$FMNH^-$. Regarding the NOS isozymes, the increase of broad peak at 520–530 nm indicates the conversion of $FMNH^-$-$FMNH^\bullet$ to $FADH^\bullet$-$FMNH^-$ [84]. Thus, an increase of this peak observed during the reduction of FAD-$FMNH^\bullet$ by NADPH indicates the internal ET between the two flavins [84], and CaM accelerates the rate of the interflavin ET. As determined from the increase of the absorbance peak for NOS isozymes [84–86], the order of conversion is iNOS > nNOS > eNOS. In the case of nNOS isozyme (Fig. 7), values of redox potentials of $NADP^+$-$FADH^-$ and NADPH-$FADH^\bullet$ are near each other. Thus, these redox states exist in the dynamic

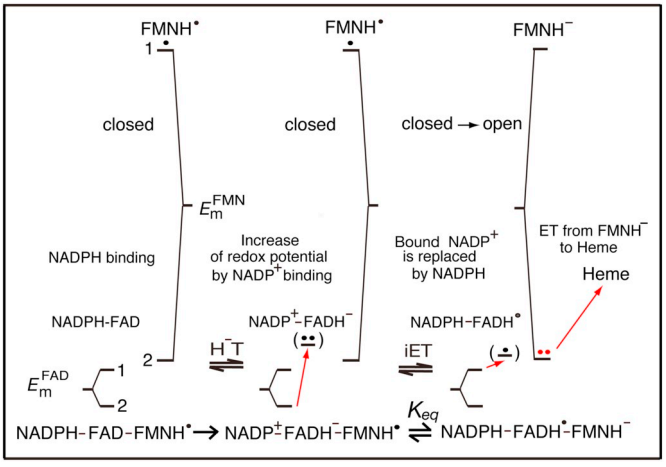

Fig. 7. The reduction processes of the CaM-bound one-electron reduced nNOS reductase domain (FAD-$FMNH^\bullet$) by NADPH. In the first step, NADPH is bound to FAD, and then $NADP^+$-$FADH^-$-$FMNH^\bullet$ complex is formed by the hydride ion transfer (H^-T) from NADPH to FAD, and in the next step the $NADP^+$-$FADH^\bullet$-$FMNH^-$ is formed during interflavin ET (iET) in which bound $NADP^+$ is replaced by NADPH in the presence of excess NADPH [84,87], resulting the NADPH-$FADH^\bullet$-$FMNH^-$. The reduction potentials of $NADP^+$-$FADH^-$ and NADPH-$FADH^\bullet$ are shown in the bracket as a working hypothesis, respectively. In the final step, the $FMNH^-$ (−274 mV [93]) donates electrons to heme (−251 mV [134]). 1 and 2 indicate a one-electron reduction potentials for $E_{ox/sq}$ and $E_{sq/red}$, and couples, respectively (see nNOS (FAD-FMN) of Fig. 5).

equilibrium in which $NADP^+$/NADPH-binding could modulate the equilibrium between the following two states, depending on the $NADP^+$/NADPH ratio [84]: $NADP^+$-$FADH^-$-$FMNH^\bullet$ ⇌NADPH-$FADH^\bullet$-$FMNH^-$. The fraction of active species, NADPH-$FADH^\bullet$-$FMNH^-$ donates electrons to heme iron (−251 mV for nNOS) [134]. In NOS isozymes, the fraction of active species may be different. Nishida and Ortiz de Montellano [135] constructed a chimeric enzyme in which the heme domain of one isozyme was connected to the reductase domain of another, and proposing that the increased reductase domain activity could lead to a corresponding increase in NO synthase activity. Thus, as judged from the absorbance changes at 520–530 nm, the equilibrium constant, K_{eq} between the $NADP^+$-$FADH^-$-$FMNH^\bullet$ and NADPH-$FADH^\bullet$-$FMNH^-$ is differentially controlled in NOS isozymes (Fig. 7); in iNOS, it lies to the right, but in nNOS to the left, and in eNOS lies far to the left.

4.2.4. Catalytic cycle of the diflavin reductases

The one-electron reduced, FAD-$FMNH^\bullet$ state of cyt P450 reductase is stable in the intact microsome [9], in which ferric cyt P450 exists in a low spin state. The FAD-$FMNH^\bullet$ state is observed in the isolated enzyme [9], and is also observed in isolated NOS isozymes [16,86,94]. Thus, during the catalytic cycle of both enzymes, one-electron reduced FAD-$FMNH^\bullet$ state is the key intermediate. Unlike cyt P450 reductase, the reductase domains of nNOS and eNOS isozymes are strictly regulated by CaM [18] (see Section 5 and Fig. 10).

The priming reaction starts from the oxidized form in which the disemiquinone, $FADH^\bullet$-$FMNH^\bullet$ is formed (Scheme 4), by the catalytic cycle starts from one-electron reduced FAD-$FMNH^\bullet$ state. The cyt P450 reductase cycles predominantly between the one- and three-electron reduced states (1-3-2-1 electron cycle). More recently, Xia et al. [126] proposed the 1-3-2-1 electron cycle on the basis of structures (see Fig. 13 of Ref. [126]). This cycle begins via hydride ion transfer from enzyme bound NADPH to a one-electron reduced FAD-$FMNH^\bullet$ in which the charge transfer complex, $NADP^+$-$FADH^-$-$FMNH^\bullet$ is formed [6]. This could cause a positive shift in the redox potential induced by preferential $NADP^+$-binding for reduced FAD, as reported in cyt b_5 reductase [3], in which the internal flavin ET from the $NADP^+$-$FADH^-$-$FMNH^\bullet$ to the $NADP^+$-$FADH^\bullet$-$FMNH^-$ occurs without any lag phase, indicating that the reduction of FAD by NADPH is rate-limiting step [6]. As judged by redox potential, the rate of internal flavin ET in the $NADP^+$-$FADH^-$-$FMNH^\bullet$ could be slower than that of the $NADP^+$-$FADH^-$-FMN [see Fig. 6]. The $FADH^\bullet$-$FMNH^-$ state donates a single electron to its acceptors such as cyt *c* and cyt P450s, in which the enzyme must be converted to its open form. The 2-4-3-2 electron cycle is also possible, depending on the $NADP^+$/NADPH ratio. These processes are also kinetically coupled to the conformational changes. Both cycles are controlled by several factors including the (i) redox potentials of each flavins and their semiquinone states, (ii) redox potential of final electron acceptors, including metal-containing redox center, (iii) rate-limiting step of the reactions, (iv) rate of conformational changes between closed (c) and open (o) forms, and (v) $NADP^+$/NADPH ratio. In addition, it is possible that the cyt P450 reductase shares a similar mechanism with the related family members, including NOS reductase domains [120,121], MS reductase [136], the cancer-related novel reductase 1(NR1) [137], as well as flavoprotein subunits of bacterial sulfite reductase (SiR) [138].

4.2.5. ET from FMN to heme

The cyt P450 reductase and cyt P450 are microsomal membrane-anchored proteins that contain the membrane-binding hydrophobic anchors necessary for the interactions with the microsomal membrane [139,140]. Cyt b_5 [141,142], heme oxygenase (HO) [101,143] and squalene monooxygenase [144] are also physiological redox partners of cyt P450 reductase. This gives rise to an important question. How does cyt P450 reductase that is encoded by a single gene interact specifically with these many different electron acceptors, in addition to ~50 microsomal cyt P450s (see Section 9). The cyt P450 isozymes contain the

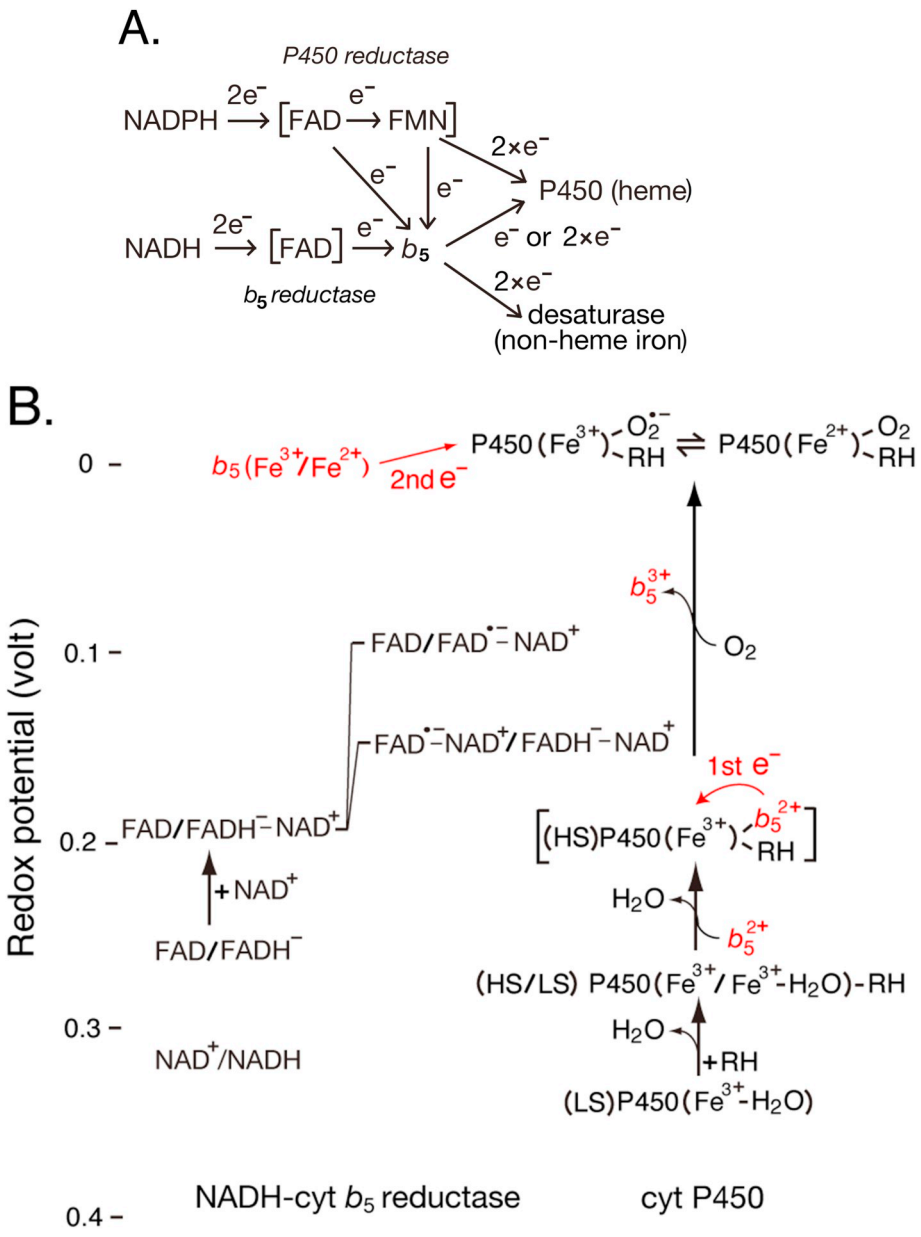

Fig. 8. Role of cyt b_5 in the NADPH-cyt P450 ET and NADH-cyt b_5 ET systems. A, The ET pathway in the microsomal cyt P450 ET and cyt b_5 ET systems. The cyt P450 reductase transfers the first electron (1st e^-) and second electrons (2nd e^-) from the fully reduced FMN, respectively. While, cyt b_5 transfers 2nd e^- or both the 1st e^- and 2nd e^-. B, the reduction potentials of redox cofactors of the NADH-cyt b_5 ET systems (see Section 7 for more detail). The reduction potential of the proposed cyt b_5 (Fe^{+2})-high spin (HS) cyt P450 (Fe^{+3})-substrate (RH) complex is shown in the parenthesis as a working hypotheses. The HS/LS P450 indicates an equilibrium between high spin (HS) and low spin (LS) of cyt P450.

highly conserved positively charged amino acid cluster that is located at the proximal surface of microsomal cyt P450 molecules [28,110,145]. This region can interact with the negatively charged surface of the FMN domain of cyt P450 reductase, including loops around the isoalloxazine ring of FMN [34]. The docked model of a complex between cyt P450 reductase and cyt P450 (CYP2B4) has been proposed, in which a positively charged surface of cyt P450 can interact with a negatively charged surface of the FMN domain of cyt P450 reductase [28], indicating that the highly conserved conformational motifs of the P450s play a role in the molecular recognition process. Thus, a single cyt P450 reductase can donate electron to all microsomal cyt P450 isozymes. The distance between cyt P450 (CYP2B4) heme and dimethylbenzene ring of the FMN molecule is estimated to be ~12 Å, and the two residues of cyt P450 (Phe429 and Glu439) lie in between the two cofactors, suggesting a possible ET pathway: FMN → Glu439 → Phe429 → heme [28]. The distance between FMN and heme of aromatase (CYP19) is ~19 Å in which the ET pathway is proposed: FMN → H_2O → Phe432 → heme [146]. Additionally, the ΔGly-141 mutant of rat cyt P450 reductase is inactive with cyt P450, but fully active in reducing cyt *c*. This mutation might cause the change in the structure and dynamics of the 140 s loop, which is located along the FMN-binding site [34], indicating that the loop structure is important in the interactions with cyt P450.

Additionally, the spin switching of the cyt P450 heme iron by the substrate binding could provide the driving force for the heme reduction. The substrate for the cyt P450 interacts with the active site of the heme center in which a distal water molecule as axial ligands is excluded. This induces a shift in ferric iron spin state (from low-spin to high-spin) [147,148]. Das et al. [149] showed that substrate binding to microsomal CYP3A4 induced a > 90% spin conversion to the high spin and shifted the redox potential by +10 to 80 mV depending on the type 1 substrates. The conversion to a high spin state of low spin ferric heme iron increases the rate of electron flow from the FMN domain of cyt P450 reductase to a high spin state cyt P450 [150,151]. The redox potential of mitochondrial cyt P450 also shifts to more positive by the binding of substrate (see Section 6). On the other hand, the soluble bacterial cyt P450, such as cyt P450cam [147] and P450BM3 [152] bind the substrates with higher specificity, and increase in the heme reduction potential, as compared with microsomal and mitochondrial cyt P450s (see Section 9).

4.2.6. Role of cyt b_5 in the cyt P450 system

In 1971, Hildebrandt and Estabrook [153] first evidenced the participation of cyt b_5 in the NADPH-dependent monooxidation reactions in which cyt b_5 provides one of the two electrons required for cyt P450 function. Bonfils et al. [154] demonstrated the first systematic study on the direct ET from ferrous cyt b_5 to oxygenated cyt P450. Both cyt P450 and cyt b_5 ET systems are localized on the cytosolic surface of ER. At present, two hypotheses have been proposed: for some cyt P450s, cyt b_5 acts as an electron donor, though it can also act as an activator. The FMN domain of cyt P450 reductase and cyt b_5 share the same binding site on the proximal surface of cyt P450 [155]. The docked model between cyt P450 and cyt b_5 suggests also an electrostatic interactions between the two proteins. In contrast to serving as an electron donor, Estrada et al. [110] have proposed that cyt b_5 acts as an allosteric modulator. Cyt b_5 binding induces the structural changes of cyt P45017A1 so that cyt P450 reductase is tightly associated with cyt P450. In contrast, the recent report by Duggal et al. [156] suggests that wild type cyt b_5 donates the second electron in the CYP17A1 system in which the lyase activity increases 5-fold, but the redox inactive Mn-substituted cyt b_5 has no effect on the lyase activity. This observation strongly suggests that cyt b_5 has a redox effector role in enhancement of the CYT17A1 mediated lyase reaction. However, the cumulative data strongly support that cyt b_5 can act as a dual redox active or activator proteins.

Henderson et al. [157] provided strong evidence that cyt b_5 reductase-cyt b_5 ET system can act as a sole electron donor to the cyt P450 system in vivo and vitro, based on the cyt P450 reductase and cyt b_5 knockout mouse. Stiborova et al. [158] also demonstrated that a cyt b_5 system catalyses the oxidation of Benzo[*a*]pyrene, supporting a sequential two electron transfer from the cyt b_5 system. Additionally, the fungal cyt b_5 reductase-cyt b_5 system can donate both the first and second electron to fungal cyt P450s (CYP5150A2) [159]. Thereby, cyt b_5 can act as the sole electron donor in these systems. However, the first electron (1st e^-) transfer reaction from cyt b_5 to oxidized cyt P450 is thermodynamically unfavorable (see Fig. 8B). The fully reduced cyt b_5 state in the reaction systems could be a driving force for the reduction of cyt P450-substrate complex, where the redox potential of the cyt b_5 is considerably more negative than its midpoint potential. Cyt b_5 is actually in the reduced state in liver cells [62]. As described in the Section, 4.2.5, the reduction potential of cyt P450 in the cyt P450-substrate complex shifts to positive. Furthermore, the binding of reduced cyt cyt b_5 to ferric cyt P450-substrate complex could lead to an additional conversion to high spin states. Recently, Ravula et al. [58] reported that ferric cyt b_5 (Fe^{3+}) binding to ferric cyt P450 (Fe^{+3}) induces a conversion from low to high spin states in the membrane systems. Thus, the first electron (1st e^-) could be transferred directly from cyt b_5 to cyt P450 within the cyt b_5-cyt P450-substrate complex (see Fig. 8B). The reduced cyt P450 binds with O_2, resulting in an oxyferrous species with a significantly more positive redox potential (+6 mV) [160], in which the oxygenated cyt P450-substrate complex accepts a second electron (2nd e^-) from cyt b_5.

From NMR and mutagenesis data, Ahuja et al. [141] have proposed that the cyt b_5-cyt P450 complex models based on the binding interface of the membrane-bound forms, clusters I and II, in which the shortest distance between the heme propionate-edge of cyt b_5 and cyt P450 is 9.0 Å and 7.4 Å, respectively. ET from cyt b_5 to cyt P450 proceeds via conserved Arg125. In contrast, cyt P450 reductase can donate electron to cyt b_5 [5,161], but its activity is lower than that of cyt b_5 reductase. Therefore, the cyt b_5 reductase system is the major electron donating source in which cyt cyt b_5 reductase switches from a two electron donor, NADH (−320 mV) to a one-electron acceptor (cyt b_5). More recently, however, Niu et al. [162] reported that negatively charged cyt b_5 accepts electron from positively charged FAD sites in the plant cyt P450 reductase (see Fig. 8A). As described above, the cumulative data suggest that cyt b_5 serves multiple functions, as an electron donor for cyt P450s and fatty acid desaturases. These effects might be dependent on the cyt P450 and desaturase species and their substrates. At present, the roles of cyt b_5 in the microsomal cyt P450 ET system could be summarized as shown in Fig. 8A and B.

4.2.7. Role of the membrane-binding domain

In this Subsection, a role of the ER in the cyt P450 ET system is discussed. Eukaryotic cyt P450 reductase and cyt P450s retain a N-terminal membrane-binding anchor, and are located on the cytoplasmic surface of the ER. The localization of these two proteins on the two-dimensional surface of the ER membrane serves to both concentrate reactants and therefore to increase the frequency of their interaction. The membrane-anchored proteins are mobile on the lipid bilayer, but their movements are much smaller than those of the lipids, indicating that the motion of lipids is a driving force for the mobility of the membrane-bound proteins. Two possible mechanisms are conceivable for the functional interactions between the cyt P450 reductase and cyt P450 on the ER membranes: (i) the interactions are brought about by the lateral motion and subsequent collision of these proteins on the plane of ER membrane [163], and (ii) both proteins exist in the ER membrane as ordered functional clusters in which the interaction can take place directly [164]. Although hydrophilic domains of both enzymes are exposed to the cytosolic compartment, the hydrophobic anchor region between the proteins might ensure the correct orientation and position of the binding sites at the proximal surface of cyt P450 heme and the dimethylbenzene ring of the FMN molecule in which an interactions between the hydrophobic anchors might promote the formation of the functional complex, cyt P450 reductase-cyt P450.

Meanwhile, the anchors of ER membrane proteins are highly dynamic in lipid membranes, with movement occurring on a submillisecond timescale, including the rotational diffusion of the entire helix and fluctuation of the helical director axis [139,140]. This motion might cause the movements of the soluble domains of cyt P450 reductase, and promotes the likelihood of forming an electrostatic complex between the negatively charged residues of the FMN domain and the positively charged residues of the proximal surface of cyt P450 (Fig. 9). The anchor-anchor interactions between ER proteins remain unclear, but the interactions between the anchors could stabilize an interactions between the soluble domains of cyt P450 reductase and cyt P450. This interactions might enhance electron transfer between these proteins. More recently, Jerabek et al. [165] proposed an X-shaped contact model between antiparallel transmembrane helices for the cyt P450-cyt b_5 complex. These interactions are relatively weak and occurs on smaller contact surfaces than an antiparallel-shaped contact. Thus, an possible X-shaped contact model for the cyt P450 reductase-cyt P450 complex is shown in Fig. 9. Taken together, the concentration of cyt P450 reductase in the ER membranes has been estimated to be 1/10–1/

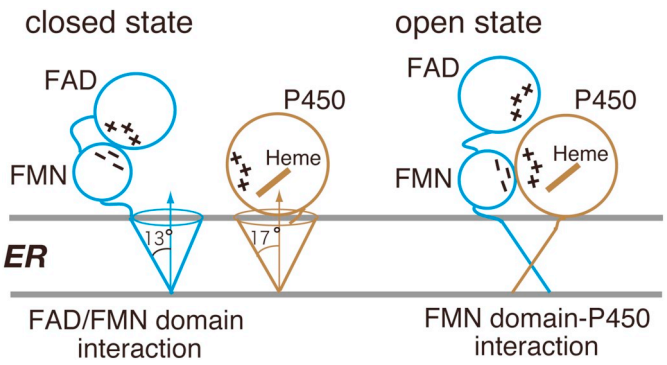

Fig. 9. The dynamic docked model between cyt P450 reductase and cyt P450 in the membrane-anchored states. The closed state of cyt P450 reductase does not interact with P450, but its open state interacts with cyt P450. The tilt angle of 13° for the membrane-binding helix of cyt P450 reductase [139] and 17° for cyt P450 [140]. The plus (+) and minus (−) indicate a positive and negative charges, respectively.

40 of the total cyt P450s [166,167], indicating that a single cyt P450 reductase must interact with 50 microsomal cyt P450s. It is likely that the interactions between cyt P450 reductase and cyt P450s are relatively weak, including interactions between the soluble domains and their anchors. Thus, a single cyt P450 reductase could enable such interactions with various structural partners, such as heme oxygenase and cyt b_5. The redox states of cyt P450 reductase are also important factors for interactions with cyt P450 (see Fig. 6). As described in the Section 4.2.1, the structure and function of the FMN domain of cyt P450 reductase is similar to those of Fldxs, which have a strong dipole moment with the positive and negative regions located towards the two terminal helices and near the FMN-binding site [168].

Brignac-Huber et al. [169] have reported that the roles of membrane lipids include (i) altering the conformation of the proteins, (ii) influencing the cyt P450 interactions with the cyt P450 reductase, and (iii) affecting the localization of the proteins into specific membrane microdomains. The lipid-protein interactions are influenced by the microsomal lipids components in the reconstituted system [170]. Meanwhile, new hypotheses have recently proposed by Barnaba et al. [171], in which the oxidized cyt P450 reductase exists in a peripheral state, and its reduced form is converted to the integral state. Thus, the peripheral state with an anchored membrane can efficiently find its redox partner cyt P450, and its integrated state formed by the reduction of NADPH interacts with cyt P450 in which the reduced cyt P450 reductase forms have a much higher association constant than its oxidized form to cyt P450.

Recently, new Nanodisc technology has been applied in the membrane protein studies, including cyt P450 reductase and cyt P450 [172]. Nanodiscs are composed of phospholipids and an encircling amphipathic helical belt protein, and provide a new and powerful tool for a broad spectrum of biochemical and biophysical studies of membrane proteins. Using this technology, Das and Sligar [91] measured the redox potentials of cyt P450 reductase [see Section 4.2.1]. In contrast, Liu et al. [170] reported that when cyt P450 reductase and cyt P450 are only localized within the same nanodiscs, the electrons from NADPH to cyt P450 via cyt P450 reductase are transferred, but when both enzyme are each incorporated separately into nanodiscs, electron transfer between nanodiscs does not occur. Laursen et al. [173] have demonstrated the presence of at least two states of plant cyt P450 reductase with dramatically different activity levels, indicating that the dynamic conformational changes of the FMN and FAD domains. Additionally, an increase of the ionic strength caused cyt P450 reductase to redistribute its conformational equilibrium and populate more open conformations [174]. The cyt b_5 drives low spin cyt P450's to high form in the nanodisc reconstituted system [58].

5. Modeling for the full-length structure of NOS

NO radicals are a signal molecule for neurotransmission, cardiovascular function, and cellular defense [18]. The three tissue-specific NOS isozymes generate NO radical, while soluble guanylate cyclase (sGC) accepts NO. NOS isozymes are activated by CaM binding, while sGC is activated by NO. During this process, 3,5-cyclic guanosine monophosphate (cGMP) as a second messenger is formed from GTP [175]. Thus, both enzymes are linked in the NO-cGMP signaling pathway. The NOS isozymes and sGC are multi-domain redox enzymes, bearing multiple conformations in solution. The flexibility and mobility of the NOS and sGC domains are likely a major reasons for the failure of crystallization of intact forms. Information regarding the entire structure of an NOS isozymes and sGC have been limited. Recently, cryo electron microscopy (cryo-EM) methods have provided structural information with the aid of partial structures determined from X-ray crystallography.

In 2002, Daff and co-workers [176] proposed a model to explain how the movement of the nNOS reductase domain is controlled by conformational changes during catalysis, in which the CaM-free reductase domain is a closed form whereas the CaM-bound form is an open form, which can donate an electron to the heme center (see Section 4.2.3). In 2009, Xia et al. [20] constructed the first model of the structure of the entire molecule of an NOS isozyme, based on the crystal structures of the iNOS CaM-FMN complex and the CaM-free nNOS reductase domain [17]. The model indicates that the CaM binding region of the iNOS isoform is converted to a tight α-helix and forms a structural unit, CaM-FMN complex is formed, whereas a relatively random structure in the absence of CaM [177]. These structural changes could be the main driving force for the opening of the closed state (input state) of the reductase domain in which ET occurs directly from FAD to FMN. The open state (output state) facilitates the interaction between the FMN-binding domain and heme-binding oxygenase domain. The distance between the FMN and heme cofactors is ~12–15 Å [20], through which a long-range ET occurs from the fully reduced FMN to the heme center. The Trp372 in iNOS and Trp587 in nNOS are positioned between the heme and FMN cofactors, and these aromatic residues that contain π electron system might act as an electron conduit between FMN and the heme center [20,178]. These Trp residues are conserved in all eukaryotic NOSs. Smith et al. [179] demonstrated this possibility by constructing a mutant enzyme in which the conserved Trp residues are replaced with alanine (Ala). The rate of heme reduction is decreased drastically to 0.0047 s^{-1} in mutant enzymes, as compared to 3.79 s^{-1} of the wild-type enzyme. These data suggest that heme reduction by the $FMNH^-$ proceeds via two step tunneling through a tryptophan radical intermediate. Meanwhile, Sheng et al. [180] have proposed possible three pathways for ET from FMN to heme: (i) FMN → Phe593 → Trp372 → heme center; (ii) FMN → 372Trp → heme center; and (iii) FMN → Tyr631 → Trp372 → heme center. By using hydrogen-deuterium exchange methods, Chen et al. [181] proposed that pathway iii is the most likely pathway. ET from $FMNH_2$ to the heme center is proton-coupled such that human iNOS Tyr631 acts as an intermediary proton shuttle between anionic FMN hydroquinone ($FMNH^-$) and water as a solvent: $FMNH_2$ + Heme (Fe^{3+}) → $FMNH^{\bullet}$ + Heme (Fe^{2+}) + H^+. The surface-enhanced Raman scattering spectra of the FMN domain of nNOS demonstrated that the fully reduced FMN is neutral (i.e. the $FMNH_2$ form) [182]. Regarding cyt P450 reductase, the isoalloxazine ring of FMN is staking between two aromatic residues (Tyr). The substitution of both Tyr to Phe has no effect on the catalytic activity, suggesting that Tyr does not act as a proton shuttle [183]. Smith et al. [179] have also examined the surface interactions between the oxygenase domain, FMN domain, and CaM. Taken together, these reports confirm that the CaM-dependent rearrangement of the reductase domain drives electron transfer to the heme oxygenase domain, as discussed by Xia et al. [20].

Recently, cryo-EM methods have been utilized to visualize the structure of NOS isozymes in different conformational states [35–37,184]. These reports suggest that the oxygenase domain of NOS isoforms is a homodimer, and the CaM-bound structure at starting point is initially linear, as shown in the left box of Fig. 10. Note that the reductase domains do not interact with each other, although the crystal structure of the reductase domain is a dimer [17]. By using a chemically cross-linked nNOS-CaM complex, Yokom et al. [35] presented a synchronous ET model that demonstrated that the dimer structure of the nNOS isozyme exists primarily in equilibrium with the extended (input state), intermediate, and closed (output state) states. The proposed states are very similar to those of the model proposed by Xia et al. [20]. In addition, Volkmann et al. [37] reported the synchronous ET model for eNOS isozyme, demonstrating a similar structure to the nNOS isoform that is proposed by Yokom et al. [35]. However, Campbell et al. [36] reported that for all three NOS isozymes, only a single reductase domain at a time contributes to NOS catalysis, while the other reductase domain remains in the input state or intermediate state. This data strongly suggest that the reductase domain of all three NOS isozymes do not function synchronously. Although the discrepancies between these reports are unclear, the structure in the input-output state

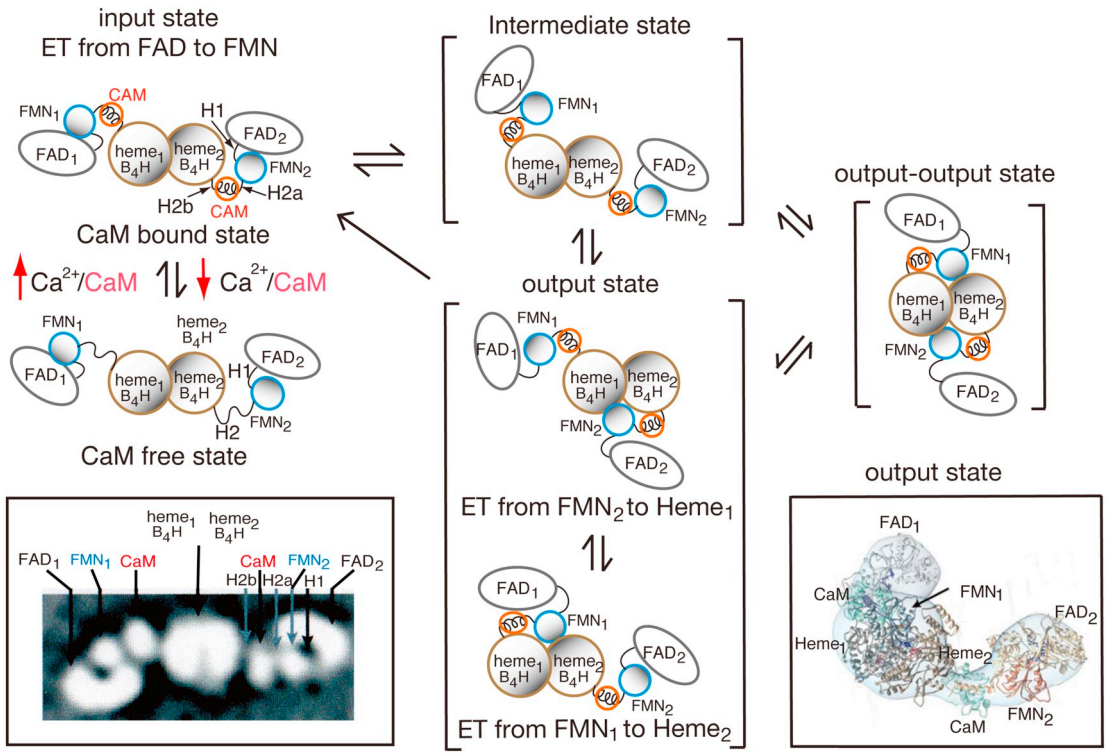

Fig. 10. Dynamic conformational model for NOS isozymes. The input state indicates ET from the FAD to FMN, while the output-state indicates ET from the FMN to the heme center. In the left box, the domain assignment of CaM-bound iNOS is shown as the example for NOS isozymes in which the FMN domain interacts with the FAD/NADPH domain. While, the right box indicates that the FMN domain docks to the oxygenase domain allowing ET from FMN_1 to $Heme_2$. The arrow (red) indicates the increase (up) or decrease (down) of Ca^{2+} concentrations. The cryoEM data of the right and left boxes were adapted from Ref. [36] with some modifications.

may be more energetically favorable than that of output-output state. All models deduced from the cryo-EM were constructed on the basis of the cross-electron transfer from the reductase of one monomer to the heme of the opposite monomer, as was already suggested by biochemical research [185]. CaM binding causes the conformational equilibrium to shift from closed (input state) to open (output state) forms, and it enables the one-electron transfer reaction from the FMN to heme center. As previously described, the cryo-EM method has demonstrated both the synchronous and nonsynchronous ET models. At present, several reports can be summarized as following (Fig. 10).

For the synchronous ET model, both oxygenase domains are simultaneously reduced by NADPH. For the nonsynchronous ET model, half of the oxygenase domain could be rapidly reduced. However, both oxygenase domains of three NOS isozymes are rapidly reduced simultaneously by NADPH, with the order of iNOS > nNOS > eNOS [186], in which the rate of flavin reduction is much faster than that of heme reduction [31]. If the rate of conversion between the two input states is faster than heme reduction, the reduction of both hemes could occur at the same time (see Fig. 3A of Ref. [187]). An alternative possibility is that an unstable output-output state that is not observed by cryo-EM is formed, in which each heme center could be reduced at the same time. However, the detailed mechanism for the reduction of both hemes remains to be explored.

All three NOS isozymes catalyse the NADPH- and oxygen-dependent conversion of L-arginine to L-citrulline and NO via two consecutive mono-oxygenation reactions (Scheme 5A). All dimeric NOS isozymes accept four electrons from 2NADPH during these reactions, and three electrons are used in the formation of L-citrulline (Cit) and NO [100], in which the first mono-oxygenation reaction (step 1) consumes two electrons, and the second mono-oxygenation reaction (step 2) consumes one electron (Scheme 5A). The FAD-$FMNH^{\bullet}$ state is formed during the priming reaction. Thus, the catalytic cycle that involves 2 × ($2e^{-}$-$1e^{-}$ pair) reactions could proceed in the following way (Scheme 5B).

However, the reductase and oxygenase domains leak electrons by an uncoupling reaction in which a superoxide radical is formed during the catalytic cycle. The nNOS isozyme is 75–80% coupled [188], whereas, eNOS isozyme is highly coupled (> 90%) [189]. Thus, the constitutive NOS isozymes are tightly coupled in the presence of L-arginine and BH_4. Meanwhile, iNOS generates the reactive oxygen species involved in killing bacteria and a highly reactive oxidant peroxynitrite, $ONOO^{-}$ is also formed from NO and superoxide ($NO + O_2^{\bullet -} \rightarrow ONOO^{-}$). By using a rapid freeze EPR technique, Berka et al. [190] demonstrated the different regulatory roles of L-arginine and BH_4. In the presence of L-arginine and BH_4, iNOS isozyme produces NO, but an uncoupling reaction occurs in the absence of L-arginine and BH_4, forming a superoxide anion. Thus, the metabolic pathways that control the level of BH_4 and L-arginine play a critical role in regulating the coupling of the three NOS isozymes catalysis and in determining the $NO/O_2^{\bullet -}$ ratio. Taken together, the electron leakage suggests that the catalytic cycle (see Scheme 5B) is not precisely maintained in vitro.

Several groups have investigated the dynamic conformational changes using the biophysical methods. Astashkin and co-workers [191] have used a pulsed EPR technique, which is sensitive to the magnetic dipole interactions. The authors constructed a nitroxide spin-labelled CaM by using an engineering method, and using the spin-labelled CaM-bound NOSoxyFMN construct of nNOS, a magnetic dipole interactions between spin-labelled CaM and low-spin heme center has been analysed [192,193]. Their results indicate that a magnetic dipole interactions are highly dynamic. Their results also indicate that the docked state (output state) for ET between FMN and heme are approx. 15% of the CaM-bound NOSoxyFMN-heme construct, while the remaining 85% of the protein exists in the unlocked conformations characterized by a wide distribution of distances between the bound CaM and heme domain. In these investigations, the FMN-CaM complex

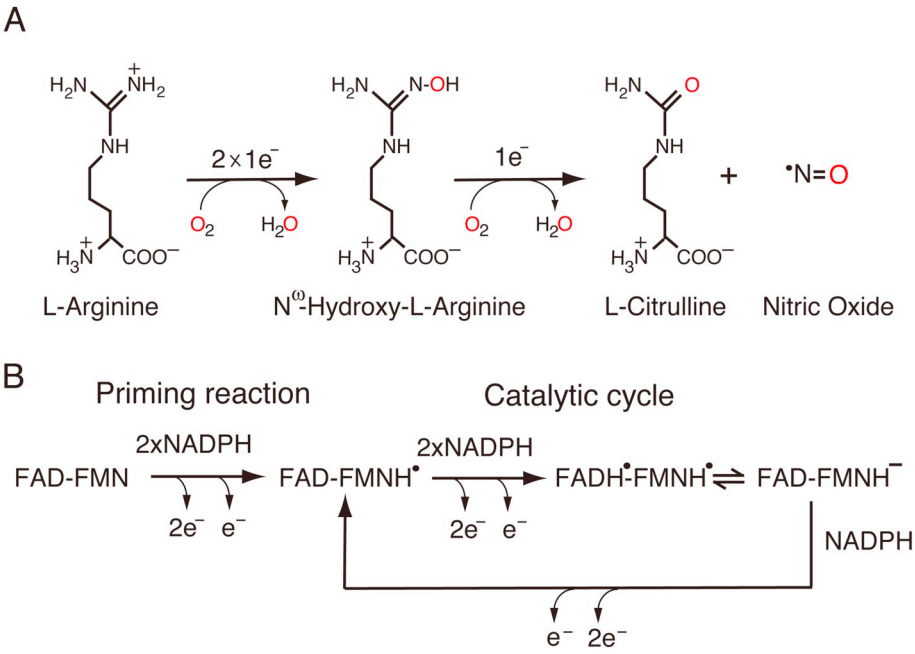

Scheme 5. (A) The two-step oxidation of L-arginine. (B) In the priming reaction, the oxidized FAD-FMN accepts four electrons from 2 × NADPH, and three electrons are consumed during first and second mono-oxygenation reactions, resulting the FAD-FMNH• intermediate. The catalytic cycle starts from the FAD-FMNH• in which 6 (2 × 3e⁻) electrons from 3 × NADPH (3 × 2e⁻) are consumed, and then backs to the starting point, FAD-FMNH•.

could switch between the FAD and FMN domains and between the FMN and heme oxygenase domains, as reported by Xia et al. [20]. In addition, Hollingsworth et al. [38] evaluated a model of the oxygenase domain-FMN-CaM by using the molecular dynamics simulation methods and provided a detailed prediction of the interdomain contacts required for stabilizing the NOS output state.

Sobolewska-Stawiarz et al. [116] have analysed a magnetic dipole interaction between the FADH• and FMNH• of the reductase domain or of holoenzyme of nNOS and suggested an exciting working hypothesis: in the absence of NADPH and CaM, the resting state (input state) adopts the multiple conformations with relatively large inter-flavin distances, and with the equilibrium shifting to shorter inter-flavin distances upon binding of NADPH, where FAD directly accepts hydride ions from NADPH. In the presence of CaM, the FMN domain has access to both the heme and FAD domains. The distances for multiple conformations range from 24 to 35 Å in solution, indicating that the structure in solution is significantly different from the crystalline structure [17]. In addition to the nNOS isozyme, cyt P450 reductase and MS reductase also range in distances from 19 to 36 Å and 27–39 Å in solution, respectively [31,106,194]. They also used the fluorescence spectroscopy methods and demonstrated that the NOS conformational landscape relates to enzyme turnover and catalysis [119].

In addition to the above approaches, Dai et al. [195] studied an internal ET rate between the NADPH/FAD and FMN domains, in which the domains are fixed by disulfide bond, as reported by Xia et al. [30]. The FMN domain movement is altered by a series of bismaleimide cross-linkers of varying lengths. The rate of interflavin ET increased by domain cross-linking, but the rate of flavin reduction became progressively slower as the cross-linker length increased. In the presence of CaM, inter-flavin ET of wild type enzymes is controlled by a combination of the rate of dynamic equilibrium between the closed and open conformations, and the distance between the FAD and FMN. Regarding cyt P450 reductase, the rate of inter-flavin ET decreases significantly in the disulfide-linked enzyme (see Section of 4.2.3).

6. Mitochondrial cyt P450 ET system

The mitochondrial steroid hydroxylating cyt P450 ET system is localized in the matrix face of the inner mitochondrial membrane [39]. The Adrenodoxin reductase (Adx reductase), Adrenodoxin (Adx) and cyt P450s are associated with this membrane. The FAD-containing Adx reductase belongs to the glutathione reductase family. Adx is an iron sulfur protein contains the [2Fe-2S] cluster as a prosthetic group and can act as a mobile one-electron carrier. Adx reductase transfers two electrons via Adx from NADPH to mitochondrial cyt P450s (Figs. 1 and 2), in which Adx is bound at the proximal surface of cyt P450s, resulting the Adx-cyt P450 complex (see Fig. 2 and Refs. [196–199]).

The midpoint reduction potential (E_m) is −292 mV at pH 7.5 for Adx reductase and −273 mV for Adx. Adx reductase forms a 1:1 complex when both proteins are in the oxidized form in which the reduction potential of Adx reductase is not altered, however, Adx's potential decreases by 40 mV when associated with Adx reductase [200], indicating the structural changes in the vicinity of the [2Fe-2S] cluster. On the other hand, the cholesterol-free cyt P450scc (CYP11A1) that catalyses the conversion of cholesterol to pregnenolone during the three sequential oxidation reactions is predominantly in the low spin form, and its reduction potential is −412 mV. The binding of cholesterol causes the conversion to a high spin form with a reduction potential of −282 mV [201] in which Adx binding promotes a complete conversion to a pure high-spin state [202]. The reduction potential of substrate-bound cyt P450scc is increased by ~130 mV, indicating that the reduction of the cholesterol-bound cyt P450scc by Adx is more favorable than that of the cholesterol-free form. Thus, the change of spin state increases the rate of first ET from reduced Adx to ferric cyt P450-substrate complex, but other factors (i.e. steric requirements and binding groups within the steroid-binding site) regulate the strength of steroid binding [203].

The crystal structure of the Adx reductase-Adx complex indicates that the [2Fe-2S] cluster of Adx and the isoalloxazine rings of FAD moiety of Adx reductase (AdxR) are ~10 Å apart, suggesting a possible electron transfer route between these redox centers [198]: the FAD isoalloxazine ring → $Ile376_{AdxR}$ → $Thr377_{AdxR}$ → $Cys52_{Adx}$. The distances between Adx and Adx reductase in solution are not substantially different from those in the crystallized complex [204]. The crystal structure of Adx-cyt P450scc complex indicates that the cyt P450scc proximal surface can accommodate only one molecule of Adx [205]. The distance between redox centers, Adx [2Fe-2S] and cyt P450 (heme) is 17.4 Å, suggesting a possible electron transfer route: $[2Fe\text{-}2S]_{Adx}$ → $Gln422_{CYP11A1}$ → Cys423CYP11A1 → heme iron, in which Adx donates electron to CYP11A1 heme (see Figs. 2 and 4B of Ref. [205]). Adx binding exerts an impact effect on the oxygen activation by cyt P450s [40].

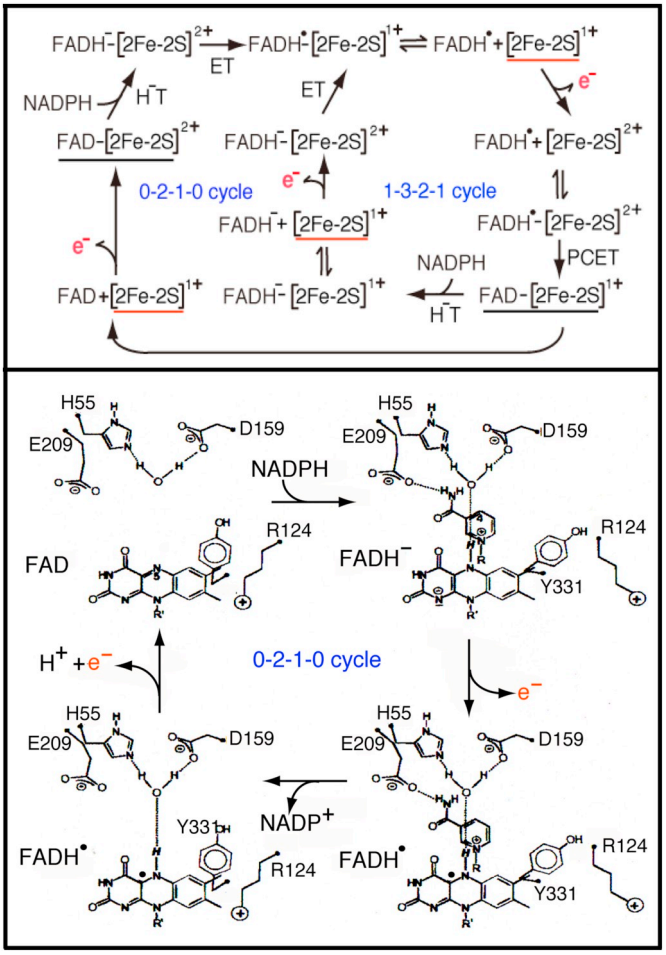

Fig. 11. Proposed catalytic cycle for the mitochondrial cyt P450 ET system. Top: the proposed catalytic 0-2-1-0 and 1-3-2-1 electron cycles. The reduced Adx, $[2Fe\text{-}2S]^{1+}$ state (red underline) that dissociates from the Adx reductase-Adx complexes can donate electrons to cyt P450. The 0-2-1-0 cycle starts from the FAD-$[2Fe\text{-}2S]^{2+}$, whereas 1-3-2-1 cycle starts from the FAD-$[2Fe\text{-}2S]^{1+}$. Bottom: the role of amino acid residues during the 0-2-1-0 catalytic cycle (see Text and Ref. [197]). Figure was adapted from Ref. [197] with some modifications.

In 2000, Ziegler and Schulz. [197] proposed a mechanism of catalytic cycle based on the structures of NADP-free Adx reductase. In the first step of enzyme reduction, a hydride ion is transferred from the C4 position of the nicotinamide ring of NADPH to the N5 position of isoalloxazine ring of FAD, resulting in the $NADP^+$-$FADH^-$ complex (Fig. 11). The $NADP^+$ binding to the reduced enzyme induces a positive shift in the redox potential, which is a driving force for the reduction of the enzyme by NADPH [206]. In the second step, the reduced form ($NADP^+$-$FADH^-$) donates electrons to Adx as a one-electron carrier, resulting in the neutral semiquinone ($FADH^•$) [206,207] which is stabilized by the hydrogen bond between its N5 atom of FAD and the water molecule that is in close contact to the central water between His (H)55 and Asp(D)159 (see bottom of Fig. 11) [197]. In the third step, $FADH^•$ transfers the second electron to the Adx molecule, in which Arg124 may accept a proton from the N5 position of isoalloxazine ring of FAD. This may be a major driving force for proton-coupled electron transfer ($FADH^• \rightarrow FAD + e^- + H^+$) in which the ET rate is lower than that of a single electron ($FADH^- \rightarrow FADH^• + e^-$) for the first electron transfer, as described in Section 7. Finally, the mitochondrial cyt P450s accepts two electrons through two sequential one-electron transfers from Adx in which molecular oxygen is activated. During the catalytic cycle, the Adx reductase-Adx complex might cycle between 1-electron reduced (FAD-$[2Fe\text{-}2S]^{1+}$) and 3-electron reduced ($FADH^-$-$[2Fe\text{-}2S]^{1+}$) states, via a two-electron intermediate ($FADH^•$-$[2Fe\text{-}2S]^{1+}$) in which two electrons are sequentially transferred to cyt P450, as previously discussed regarding cyt P450 reductase (see Fig. 5 and Ref. [206]). The 0-2-1-0 electron cycle between the oxidized (FAD-$[2Fe\text{-}2S]^{2+}$) and 2-electron reduced ($FADH^-$-$[2Fe\text{-}2S]^{2+}$) is also possible.

7. Cyt b_5 ET systems

The fatty acid desaturase family bears non-heme di-iron center [43,208], which catalyses monooxygenase reactions. The two electrons are supplied from NADH-cyt b_5 reductase/cyt b_5 system (Fig. 1). The FAD-containing cyt b_5 reductase is a member of the plant FNR family [209]. Despite their low sequence similarity, the overall structure is highly conserved. However, its redox properties are significantly different from those of the plant FNR family (see Figs. 4 and 5). The FAD semiquinone state is also significantly different from those of cyt P450 reductase, MS reductase and NOS isoforms. In addition, the adenosine moiety of the FAD folds backwards, and its isoalloxazine ring is staking between two aromatic amino acid residues, Tyr and Phe [55,210,211].

In the first step, the FAD accepts a hydride ion from NADH with concomitant production of a long-wavelength-absorbing NAD^+-reduced FAD charge-transfer complex, NAD^+-$FADH^-$, and it is oxidized through semiquinone intermediates by cyt b_5 in two one-electron transfer steps (Fig. 12). Kobayashi et al. [212] observed the conversion of the neutral semiquinone to anionic semiquinone in the presence of NAD^+ using a pulse radiolysis technique: NAD^+-$FADH^• \rightarrow NAD^+$-$FAD^{•-} + H^+$, whose p*K*a is ~6.3, which is lower than that of the free flavin p*K*a of 8.3. The stable NAD^+-bound semiquinone is the red form at physiological pH. Yamada et al. [55] recently analysed the mechanism of conversion on the basis of the high resolution X-ray of the crystal structure of porcine cyt b_5 reductase. The authors proposed that a lone pair of the Thr66 Oγ atoms that sits near the N5 atom of the isoalloxazine ring of FAD accepts a proton released from the N5 atom of the isoalloxazine ring (Fig. 12). Thus, the neutralization of the positive charge of nicotinamide by the negative charge of the anionic semiquinone form of FAD is considered to be the driving forces for the rapid conversion in the neutral to anionic semiquinone forms. In contrast, the mutant of Thr66Val mutant in which the hydroxyl group of Thr is replaced with methyl group stabilized the neutral semiquinone form, and its activities for ferricyanide and cyt b_5 (both one-electron acceptors) are nearly 9% and 4% of that of the wild type, respectively [54], suggesting that the anionic form is more active than the neutral form. It is likely that the oxidation of the neutral semiquinone associated with proton transfer is kinetically gated by the deprotonation of a semiquinone, as discussed for cyt P450 reductase (see Sections 4.2.1 and 4.2.3).

The cyt b_5 reductase-cyt b_5 complex is stabilized by an electrostatic charge between the two proteins. The docking model shows a distance of 6.58 Å between the methyl group at C8 (C8M) of the isoalloxazine ring of FAD and a heme propionate carboxylate oxygens of cyt b_5, suggesting the ET from C8M to heme [213]. While, Takaba et al. [214] reported that the N5 atom of the isoalloxazine ring of FAD is stabilized by hydrogen bonding with Tyr65 and Thr66, and this network leads to the highly conserved His49 that is located near the cyt b_5-binding site [215]. Takaba et al.[214] proposed that the ET pathway is directly along the hydrogen−bond paths (FAD-N5···Tyr65/Thr66···His49···cyt b_5). It is likely that the proton and electron transfers share the same route. In contrast, the docking model for the desaturase illustrates a possible route for ET from cyt b_5 (~0 mV) to the non-heme diiron center of desaturase (~ −30 mV [216]) [43].

Meanwhile, a novel 58-kDa flavoheme protein (NADH-cyt b_5 oxidoreductase, Ncb5or) is a fusion enzyme that contains the cyt b_5-like domain at the N-terminus and the cyt b_5 reductase-like domain at the C-terminus [217]. The two domains are connected by hinge region that has a 90-residue spacer of unique sequence. Ncb5or may be loosely

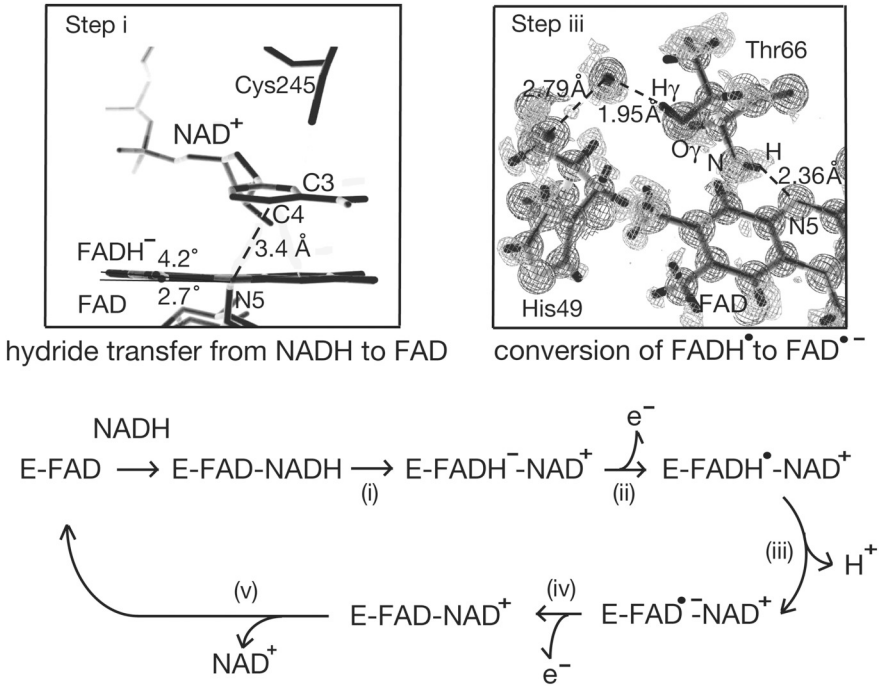

Fig. 12. Stabilization of anionic semiquinone in the NADH-cyt b_5 reductase. Figure was adapted from Refs. [54,55] with some modifications.

associated with the ER membrane, and it donates electrons to membrane-bound desaturase. The knockout mice show a defective Δ9 desaturase activity of fatty acids, suggesting that the cyt b_5-like domain can function as a one-electron carrier, and donates two electrons to desaturase [218]. Taken together, the conformational changes of the FAD-cyt b_5 pair is necessary in the ET process from NADH to desaturase, as described in the FAD-FMN pair of the P450 systems (see Section 4.2.2). Thus, the FAD-cyt b_5 pair can participate in the conversion of a two-electron donor to a one-electron acceptor. Additionally, the cyt b_5 ET system that is localized in the outer membrane of mitochondria has been reported [219]. This ET system contains three components: NADH-cyt b_5 reductase, cyt b_5, and molybdopterin-containing amidoxime-reducing component (mARC). The isoforms mARC-1 and mARC-2 are able to catalyse the reduction of nitrite, generating the nitric oxide radical (NO). In contrast, the soluble cyt b_5 reductase-cyt b_5 system donates an electron to cytoglobin, in which the ferrous cytoglobin (Fe^{2+}) can bind oxygen, resulting the oxygenated cytoglobin ($Fe^{2+}O_2$), and then oxidizes NO to nitrate ion (cytoglobin Fe^{2+}–O_2 + NO → cytoglobin Fe^{3+} + NO_3^-) oxidizes NO to nitrate [220]. These reactions provide a pathway to regulate NO concentrations in response to the oxygen tension [221]. Thereby, the cyt b_5 reductase-cyt b_5 system exhibits diverse functionality as an electron donor system.

8. Methione synthase (MS) reductase

In addition to plant FNR, a FAD-containing bacteria Fldx reductase also catalyses the reversible transfer of electrons between NADPH and Fldx or Fdx [63,65]. In *Escherichia. coli*, Fldx reductase and Fldx are physiological reducing systems in a cobalamin-dependent methionine synthesis. The overall structure of Fldx reductase is similar to that of FNR despite the low sequence similarities [209]. However, in the eukaryotic reducing system, methione synthase (MS) reductase has a similar prosthetic groups to those of cyt P450 reductase [104,222]. Thus, it has been hypothesized that a mammalian two-component system containing FAD-FMN arose from the gene fusion of FNR or Fldx reductase and Fldx (Eqs. (12) and (13)), as described for the microsomal cyt P450 ET system. The mechanism of ET is similar to that of cyt P450 reductase [223], and the similarities and differences between microsomal cyt P450 ET system and MS system have been studied extensively.

$$\text{NADPH} \rightarrow \text{Fldx reductase (FAD)} \rightarrow \text{Fldx (FMN)} \rightarrow \text{MS} - \text{cob(II)alamin} \quad (12)$$

$$\text{NADPH} \rightarrow \text{MS reductase (FAD} - \text{FMN)} \rightarrow \text{MS} - \text{cob(II)alamin} \quad (13)$$

For bacterial three-component systems (Eq. (12)), the redox potentials of Fldx reductase, E_m (FAD/$FADH^-$ couple) value for the overall two-electron reduction potential is E_m, −288 mV, and $E_{ox/sq}$, −308 mV and $E_{sq/red}$, −268 mV for the individual one-electron reduction potential, respectively, while the value for E_m (FMN/$FMNH^-$ couple) is −343 mV, and the values of $E_{ox/sq}$ and $E_{sq/red}$ for fldx (FMN) are −254 mV and −433 mV, respectively [224]. For eukaryotic two-component systems (Eq. (13)), the values of $E_{ox/sq}$ and $E_{sq/red}$ for FAD are −254 mV and −291 mV, respectively, while the values of $E_{ox/sq}$ and $E_{sq/red}$ for FMN are −109 mV and −227 mV, respectively [136] (Fig. 5). Thus, both enzymes share similar one-electron midpoint potentials, indicating conservative evolution.

Both ET systems donate electrons to inactive MS-cob(II)alamin that is occasionally formed by one-electron oxidation. In the analogy with cyt P450 reductase, the FMN of Fldx and MS reductase donates electrons to inactive MS-cob(II)alamin [136,225,226]. The cobalt of MS-cob(II)alamin is five-coordinated, of which the axial nitrogen atom is derived from the histidine (His) or the 5,6-dimethylbenzimidazole that extends from one edge of the corrin ring. The one-electron reduction potential is −500 mV for Co(I)/Co(II) couple [227]. Thus, the ET from NADPH (−320 mV) to MS-cob(II)alamin is thermodynamically unfavorable in both systems. Hoover et al. [228] proposed that the binding of Fldx to MS-cob(II)alamin results in a change in the coordination geometry of the cobalt from five-coordination to four-coordination in which one-electron reduction potential raises ~100 mV. Whereas Stich et al. [229] proposed an increase of ~250 mV on the stabilization of the $3dz_2$ orbital of the cobalt ion in the four-coordinate state. The increase in reduction potential could promote the reduction of MS-cob(II)alamin to its active state under the physiological conditions. The active MS-cob(I)alamin is methylated and this form can

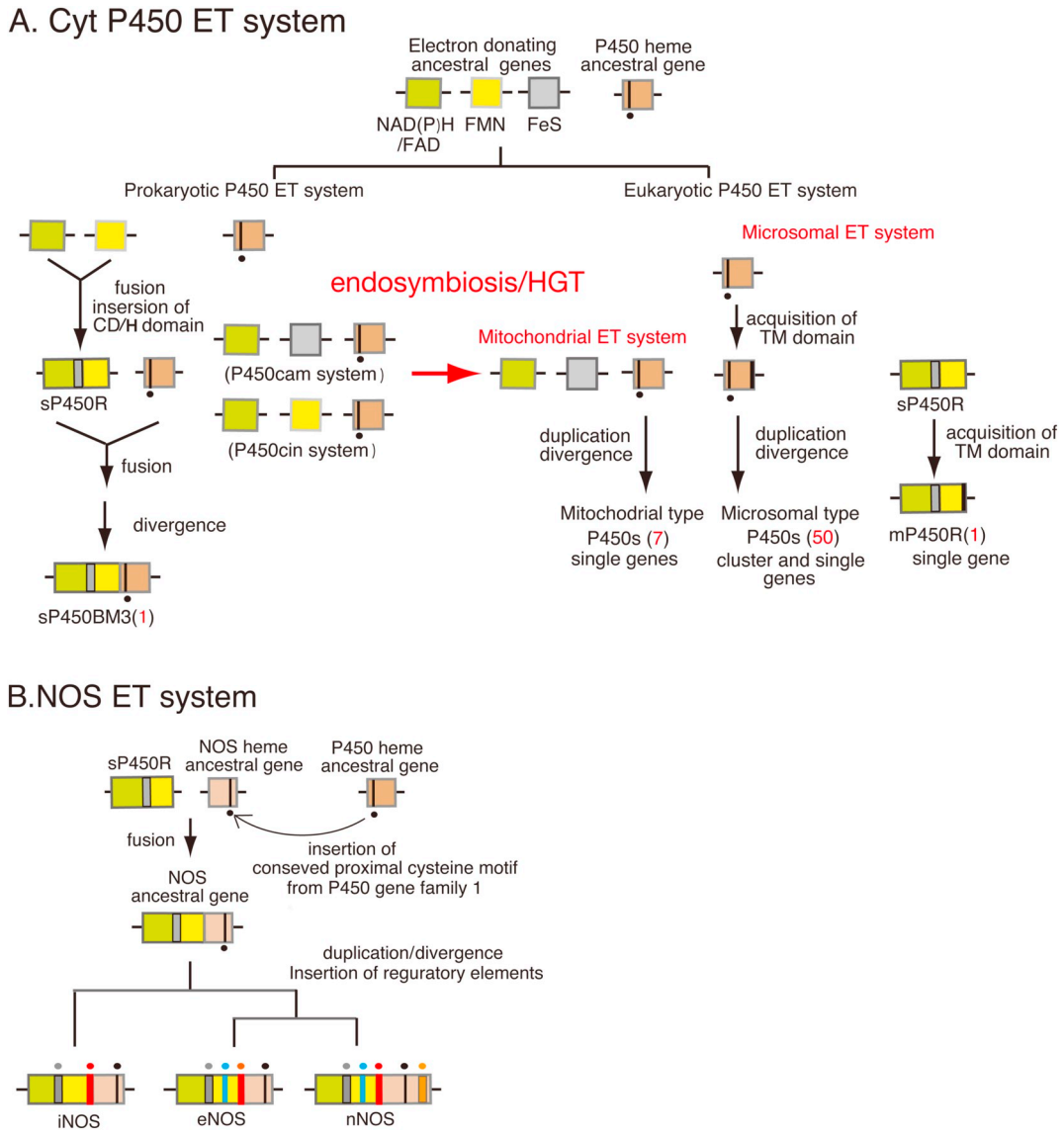

Fig. 13. A model for the evolution of functional domains in cyt P450 ET system (A) and nitric oxide synthase system (B) genes. For cyt P450 ET system (A): NAD(P)H/FAD, FMN, Fe-sulfur cluster (FeS) domain, and P450 heme indicate ancestral domains of each gene. sP450R, a soluble cyt P450 reductase; mP450R, membrane-bound cyt P450 reductase; sP450BM3, a soluble flavocytochrome P450BM3 from *Bacillus megaterium*; P450cam, cyt $P450_{CAM}$ from *Pseudomonas putida* cyt P450; $P450_{cin}$, cyt $P450_{cin}$ from *Citrobacter braakdii*. CD/H indicates the connecting (C) and hinge (H) domains. HGT, horizontal gene transfer. For cyt P450, dot indicates conserved proximal cysteine residue. The number of functional isozymes are shown as red numbers in parentheses. For the NOS ET system (B): an autoregulatory region (blue), calmodulin-binding region (red), and conserved proximal cysteine motif as the thiolate ligand (black), and PDZ domain for nNOS (orange). (A and B): All domains are arranged in order of the C-terminal (left) to the N-terminal (right). Thus, ET occurs from the electron donor, NAD(P)H to the final electron acceptor oxygenases: NAD(P)H → FAD→FMN/or [2Fe-2S] → oxygenase.

transfer the methyl group to homocysteine, forming the methionine. These reactions involve the heterolytic cleavage of the Co(III)-carbon bonds, generating the Co(I) and CH^{3+}. The paired electron of homocysteine ($R\text{-}S:^-$) shares the CH_3^+, forming the methionine ($R\text{-}CH_3$) [104].

9. Evolutionary aspects of NAD(P)H-dependent multi-domain ET systems

The NAD(P)H-dependent ET systems include a combination of multi-domain (Figs. 1, 2, 13). In both prokaryotic and eukaryotic systems, their multi-domain organizations display similarities as well as differences in their components. Thus, it is thought that the ancestral genes for these ET systems have evolved from a combination of the flavin-containing NAD(P)H-dehydrogenase, one-electron carrier, and metal-containing proteins through gene duplication and gene fusion providing a basic working for the organization of ET chains [230,231]. For origins of eukaryotic enzymes, Ku et al. [232] have proposed that a horizontal gene transfer (HGT) from bacteria to eukaryotes is primarily mediated through endosymbiosis.

The most interesting examples for the gene organization of the multi-domain ET systems are the cyt P450 ET systems [11,233] and nitric oxide synthases [4,15,234]. The evolutionary aspects of microsomal cyt P450 ET system and NOS isozymes have shed a new light on the origin of NAD(P)H-dependent ET systems. As shown in Fig. 13A and B, it is thought that the ancestor of cyt P450 ET systems and NOSs in terms of the structure and function of one-electron carriers, ferredoxin (Fdx), and flavodoxin (Fldx) may have evolved from at least four discrete genes, which encode Fdx/Fldx reductase (FAD), Fdx (2Fe-2S), Fldx (FMN) and heme-containing proteins. These genes provide the

common ancestral components for some eukaryotic ET systems. In 1996, a heme-containing archaeal cyt P450 (CYP119) gene was cloned from an acidothermophilic archaeon *S. solfataricus* [235], which shares the heme-binding conserved cysteine (C) motif, and an amino acid sequence shares 35% identical residues with the bacterium *Bacillus subtilis* cyt P450. The cyt P450 gene superfamily is likely a product of gene duplication and divergence from an ancient archaeal cyt P450 gene. The prokaryotic cyt P450 ET systems are three-component systems, consisted of NAD(P)H/FAD, Fdx (2Fe-2S)/Fldx (FMN) and cyt P450 (heme). For example, the cyt $P450_{cam}$ from *Pseudomonas putida* [236] and the cyt $P450_{cin}$ from *Citrobacter braakdii* [237] are three-component systems. The eukaryotic cyt P450 ET systems located in the inner membrane of mitochondria also contain three-components (see Section 6). Therefore, this eukaryotic system is thought to have originated from bacteria during the endosymbiosis/HGT (Fig. 13A). Recently, a soluble cyt P450 reductase from *Bacillus megaterium* was reported [41], which reveals the sequence homology to the mammalian cyt P450 reductase. These findings strongly suggest that eukaryotic multi-component NAD(P)H-dependent cyt P450 ET systems was acquired by endosymbiosis/HGT from bacteria. Unlike the mitochondrial cyt P450 ET system, the microsomal cyt P450 system is a two-component system in which cyt P450 reductase is a multi-domain enzyme. This is a fusion enzyme derived from a FNR-like and Fldx-like flavoproteins, but the fldx-like FMN protein is not found in eukaryotic cells [238]. Knowing this information, it is of evolutionary interest that cyt P450 reductase selects an Fldx as a one-electron carrier, rather than an Fdx, suggesting that Fldx is more efficient as a partner with the FAD domain (see Fig. 13A). The human cyt P450 reductase is encoded by a single gene located on 7q11.2 [239], whereas its partner cyt P450s are encoded by distinct genes. Knowing whether exons encode the functional units or structural units in these proteins is of interest. The cyt P450 reductase gene comprises 16 exons; the membrane binding regions (as 1–60) is encoded by exon 2, and exon 3 encodes as 61–76, which links the membrane binding domain and the FMN domain. The exons 4–7 encode the FMN-binding domain, and exons 8–16 encode the FAD/NADPH-binding domain [240]. A soluble mammalian MS reductase (FAD-FMN) shares the same cofactors as a cyt P450 reductase (see Section 8). The positions of several junctions of human gene that comprises 15 exons are conserved. This is also true for the cyt P450 reductase gene, but its gene lacks the membrane-binding anchor exon [241]. Consequently, the microsomal P450 ET system has acquired the membrane-binding anchor exon. A typical oxidative Phase I cyt P450 reductase/cyt P450 system is localized on the cytosolic side of the ER membrane, whereas conjugative Phase II UDP-glucuronosyltransferases (UGTs) are localized on the luminal side [23]. Thus, the cyt P450 ET system and UGT are effectively coupled in the biotransformations of small exogenous and endogenous compounds. This causes the question why both systems are localized in the different compartment. In addition, UGT system requires the transport of UDP-glucuronic acid from the cytosolic side to luminal side [23,242]. Detailed evolutionally explanation for these questions remains unclear.

The NOS reductase domain shares a structural similarity to cyt P450 reductase [12,17]. The heme-containing bacterial nitric-oxide synthases (bNOSs) lack an essential reductase domain. However, the structure of bNOS is similar to those of mammalian NOSs, and its dimer form produces NO in the presence of an electron donor system such as NADPH-flavodoxin reductase (FAD) and flavodoxin (FMN) [243]. This suggests that bNOS is an early precursor to eukaryotic NOS and that it acquired the reductase domain later in evolution [244]. The oxygenase domain was acquired by endosymbiosis/HGT from bacteria, and the reductase domain of three NOS isozymes shares a bacterial cyt P450 reductase- or sulfite reductase-like domains, suggesting that a mammalian NOS reductase domain was evolved from a bacterial diflavin reductase acquired from the proto-mitochondrial endosymbiont [245]. A comparative analysis of the intron splice location for the rat cyt P450 reductase and the human NOS genes suggests that the location and size of exons/introns in the three human NOS genes are similar to each other. Therefore, the three human NOS genes are derived from a common ancestor by duplication [246]. However, NOS isozymes are distributed on different chromosomes, 12q24.2 for nNOS (NOS I), 17q11.2 for iNOS (NOS II) and 7q36 for eNOS (NOS III). After the duplication of a common ancestral gene, NOS isoforms acquired the regulatory elements within its gene (Fig. 13B). The CaM binding motif is inserted between the FMN and heme domains. The autoregulatory motif is inserted within FMN domain of nNOS and eNOS, but iNOS does not contain this motif. The CaM act as a precise conformational switch for a one-electron transfer reaction from FMN to the oxygenase domain (see Fig. 10). However, the oxygenase domains of NOS isoforms do not reveal any sequence homology with known cyt P450s, although they share a common cysteine residue as the proximal thiol ligand [247]. This suggests that the origin of the NOS oxygenase domain may be different from those of microsomal or mitochondrial cyt P450. However, the heme domains for the bacterial and mammalian NOS isoforms share a sequence motif, (R/K)**C**(I/V)G in the conserved proximal cysteine residues, which is found in the cyt P450 gene family 1 [248,249]. Although its detailed mechanism is unknown, the NOS oxygenase domain might have acquired this motif from a member of the cyt P450 family 1 through an intergenetic gene conversion (see Fig. 13B). The NOS system acquired a CaM binding site for the regulation of ET. $P450_{BM3}$ (CYP102A1) from *B. megaterium* is a single peptide enzyme, which shares cyt P450 reductase-like and cyt P450-like domains [250], and a dimer is its active form [47,48]. Thus, this system has evolved through the fusion of cyt P450 and cyt P450 reductase genes. An another interesting example is that the P450 ET system is present in the plants, but NOS isozymes are not present in the land plants, although NOSs are present in a few algal species. The question of how NO is produced in plants is interesting subject. A possible hypothesis has been discussed by Jeandroz et al. [251]: (i) vertical gene transmission from a eukaryotic ancestor before the separation of the eukaryotic supergroups, followed by gene loss in some lineages, including all land plants; (ii) acquisition by horizontal gene transfer (HGT) in algal lineages (the losses or gains of NOS encoding genes in the plants). In plants, nitrate assimilation consists of two reactions: nitrate reduction and nitrite reduction. These reactions are catalyzed by NAD(P)H-dependent nitrate reductase, which includes the two redox centers, containing a FAD-heme, and a molybdopterin [252]. The former center shares sequence homology with cyt b_5 reductase and cyt b_5, respectively. The NO is produced by the reduction of nitrite at the molybdopterin active site ($NO_2^- + e^- + 2H^+ \rightarrow NO + H_2O$) [253]. Thus, land plants seem to have evolved a finely regulated single component nitrate reductase. On the other hand, mammal mitochondrial mARC-1/2 systems are composed of three components, as described in Section 7. These suggest that the plant nitrate reductase is a fusion enzyme consisting of cyt b_5 reductase (FAD), cyt b_5 (heme) and molybdopterin binding protein.

The microsomal cyt b_5 and the cyt P450 reductase ET systems can donate electrons to several metabolic electron acceptors [254], in which both the cyt b_5 and FMN domains of cyt P450 reductase can act as a multi-functional one-electron donor sites, suggesting that the interfaces of the cyt b_5 and the FMN domain have evolved to interact with several electron acceptors. While, mammal cyt P450s are localized in both microsomes and mitochondria, and they share a similar structures. In plants and fungi, cyt P450s are localized in the ER, but mitochondrial cyt P450 has yet to be reported [255]. These reports suggest that a microsomal cyt P450 is an ancestor of animal mitochondrial cyt P450, in which the ER-targeting sequence of a microsomal cyt P450 is converted to a mitochondrial-targeting sequence. Meanwhile, cyt b_5 reductase is encoded by a single gene located on chromosome 22q13.2-q13.31 [256]. Thus, microsomal and mitochondrial cyt b_5 ET systems share the same proteins, but their partner is different (see Section 7). These ET systems have acquired a functional diversity over the course of the evolution of animals. Taken together, the microsomal and

mitochondrial cyt P450s have evolved synergistically for the biosynthesis of endobiotics, such as steroid hormones and vitamin D. These metabolic ET networks raise the question of how specific protein-protein interactions are acquired.

Regarding the metabolic functions, the prokaryotic cyt P450s generally exhibit a high substrate specificity and activity, while the eukaryotic microsomal P450 systems display broad, overlapping substrate specificities and low activity [23]; this indicates that highly plastic active sites accommodate a wide variety of substrates as compared to bacterial cyt P450s. On the other hand, the prokaryotic cyt P450 ET systems utilize the substrates as an energy source in where a high catalytic activity is needed, but eukaryotic cyt P450 ET system is not necessarily the case. As described in Section, 4.2.1, the anionic FMN semiquinone can donate electrons effectively to the heme center. Although a cyt P450 reductase is the product of a single gene in animal cells, it can donate electrons to ~50 microsomal cyt P450 isoforms in which most conserved residues are found at the functional interface residues between the FMN domain of cyt P450 reductase and cyt P450s, but the diversity of cyt P450 isoforms is associated with changes in the substrate specificity. This raises serious question in that a defect of single cyt P450 reductase affects in the function of all microsomal cyt P450 isoforms, including three steroidogenic microsomal cyt P450s [4]. In contrast, a mitochondrial cyt P450 ET system can donate an electron to seven cyt P450 isoforms, which all have high substrate specificity. Meanwhile, the rate of NAD(P)H supply modulates the substrate oxidation by the NAD(P)H-dependent cyt P450 ET systems in intact cells [22,23,257].

Finally, the NAD(P)H-dependent ET systems have been adapted in the diverse metabolic pathways during the processes of evolution. The fittest genes for metabolic NAD(P)H-dependent ET systems may be the result of the relentless shuffling, mixing and recombination of genes that encode the diversity of prokaryote-eukaryote redox enzymes [232–234,258]. The NAD(P)H-dependent ET systems (Fig. 13) are the products of natural evolution, but the direct laboratory evolution [259] could throw new light on the origin of structure and function of the multi-domain enzyme systems.

Conflict interest

The author has no conflicts of interest to declare.

Transparency document

The Transparency document associated with this article can be found, in online version.

Acknowledgements

The author thanks Drs. Chuanwu Xia and Jung-Ja Kim (Medical College of Wisconsin, USA) for the construction of Fig. 2. The author also thanks Dr. Jung-Ja Kim and the reviewers for his/her critical and helpful comments.

References

[1] L. Michaelis, Theory of the reversible two-step oxidation, J. Biol. Chem. 96 (1932) 703–715.
[2] U. Deichmann, S. Schuster, J.P. Mazat, A. Cornish-Bowden, Commemorating the 1913 Michaelis–Menten paper Die Kinetik der Invertinwirkung: three perspectives, FEBS J. 281 (2014) 435–463.
[3] T. Iyanagi, S. Watanabe, K.F. Anan, One-electron oxidation-reduction properties of hepatic NADH-cytochrome b5 reductase, Biochemistry 23 (1984) 1418–1425.
[4] T. Iyanagi, C. Xia, J.J. Kim, NADPH-cytochrome P450 oxidoreductase:prototypic member of the diflavin reductase family, Arch. Biochem. Biophys. 528 (2012) 72–89.
[5] T. Iyanagi, N. Makino, H.S. Mason, Redox properties of the reduced nicotinamide adenine dinucleotide phosphate-cytochrome P-450 and reduced nicotinamide adenine dinucleotide-cytochrome b_5 reductases, Biochemistry 13 (1974) 1701–1710.
[6] T. Iyanagi, R. Makino, F.K. Anan, Studies on the microsomal mixed-function oxidase system: mechanism of action of hepatic NADPH-cytochrome P-450 reductase, Biochemistry 20 (1981) 1722–1730.
[7] T. Omura, E. Sanders, R.W. Estabrook, D.Y. Cooper, O. Rosenthal, Isolation from adrenal cortex of a nonheme iron protein and a flavoprotein functional as a reduced triphosphopyridine nucleotide-cytochrome P-450 reductase, Arch. Biochem. Biophys. 117 (1966) 660–673.
[8] T. Omura, Pioneers in the early years of cytochrome P450 research, in: H. Yamazaki (Ed.), In Fifty Years of Cytochrome P450 Research, Springer, Japan, 2014, pp. 3–16.
[9] T. Iyanagi, H.S. Mason, Some properties of hepatic reduced nicotinamide adenine dinucleotide phosphate-cytochrome *c* reductase, Biochemistry 12 (1973) 2297–2308.
[10] J.L. Vermilion, D.P. Ballou, V. Massey, M.J. Coon, Separate roles for FMN and FAD in catalysis by liver microsomal NADPH-cytochrome P-450 reductase, J. Biol. Chem. 256 (1981) 266–277.
[11] T.D. Porter, C.B. Kasper, NADPH-cytochrome P-450 oxidoreductase: flavin mononucleotide and flavin adenine dinucleotide domains evolved from different flavoproteins, Biochemistry 25 (1986) 1682–1687.
[12] M. Wang, D.L. Roberts, R. Paschke, T.M. Shea, B.S.S. Masters, J.J.P. Kim, Three-dimensional structure of NADPH-cytochrome P450 reductase: prototype for FMN- and FAD-containing enzymes, Proc. Natl. Acad. Sci. U. S. A. 94 (1997) 8411–8416.
[13] M. Haniu, T. Iyanagi, P. Miller, T.D. Lee, J.E. Shively, Complete amino acid sequence of NADPH-cytochrome P-450 reductase from porcine hepatic microsomes, Biochemistry 25 (1986) 7906–7911.
[14] A.W. Munro, M.A. Noble, L. Robledo, S.N. Daff, S.K. Chapman, Determination of the redox properties of human NADPH-cytochrome P450 reductase, Biochemistry 40 (2001) 1956–1963.
[15] D.S. Bredt, P.M. Hwang, C.E. Glatt, C. Lowenstein, R.R. Reed, S.H. Snyder, Cloned and expressed nitric oxide synthase structurally resembles cytochrome P-450 reductase, Nature 351 (1991) 714–718.
[16] D.J. Stuehr, M. Ikeda-Saito, Spectral characterization of brain and macrophage nitric oxide synthases. Cytochrome P-450-like hemeproteins that contain a flavin semiquinone radical, J. Biol. Chem. 267 (1992) 20547–20550.
[17] E.D. Garcin, C.M. Bruns, S.J. Lloyd, D.J. Hosfield, M. Tiso, R. Gachhui, D.J. Stuehr, J.A. Tainer, E.D. Getzoff, Structural basis for isozyme-specific regulation of electron transfer in nitric-oxide synthase, J. Biol. Chem. 279 (2004) 37918–37927.
[18] W.K. Alderton, C.E. Cooper, R.G. Knowles, Nitric oxide synthases: structure, function and inhibition, Biochem. J. 357 (2001) 593–615.
[19] L.J. Roman, P. Martásek, B.S.S. Masters, Intrinsic and extrinsic modulation of nitric oxide synthase activity, Chem. Rev. 102 (2002) 1179–1190.
[20] C. Xia, I. Misra, T. Iyanagi, J.J.P. Kim, Regulation of interdomain interactions by calmodulin in inducible nitric-oxide synthase, J. Biol. Chem. 284 (2009) 30708–30717.
[21] M.B. Murataliev, R. Feyereisen, F.A. Walker, Electron transfer by diflavin reductases, Biochim. Biophys. Acta 1698 (2004) 1–26.
[22] T. Iyanagi, Structure and function of NADPH-cytochrome P450 reductase and nitric oxide synthase reductase domain, Biochem. Biophys. Res. Commun. 338 (2005) 520–528.
[23] T. Iyanagi, Molecular mechanism of phase I and phase II drug-metabolizing enzymes: implications for detoxification, Int. Rev. Cytol. 260 (2007) 35–112.
[24] S. Daff, NO synthase: structures and mechanisms, Nitric Oxide 23 (2010) 1–11.
[25] C. Feng, Mechanism of nitric oxide synthase regulation: electron transfer and interdomain interactions, Coord. Chem. Rev. 256 (2012) 393–411.
[26] L. Waskell, J.J.P. Kim, Electron transfer partners of cytochrome P450, in: Paul R. Ortiz de Montellano (Ed.), Cytochrome P450, 5th edition, Springer International Publishing, Switzerland, 2015, pp. 33–68.
[27] P. Hlavica, Mechanistic basis of electron transfer to cytochromes P450 by natural redox partners and artificial donor constructs, in: E.G. Hrycay, S.M. Bandiera (Eds.), In Monooxygenase, Peroxidase and Peroxygenase Properties and Mechanisms of Cytochrome P450, Advances in Experimental Medicine and Biology 851, Springer International Publishing, Switzerland, 2015, pp. 247–297.
[28] D. Hamdane, C. Xia, S.C. Im, H. Zhang, J.J.P. Kim, L. Waskell, Structure and function of an NADPH-cytochrome P450 oxidoreductase in an open conformation capable of reducing cytochrome P450, J. Biol. Chem. 284 (2009) 11374–11384.
[29] A. Welland, S. Daff, Conformation-dependent hydride transfer in neuronal nitric oxide synthase reductase domain, FEBS J. 277 (2010) 3833–3834.
[30] C. Xia, D. Hamdane, A.L. Shen, V. Choi, C.B. Kasper, N.M. Pearl, H. Zhang, S. Im, L. Waskell, J.J. Kim, Conformational changes of NADPH-cytochrome P450 oxidoreductase are essential for catalysis and cofactor binding, J. Biol. Chem. 286 (2011) 16246–16260.
[31] N.G. Leferink, S. Hay, S.E. Rigby, N.S. Scrutton, Towards the free energy landscape for catalysis in mammalian nitric oxide synthases, FEBS J. 282 (2015) 3016–3029.
[32] W.C. Huang, J. Ellis, P.C. Moody, E.L. Raven, G.C. Roberts, Redox-linked domain movements in the catalytic cycle of cytochrome *p*450 reductase, Structure 21 (2013) 1581–1589.
[33] H. Li, A. Das, H. Sibhatu, J. Jamal, S.G. Sligar, T.L. Poulos, Exploring the electron transfer properties of neuronal nitric-oxide synthase by reversal of the FMN redox potential, J. Biol. Chem. 283 (2008) 34762–34772.
[34] F. Rwere, C. Xia, S. Im, M.M. Haque, D.J. Stuehr, L. Waskell, J.J.P. Kim, Mutants of cytochrome P450 reductase lacking either Gly-141 or Gly-143 destabilize its FMN semiquinone, J. Biol. Chem. 291 (2016) 14639–14661.
[35] A.L. Yokom, Y. Morishima, M. Lau, M. Su, A. Glukhova, Y. Osawa, D.R. Southworth, Architecture of the nitric-oxide synthase holoenzyme reveals large conformational changes and a calmodulin-driven release of the FMN domain, J. Biol. Chem. 289 (2014) 16855–16865.

[36] M.G. Campbell, B.C. Smith, C.S. Potter, B. Carragher, M.A. Marletta, Molecular architecture of mammalian nitric oxide synthases, Proc. Natl. Acad. Sci. U. S. A. 111 (2014) E3614–E3623.

[37] N. Volkmann, P. Martásek, L.J. Roman, X. Xu, C. Page, M. Swift, D. Hanein, B.S. Masters, Holoenzyme structures of endothelial nitric oxide synthase—an allosteric role for calmodulin in pivoting the FMN domain for electron transfer, J. Struct. Biol. 188 (2014) 46–54.

[38] S.A. Hollingsworth, J.K. Holden, H. Li, T.L. Poulos, Elucidating nitric oxide synthase domain interactions by molecular dynamics, Protein Sci. 25 (2016) 374–382.

[39] I. Hanukoglu, Conservation of the enzyme–coenzyme interfaces in FAD and NADP binding adrenodoxin reductase — a ubiquitous enzyme, J. Mol. Evol. 85 (2017) 205–218.

[40] Q. Zhu, P.J. Mak, R.C. Tuckey, J.R. Kincaid, Active site structures of CYP11A1 in the presence of its physiological substrates and alterations upon binding of adrenodoxin, Biochemistry 56 (2017) 5786–5797.

[41] M. Milhim, A. Gerber, J. Neunzig, F. Hannemann, R. Bernhardt, A. Novel, NADPH-dependent flavoprotein reductase from *Bacillus megaterium* acts as an efficient cytochrome P450 reductase, J. Biotechnol. 231 (2016) 83–94.

[42] H.G. Enoch, A. Catala, P. Strittmatter, Mechanism of rat liver microsomal stearyl-CoA desaturase, studies of the substrate specificity, enzyme-substrate interactions, and the function of lipid, J. Biol. Chem. 251 (1976) 5095–5103.

[43] Y. Bai, J.G. McCoy, E.J. Levin, P. Sobrado, K.R. Rajashankar, B.G. Fox, M. Zhou, X-ray structure of a mammalian stearoyl-CoA desaturase, Nature 524 (2015) 252–256.

[44] K. Larade, Z. Jiang, Y. Zhang, W. Wang, S. Bonner-Weir, H. Zhu, H.F. Bunn, Loss of Ncb5or results in impaired fatty acid desaturation, lipoatrophy, and diabetes, J. Biol. Chem. 283 (2008) 29285–29291.

[45] M.A. Marletta, A.R. Hurshman, K.M. Rusche, Catalysis by nitric oxide synthase, Curr. Opin. Chem. Biol. 2 (1998) 656–663.

[46] D.J. Stuehr, Catalysis by nitric oxide synthase, Biochim. Biophys. Acta 1411 (1999) 217–230.

[47] T. Kitazume, D.C. Haines, R.W. Estabrook, B. Chen, J.A. Peterson, Obligatory intermolecular electron-transfer from FAD to FMN in dimeric P450BM-3, Biochemistry 46 (2007) 11892–11901.

[48] H. Zhang, A.L. Yokom, S. Cheng, M. Su, P.F. Hollenberg, D.R. Southworth, Y. Osawa, The full-length cytochrome P450 enzyme CYP102A1 dimerizes at its reductase domains and has flexible heme domains for efficient catalysis, J. Biol. Chem. 293 (2018) 7727–7736.

[49] J. Tejero, J.R. Peregrina, M. Martínez-Júlvez, A. Gutiérrez, C. Gomez-Moreno, N.S. Scrutton, M. Medina, Catalytic mechanism of hydride transfer between $NADP^+$/H and ferredoxin-$NADP^+$ reductase from *Anabaena* PCC 7119, Arch. Biochem. Biophys. 459 (2007) 79–90.

[50] Q. Bashir, S. Scanu, M. Ubbink, Dynamics in electron transfer protein complexes, FEBS J. 278 (2011) 1391–1400.

[51] S.L. Tan, R.D. Webster, Electrochemically induced chemically reversible proton-coupled electron transfer reactions of riboflavin (vitamin B2), J. Am. Chem. Soc. 134 (2012) 5954–5964.

[52] S.G. Mayhew, The effects of pH and semiquinone formation on the oxidation–reduction potentials of flavin mononucleotide, Eur. J. Biochem. 265 (1999) 698–702.

[53] H. Ishikita, K. Saito, Proton transfer reactions and hydrogen-bond networks in protein environments, Interface 11 (2014), https://doi.org/10.1098/rsif.2013.0518.

[54] S. Kimura, M. Kawamura, T. Iyanagi, Role of Thr(66) in porcine NADH-cytochrome *b*5 reductase in catalysis and control of the rate-limiting step in electron transfer, J. Biol. Chem. 278 (2003) 3580–3589.

[55] M. Yamada, T. Tamada, K. Takeda, F. Matsumoto, H. Ohno, M. Kosugi, K. Takaba, Y. Shoyama, S. Kimura, R. Kuroki, K. Miki, Elucidations of the catalytic cycle of NADH-cytochrome *b*5 reductase by X-ray crystallography: new insights into regulation of efficient electron transfer, J. Mol. Biol. 425 (2013) 4295–4306.

[56] T. Iyanagi, F.K. Anan, Y. Imai, H.S. Mason, Studies on the microsomal mixed function oxidase system: redox properties of detergent-solubilized NADPH-cytochrome P-450 reductase, Biochemistry 17 (1978) 2224–2230.

[57] A.K. Samhan-Arias, R.M. Almeida, S. Ramos, C.M. Cordas, I. Moura, C. Gutierrez-Merino, J.J. Moura, Topography of human cytochrome *b*5/cytochrome *b*5 reductase interacting domain and redox alterations upon complex formation, Biochim. Biophys. Acta Bioenerg. 1859 (2018) 78–87.

[58] T. Ravula, C. Barnaba, M. Mahajan, G.M. Anantharamaiah, S.C. Im, L. Waskell, A. Ramamoorthy, Membrane environment drives cytochrome P450's spin transition and its interaction with cytochrome *b*5, Chem. Commun. 53 (2017) 12798–12,801.

[59] I. Yamazaki, T. Ohnishi, One-electron-transfer reactions in biochemical systems I. Kinetic analysis of the oxidation-reduction equilibrium between quinol-quinone and ferro-ferricytochrome *c*, Biochim. Biophys. Acta, Biophys. Incl. Photosynth. 112 (1966) 469–481.

[60] R.F. Anderson, Energetics of the one-electron reduction steps of riboflavin, FMN and FAD to their fully reduced forms, Biochim. Biophys. Acta Bioenerg. 722 (1983) 158–162.

[61] Y. Sawada, T. Iyanagi, I. Yamazaki, Relation between redox potentials and rate constants in reactions coupled with the system oxygen-superoxide, Biochemistry 14 (1975) 3761–3764.

[62] T. Iyanagi, On the mechanism of one-electron reduction of quinones by microsomal flavin enzymes: the kinetic analysis between cytochrome B5 and menadione, Free Radic. Res. Commun. 8 (1990) 259–268.

[63] M. Medina, Structural and mechanistic aspects of flavoproteins: photosynthetic electron transfer from photosystem I to $NADP^+$, FEBS J. 276 (2009) 3942–3958.

[64] K.M. Kean, R.A. Carpenter, V. Pandini, G. Zanetti, A.R. Hall, R. Faber, A. Aliverti, P.A. Karplus, High-resolution studies of hydride transfer in the ferredoxin: $NADP^+$ reductase superfamily, FEBS J. 284 (2017) 3302–3319.

[65] S. Saen-oon, I.C. de Vaca, D. Masone, M. Medina, V. Guallar, A theoretical multiscale treatment of protein–protein electron transfer: the ferredoxin/ferredoxin-$NADP^+$ reductase and flavodoxin/ferredoxin-$NADP^+$ reductase systems, Biochim. Biophys. Acta Bioenerg. 1847 (2015) 1530–1538.

[66] A. Aliverti, V. Pandini, A. Pennati, M. de Rosa, G. Zanetti, Structural and functional diversity of ferredoxin-NADP+ reductases, Arch. Biochem. Biophys. 474 (2008) 283–291.

[67] O. Dym, D. Eisenberg, Sequence-structure analysis of FAD-containing proteins, Protein Sci. 10 (2001) 1712–1728.

[68] I. Lans, M. Medina, E. Rosta, G. Hummer, M. García-Viloca, J.M. Lluch, A. González-Lafont, Theoretical study of the mechanism of the hydride transfer between ferredoxin-NADP+ reductase and $NADP^+$: the role of Tyr303, J. Am. Chem. Soc. 134 (2012) 20544–20553.

[69] M.E. Corrado, A. Aliverti, G. Zanetti, S.G. Mayhew, Analysis of the oxidation–reduction potentials of recombinant ferredoxin–$NADP^+$ reductase from spinach chloroplasts, Eur. J. Biochem. 239 (1996) 662–667.

[70] P. Sétif, R. Mutoh, G. Kurisu, Dynamics and energetics of cyanobacterial photosystem I: Ferredoxin complexes in different redox states, Biochim. Biophys. Acta 1858 (2017) 483–496.

[71] C.J. Batie, H. Kamin, The relation of pH and oxidation-reduction potential to the association state of the ferredoxin. Ferredoxin: $NADP^+$ reductase complex, J. Biol. Chem. 256 (1981) 7756–7763.

[72] I. Nogués, J. Tejero, J.K. Hurley, D. Paladini, S. Frago, G. Tollin, S.G. Mayhew, G. Gomez-Moreno, E.A. Ceccarelli, N. Carrillo, M. Medina, Role of the C-terminal tyrosine of ferredoxin-nicotinamide adenine dinucleotide phosphate reductase in the electron transfer processes with its protein partners ferredoxin and flavodoxin, Biochemistry 43 (2004) 6127–6137.

[73] J. Tejero, I. Pérez-Dorado, C. Maya, M. Martínez-Júlvez, J. Sanz-Aparicio, C. Gómez-Moreno, J.A. Hemoso, M. Medina, C-Terminal tyrosine of ferredoxin $NADP^+$ reductase in hydride transfer processes with NAD (P) /H, Biochemistry 44 (2005) 13477–13490.

[74] C.J. Batie, H. Kamin, Association of ferredoxin-$NADP^+$ reductase with NADP (H) specificity and oxidation-reduction properties, J. Biol. Chem. 261 (1986) 11214–11223.

[75] R.P. Swenson, G.D. Krey, Site-directed mutagenesis of tyrosine-98 in the flavodoxin from *Desulfovibrio vulgaris* (Hildenborough): regulation of oxidation-reduction properties of the bound FMN cofactor by aromatic, solvent, and electrostatic interactions, Biochemistry 33 (1994) 8505–8514.

[76] H. Ishikita, Influence of the protein environment on the redox potentials of flavodoxins from *Clostridium beijerinckii*, J. Biol. Chem. 282 (2007) 25240–25246.

[77] L.H. Bradley, R.P. Swenson, Role of glutamate-59 hydrogen bonded to N (3) H of the flavin mononucleotide cofactor in the modulation of the redox potentials of the *Clostridium beijerinckii* flavodoxin. Glutamate-59 is not responsible for the pH dependency but contributes to the stabilization of the flavin semiquinone, Biochemistry 38 (1999) 12377–12386.

[78] F.C. Chang, L.H. Bradley, R.P. Swenson, Evaluation of the hydrogen bonding interactions and their effects on the oxidation-reduction potentials for the riboflavin complex of the *Desulfovibrio vulgaris* flavodoxin, Biochim. Biophys. Acta Bioenerg. 1504 (2001) 319–328.

[79] M. Martínez-Júlvez, M. Medina, C. Gómez-Moreno, Ferredoxin-$NADP^+$ reductase uses the same site for the interaction with ferredoxin and flavodoxin, J. Biol. Inorg. Chem. 4 (1999) 568–578.

[80] G. Kurisu, M. Kusunoki, E. Katoh, T. Yamazaki, K. Teshima, Y. Onda, Y. Kimata-Ariga, T. Hase, Structure of the electron transfer complex between ferredoxin and ferredoxin-NADP(+) reductase, Nat. Struct. Biol. 8 (2001) 117–121.

[81] M. Medina, R. Abagyan, C. Gómez-Moreno, J. Fernandez-Recio, Docking analysis of transient complexes: interaction of ferredoxin-$NADP^+$ reductase with ferredoxin and flavodoxin, Proteins 72 (2008) 848–862.

[82] C.H. Williams, H. Kamin, Microsomal triphosphopyridine nucleotide-cytochrome *c* reductase of liver, J. Biol. Chem. 237 (1962) 587–595.

[83] K. Ichihara, E. Kusunose, M. Kusunose, Some properties of NADPH-cytochrome *c* reductase reconstitutively active in fatty-acid ω-hydroxylation, Eur. J. Biochem. 38 (1973) 463–472.

[84] Z.W. Guan, D. Kamatani, S. Kimura, T. Iyanagi, Mechanistic studies on the intramolecular one-electron transfer between the two flavins in the human neuronal nitric-oxide synthase and inducible nitric-oxide synthase flavin domains, J. Biol. Chem. 278 (2003) 30859–30868.

[85] K. Yamamoto, S. Kimura, Y. Shiro, T. Iyanagi, Interflavin one-electron transfer in the inducible nitric oxide synthase reductase domain and NADPH-cytochrome P450 reductase, Arch. Biochem. Biophys. 440 (2005) 65–78.

[86] Y. Nishino, K. Yamamoto, S. Kimura, A. Kikuchi, Y. Shiro, T. Iyanagi, Mechanistic studies on the intramolecular one-electron transfer between the two flavins in the human endothelial NOS reductase domain, Arch. Biochem. Biophys. 465 (2007) 254–265.

[87] Z.W. Guan, T. Iyanagi, Electron transfer is activated by calmodulin in the flavin domain of human neuronal nitric oxide synthase, Arch. Biochem. Biophys. 412 (2003) 65–76.

[88] R. Neeli, O. Roitel, N.S. Scrutton, A.W. Munro, Switching pyridine nucleotide specificity in P450BM3 mechanistic analysis of the W1046H and W1046A enzymes, J. Biol. Chem. 280 (2005) 17634–17644.

[89] A.J. Dunford, H.M. Girvan, N.S. Scrutton, A.W. Munro, Probing the molecular determinants of coenzyme selectivity in the P450BM3 FAD/NADPH domain,

Biochim. Biophys. Acta, Proteins Proteomics 1794 (2009) 1181–1189.
[90] S. Brenner, S. Hay, A.W. Munro, N.S. Scrutton, Interflavin electron transfer in cytochrome P450 reductase–effects of solvent and pH identify hidden complexity in mechanism, FEBS J. 275 (2008) 4540–4557.
[91] A. Das, G.S. Sligar, Modulation of the cytochrome P450 reductase redox potential by the phospholipid bilayer, Biochemistry 48 (2009) 12104–12112.
[92] A. Shukla, E.M. Gillam, P.V. Bernhardt, Direct electrochemistry of human and rat NADPH cytochrome P450 reductase, Electr. Commun. 8 (2006) 1845–1849.
[93] A. Welland, P.E. Garnaud, M. Kitamura, C.S. Miles, S. Daff, Importance of the domain–domain interface to the catalytic action of NO synthase reductase domain, Biochemistry 47 (2008) 9771–9780.
[94] A.J. Dunford, S.E. Rigby, S. Hay, A.W. Munro, N.S. Scrutton, Conformational and thermodynamic control of electron transfer in neuronal nitric oxide synthase, Biochemistry 46 (2007) 5018–5029.
[95] H.C. Chen, R.P. Swenson, Effect of the insertion of a glycine residue into the loop spanning residues 536–541 on the semiquinone state and redox properties of the flavin mononucleotide-binding domain of flavocytochrome P450BM-3 from *Bacillus megaterium*, Biochemistry 47 (2008) 13788–13799.
[96] S.C. Hanley, T.W. Ost, S. Daff, The unusual redox properties of flavocytochrome P450 BM3 flavodoxin domain, Biochem. Biophys. Res. Commun. 325 (2004) 1418–1423.
[97] M.B. Murataliev, M. Klein, A. Fulco, R. Feyereisen, Functional interactions in cytochrome P450BM3: flavin semiquinone intermediates, role of NADP (H), and mechanism of electron transfer by the flavoprotein domain, Biochemistry 36 (1997) 8401–8412.
[98] K.D. Dubey, S. Shaik, The choreography of the reductase and P450BM3 domains towards electron transfer is instigated by the substrate, J. Am. Chem. Soc. 140 (2018) 683–690.
[99] H. Ishikita, Redox potential difference between *Desulfovibrio vulgaris* and *Clostridium beijerinckii* flavodoxins, Biochemistry 47 (2008) 4394–4402.
[100] J. Tejero, D.J. Stuehr, Tetrahydrobiopterin in nitric oxide synthase, IUBMB Life 65 (2013) 358–365.
[101] M. Sugishima, H. Sato, Y. Higashimoto, J. Harada, K. Wada, K. Fukuyama, M. Noguchi, Structural basis for the electron transfer from an open form of NADPH-cytochrome P450 oxidoreductase to heme oxygenase, Proc. Natl. Acad. Sci. U. S. A. 111 (2014) 2524–2529.
[102] L.M. Siegel, P.S. Davis, H. Kamin, Reduced nicotinamide adenine dinucleotide phosphate-sulfite reductase of enterobacteria III. The *Escherichia coli* hemoflavinprotein: catalytic parameters and the sequence of electron flow, J. Biol. Chem. 249 (1974) 1572–1586.
[103] A. Gruez, D. Pignol, M. Zeghouf, J. Covès, M. Fontecave, J.L. Ferrer, J.C. Fontecilla-Camps, Four crystal structures of the 60 kDa flavoprotein monomer of the sulfite reductase indicate a disordered flavodoxin-like module, J. Mol. Biol. 299 (2000) 199–212.
[104] K.R. Wolthers, N.S. Scrutton, Cobalamin uptake and reactivation occurs through specific protein interactions in the methionine synthase–methionine synthase reductase complex, FEBS J. 276 (2009) 1942–1951.
[105] J. Ellis, A. Gutierrez, I.L. Barsukov, W.C. Huang, J.D. Grossmann, G.C. Roberts, Domain motion in cytochrome P450 reductase: conformational equilibria revealed by NMR and small-angle X-ray scattering, J. Biol. Chem. 284 (2009) 36628–36637.
[106] T.M. Hedison, S. Hay, N.S. Scrutton, Real-time analysis of conformational control in electron transfer reactions of human cytochrome P450 reductase with cytochrome *c*, FEBS J. 282 (2015) 4357–4375.
[107] T. Laursen, K. Jensen, B.L. Moller, Conformational changes of the NADPH-dependent cytochrome P450 reductase in the course of electron transfer to cytochromes P450, Biochim. Biophys. Acta 1814 (2011) 132–138.
[108] L. Aigrain, D. Pompon, G. Truan, Role of the interface between the FMN and FAD domains in the control of redox potential and electronic transfer of NADPH cytochrome P450 reductase, Biochem. J. 435 (2011) 197–206.
[109] A. Sündermann, C. Oostenbrink, Molecular dynamics simulations give insight into the conformational change, complex formation, and electron transfer pathway for cytochrome P450 reductase, Protein Sci. 22 (2013) 1183–1195.
[110] D.F. Estrada, J.S. Laurence, E.E. Scott, Cytochrome P450 17A1 interactions with the FMN domain of its reductase as characterized by NMR, J. Biol. Chem. 291 (2016) 3990–4003.
[111] S.L. Freeman, A. Martel, E.L. Raven, G.C. Roberts, Orchestrated domain movement in catalysis by cytochrome P450 reductase, Sci. Rep. 7 (2017) 9741.
[112] S.L. Freeman, A. Martel, J.M. Devos, J. Basran, E.L. Raven, G.C. Roberts, Solution structure of the cytochrome P450 reductase–cytochrome c complex determined by neutron scattering, J. Biol. Chem. 293 (2018) 5210–5219.
[113] C.W. Chang, T.F. He, L. Guo, J.A. Stevens, T. Li, L. Wang, D. Zhong, Mapping solvation dynamics at the function site of flavodoxin in three redox states, J. Am. Chem. Soc. 132 (2010) 12741–12747.
[114] C.R. Pudney, B. Khara, L.O. Johannissen, N.S. Scrutton, Coupled motions direct electrons along human microsomal P450 chains, PLoS Biol. 9 (2011) e1001222.
[115] E.A. Kovrigina, B. Pattengale, C. Xia, A.R. Galiakhmetov, J. Huang, J.J.P. Kim, E.L. Kovrigin, Conformational states of cytochrome P450 oxidoreductase evaluated by FRET using ultrafast transient absorption spectroscopy, Biochemistry 55 (2016) 5973–5976.
[116] A. Sobolewska-Stawiarz, N.G.E. Leferink, K. Fisher, D.J. Heyes, S. Hay, N.S.E. Rigby, N.S. Scrutton, Energy landscapes and catalysis in nitric-oxide synthase, J. Biol. Chem. 289 (2014) 11725–11738.
[117] M.M. Haque, S.S. Ray, D.J. Stuehr, Phosphorylation controls endothelial nitric-oxide synthase by regulating its conformational dynamics, J. Biol. Chem. 291 (2016) 23047–23057.
[118] T.M. Hedison, N.G. Leferink, S. Hay, N.S. Scrutton, Correlating calmodulin landscapes with chemical catalysis in neuronal nitric oxide synthase using time-resolved FRET and a 5-deazaflavin thermodynamic trap, ACS Catal. 6 (2016) 5170–5180.
[119] T.M. Hedison, S. Hay, N.S. Scrutton, A perspective on conformational control of electron transfer in nitric oxide synthases, Nitric Oxide 63 (2017) 61–67.
[120] M.M. Haque, J. Tejero, M. Bayachou, Z.Q. Wang, M. Fadlalla, D.J. Stuehr, Thermodynamic characterization of five key kinetic parameters that define neuronal nitric oxide synthase catalysis, FEBS J. 280 (2013) 4439–4453.
[121] M.M. Haque, M. Bayachou, J. Tejero, C.T. Kenney, N.M. Pearl, S.C. Im, L. Waskell, D.J. Stuehr, Distinct conformational behaviors of four mammalian dual-flavin reductases (cytochrome P450 reductase, methionine synthase reductase, neuronal nitric oxide synthase, endothelial nitric oxide synthase) determine their unique catalytic profiles, FEBS J. 281 (2014) 5325–5340.
[122] D.D. Oprian, M.J. Coon, Oxidation-reduction states of FMN and FAD in NADPH-cytochrome P-450 reductase during reduction by NADPH, J. Biol. Chem. 257 (1982) 8935–8944.
[123] P.A. Hubbard, A.L. Shen, R. Paschke, C.B. Kasper, J.J.P. Kim, NADPH-cytochrome P450 oxidoreductase structural basis for hydride and electron transfer, J. Biol. Chem. 276 (2001) 29163–29170.
[124] C.E. Meints, S. Simtchouk, K.R. Wolthers, Aromatic substitution of the FAD-shielding tryptophan reveals its differential role in regulating electron flux in methionine synthase reductase and cytochrome P450 reductase, FEBS J. 280 (2013) 1460–1474.
[125] C.E. Meints, S.M. Parke, K.R. Wolthers, Proximal FAD histidine residue influences interflavin electron transfer in cytochrome P450 reductase and methionine synthase reductase, Biochem. Biophys. 547 (2014) 18–26.
[126] C. Xia, F. Rwere, S. Im, A. Shen, L.A. Waskell, J.J.P. Kim, Structural and kinetic studies of Asp632 mutants and fully-reduced NADPH-cytochrome P450 oxidoreductase define the role of Asp632 loop dynamics in control of NADPH binding and hydride transfer, Biochemistry 57 (2018) 945–962.
[127] A. Gutierrez, M. Paine, C.R. Wolf, N.S. Scrutton, G.C. Roberts, Relaxation kinetics of cytochrome P450 reductase: internal electron transfer is limited by conformational change and regulated by coenzyme binding, Biochemistry 41 (2002) 4626–4637.
[128] C.C. Page, C.C. Moser, X.X. Chen, P.L. Dutton, Natural engineering principles of electron tunneling in biological oxidation-reduction, Nature 402 (1999) 47–52.
[129] C.E. Meints, F.S. Gustafsson, N.S. Scrutton, K.R. Wolthers, Tryptophan 697 modulates hydride and interflavin electron transfer in human methionine synthase reductase, Biochemistry 50 (2011) 11131–11142.
[130] J.I. García, M. Medina, J. Sancho, P.J. Alonso, C. Gomez-Moreno, J.A. Mayoral, J.I. Martínez, Theoretical analysis of the electron spin density distribution of the flavin semiquinone isoalloxazine ring within model protein environments, J. Phys. Chem. A 106 (2002) 4729–4735.
[131] J.I. Martinez, P.J. Alonso, I. García-Rubio, M. Medina, Methyl rotors in flavoproteins, Phys. Chem. Chem. Phys. 16 (2014) 26203–26212.
[132] P. Garnaud, A. Welland, C. Miles, S. Daff, Flavins and Flavoproteins, ARchiTeck Inc., Tokyo, Japan, 2005, pp. 465–471.
[133] H. Matsuda, T. Iyanagi, Calmodulin activates intramolecular electron transfer between the two flavins of neuronal nitric oxide synthase flavin domain, Biochim. Biophys. Acta, Gen. Subj. 1473 (1999) 345–355.
[134] A. Presta, A.M. Weber-Main, M.T. Stankovich, D.J. Stuehr, Comparative effects of substrates and pterin cofactor on the heme midpoint potential in inducible and neuronal nitric oxide synthases, J. Am. Chem. Soc. 120 (1998) (1998) 9460–9465.
[135] C.R. Nishida, P.R. Oritz de Montellano, Electron transfer and catalytic activity of nitric oxide synthases chimeric constructs of the neuronal, inducible, and endothelial isoforms, J. Biol. Chem. 273 (1998) 5566–5571.
[136] K.R. Wolthers, J. Basran, A.W. Munro, N.S. Scrutton, Molecular dissection of human methionine synthase reductase: determination of the flavin redox potentials in full-length enzyme and isolated flavin-binding domains, Biochemistry 42 (2003) 3911–3920.
[137] R.D. Finn, J. Basran, O. Roitel, C.R. Wolf, A.W. Munro, M. Paine, N.S. Scrutton, Determination of the redox potentials and electron transfer properties of the FAD- and FMN-binding domains of th human oxidoreductase NR1, Eur. J. Biochem. 270 (2003) 1164–1175.
[138] J. Ostrowski, M.J. Barber, D.C. Rueger, B.E. Miller, L.M. Siegel, N.M. Kredich, Characterization of the flavoprotein moieties of NADPH-sulfite reductase from *Salmonella typhimurium* and *Escherichia coli*. Physicochemical and catalytic properties, amino acid sequence deduced from DNA sequence of *cysJ*, and comparison with NADPH-cytochrome P-450 reductase, J. Biol. Chem. 264 (1989) 15796–15808.
[139] R. Huang, K. Yamamoto, M. Zhang, N. Popovych, I. Hung, S.C. Im, Z. Gan, A. Ramamoorthy, Probing the transmembrane structure and dynamics of microsomal NADPH-cytochrome P450 oxidoreductase by solid-state NMR, Biophys. J. 106 (2014) 2126–2133.
[140] K. Yamamoto, M. Gildenberg, S. Ahuja, S.C. Im, P. Pearcy, L. Waskell, A. Ramamoorthy, Probing the transmembrane structure and topology of microsomal cytochrome-p450 by solid-state NMR on temperature-resistant bicelles, Sci. Rep. 3 (2013) 2556.
[141] S. Ahuja, N. Jahr, S.C. Im, S. Vivekanandan, N. Popovych, S.V. Le Clair, R. Huang, R. Soong, J. Xu, K. Yamamoto, R.P. Nanga, A. Bridges, L. Waskell, A. Ramamoorthy, A model of the membrane-bound cytochrome *b*5-cytochrome P450 complex from NMR and mutagenesis data, J. Biol. Chem. 288 (2013) 22080–22095.
[142] S. Kollipara, S. Tatireddy, T. Pathirathne, L.K. Rathnayake, S.H. Northrup, Contribution of electrostatics to the kinetics of electron transfer from NADH-

cytochrome b5 reductase to Fe (III)-cytochrome b5, J. Phys. Chem. B 120 (2016) 8193–8207.
[143] A.L. Spencer, I. Bagai, D.F. Becker, E.R. Zuiderweg, S.W. Ragsdale, Protein/protein interactions in the mammalian heme degradation pathway heme oxygenase-2, cytochrome P450 reductase, and biliverdin reductase, J. Biol. Chem. 289 (2014) 29836–29858.
[144] I. Abe, T. Abe, W. Lou, T. Masuoka, H. Noguchi, Sitedirected mutagenesis of conserved aromatic residues in rat squalene epoxidase, Biochem. Biophys. Res. Commun. 352 (2007) 259–263.
[145] S.C. Im, L. Waskell, The interaction of microsomal cytochrome P450 2B4 with its redox partners, cytochrome P450 reductase and cytochrome b_5, Arch. Biochem. Biophys. 507 (2011) 144–153.
[146] Y. Dai, J. Zhen, X. Zhang, Y. Zhong, S. Liu, Z. Sun, Z. Sun, Y. Guo, Q. Wu, Analysis of the complex formation, interaction and electron transfer pathway between the "open" conformation of NADPH-cytochrome P450 reductase and aromatase, Steroids 101 (2015) 116–124.
[147] S.G. Sligar, Coupling of spin, substrate, and redox equilibriums in cytochrome P450, Biochemistry 15 (1976) 5399–5406.
[148] S.G. Sligar, D.L. Cinti, G.G. Gibson, J.B. Schenkman, Spin state control of the hepatic cytochrome P450 redox potential, Biochem. Biophys. Res. Commun. 90 (1979) 925–932.
[149] A. Das, Y.V. Grinkova, S.G. Sligar, Redox potential control by drug binding to cytochrome P450 3A4, J. Am. Chem. Soc. 129 (2007) (2007) 13778–13779.
[150] Y. Imai, R. Sato, T. Iyanagi, Rate-limiting step in the reconstituted microsomal drug hydroxylase system, J. Biochem. 82 (1977) 1237–1246.
[151] T. Iyanagi, T. Suzaki, S. Kobayashi, Oxidation-reduction states of pyridine nucleotide and cytochrome P-450 during mixed-function oxidation in perfused rat liver, J. Biol. Chem. 256 (1981) 12933–12939.
[152] T.W. Ost, J. Clark, C.G. Mowat, C.S. Miles, M.D. Walkinshaw, G.A. Reid, S.K. Chapman, S. Daff, Oxygen activation and electron transfer in flavocytochrome P450 BM3, J. Am. Chem. Soc. 125 (2003) 15010–15020.
[153] A. Hildebrandt, R.W. Estabrook, Evidence for the participation of cytochrome *b*5 in hepatic microsomal mixed-function oxidation reactions, Biochem. Biophys. 143 (1971) 66–79.
[154] C. Bonfils, C. Balny, P. Maurel, Direct evidence for electron transfer from ferrous cytochrome *b*5 to the oxyferrous intermediate of liver microsomal cytochrome P-450 LM2, J. Biol. Chem. 256 (1981) 9457–9465.
[155] K. Yamamoto, U.H. Dürr, J. Xu, S.C. Im, L. Waskell, A. Ramamoorthy, Dynamic interaction between membrane-bound full-length cytochrome P450 and cytochrome *b*5 observed by solid-state NMR spectroscopy, Sci. Rep. 3 (2013) 2538.
[156] R. Duggal, Y. Liu, M.C. Gregory, I.G. Denisov, J.R. Kincaid, S.G. Sligar, Evidence that cytochrome *b*5 acts as a redox donor in CYP17A1 mediated androgen synthesis, Biochem. Biophys. Res. Commun. 477 (2016) 202–208.
[157] C.J. Henderson, L.A. McLaughlin, C.R. Wolf, Evidence that cytochrome *b*5 and cytochrome *b*5 reductase can act as sole electron donors to the hepatic cytochrome P450 system, Mol. Pharmacol. 83 (2013) 1209–1217.
[158] M. Stiborova, R. Indra, M. Moserova, E. Frei, H.H. Schmeiser, K. Kopka, D.H. Phillips, V.M. Arlt, NADH: cytochrome b5 reductase and cytochrome *b*5 can act as sole electron donors to human cytochrome P450 1A1-mediated oxidation and DNA adduct formation by benzo [a] pyrene, Chem. Res. Toxicol. 29 (2016) 1325–1334.
[159] H. Ichinose, H. Wariishi, Heterologous expression and mechanistic investigation of a fungal cytochrome P450 (CYP5150A2): involvement of alternative redox partners, Arch. Biochem. Biophys. 518 (2012) 8–15.
[160] W.H. Koppenol, Oxygen activation by cytochrome P450: a thermodynamic analysis, J. Am. Chem. Soc. 129 (2007) 9686–9690.
[161] H.G. Enoch, P. Strittmatter, Cytochrome b5 reduction by NADPH-cytochrome P-450 reductase, J. Biol. Chem. 254 (1979) 8976–8981.
[162] G. Niu, S. Zhao, L. Wang, W. Dong, L. Liu, Y. He, Structure of the *Arabidopsis thaliana* NADPH-cytochrome P450 reductase 2 (ATR2) provides insight into its function, FEBS J. 284 (2017) 754–765.
[163] H. Taniguchi, Y. Imai, T. Iyanagi, R. Sato, Interaction between NADPH-cytochrome P-450 reductase and cytochrome P-450 in the membrane of phosphatidylcholine vesicles, Biochim. Biophys. Acta Bioenerg. 550 (1979) 341–356.
[164] J.A. Peterson, R.E. Ebel, D.H. O'keeffe, T. Matsubara, R.W. Estabrook, Temperature dependence of cytochrome P-450 reduction. A model for NADPH-cytochrome P-450 reductase: cytochrome P-450 interaction, J. Biol. Chem. 251 (1976) 4010–4016.
[165] P. Jerabek, J. Florián, V. Martínek, Membrane-anchored cytochrome P450 1A2–cytochrome *b*5 complex features an X-shaped contact between antiparallel transmembrane helices, Chem. Res. Toxicol. 29 (2016) 626–636.
[166] R.W. Estabrook, M.R. Franklin, B. Cohen, A. Shigamatzu, A.G. Hildebrandt, Influence of hepatic microsomal mixed function oxidation reactions on cellular metabolic control, Metabolism 20 (1971) 187–199.
[167] J. Watanabe, Y. Asaka, S. Fujimoto, S. Kanamura, Densities of NADPH-ferrihemoprotein reductase and cytochrome P-450 molecules in the endoplasmic reticulum membrane of rat hepatocytes, Histochem. Cytochem. 41 (1993) 43–49.
[168] I. Lans, S. Frago, M. Medina, Understanding the FMN cofactor chemistry within the *Anabaena* flavodoxin environment, Biochim. Biophys. Acta Bioenerg. 1817 (2012) 2118–2127.
[169] L.M. Brignac-Huber, J.W. Park, J.R. Reed, W.L. Backes, Cytochrome P450 organization and function are modulated by endoplasmic reticulum phospholipid heterogeneity, Drug Metab. Dispos. 44 (2016) 18591 (1866).
[170] K.C. Liu, J.M. Hughes, S. Hay, N.S. Scrutton, Liver microsomal lipid enhancesthe activity and redox coupling of co-localized cytochrome P450 reductasecytochrome P450 3A4 in nanodiscs, FEBS J. 284 (2017) 2302–2319.
[171] C. Barnaba, M.J. Martinez, E. Taylor, A.O. Barden, J.A. Brozik, Single protein tracking reveals that NADPH mediates the insertion of cytochrome P450-reductase into a biomimetic of the endoplasmic reticulum, J. Am. Chem. Soc. 139 (2017) 5420–5430.
[172] I.G. Denisov, S.G. Sligar, Nanodiscs in membrane biochemistry and biophysics, Chem. Rev. 117 (2017) 4669–4713.
[173] T. Laursen, A. Singha, N. Rantzau, M. Tutkus, J. Borch, P. Hedegard, D. Stamou, B.L. Møller, N.S. Hatzakis, Single molecule activity measurements of cytochrome P450 oxidoreductase reveal the existence of two discrete functional states, ACS Chem. Biol. 9 (2014) 630–634.
[174] K. Bavishi, D. Li, S. Eiersholt, E.N. Hooley, T.C. Petersen, B.L. Møller, N.S. Hatzakis, T. Laursen, Direct observation of multiple conformational states in cytochrome P450 oxidoreductase and their modulation by membrane environment and ionic strength, Sci. Rep. 8 (2018) 6817.
[175] M.G. Campbell, E.S. Underbakke, C.S. Potter, B. Carragher, M.A. Marletta, Single-particle EM reveals the higher-order domain architecture of soluble guanylate cyclase, Proc. Natl. Acad. Sci. U. S. A. 111 (2014) 2960–2965.
[176] D.H. Craig, S.K. Chapman, S. Daff, Calmodulin activates electron transfer through neuronal nitric-oxide synthase reductase domain by releasing an NADPH-dependent conformational lock, J. Biol. Chem. 277 (2002) 33987–33994.
[177] T.B. Dunlap, J.M. Kirk, E.A. Pena, M.S. Yoder, T.P. Creamer, Thermodynamics of binding by calmodulin correlates with target peptide α-helical propensity, Proteins 81 (2013) 607–612.
[178] J. Tejero, L. Hannibal, A. Mustovich, D.J. Stuehr, Surface charges and regulation of FMN to heme electron transfer in nitric-oxide synthase, J. Biol. Chem. 285 (2010) 27232–27240.
[179] B.C. Smith, E.S. Underbakke, D.W. Kulp, W.R. Schief, M.A. Marletta, Nitric oxide synthase domain interfaces regulate electron transfer and calmodulin activation, Proc. Natl. Acad. Sci. U. S. A. 110 (2013) E3577–E3586.
[180] Y. Sheng, L. Zhong, D. Guo, G. Lau, C. Feng, Insight into structural rearrangements and interdomain interactions related to electron transfer between flavin mononucleotide and heme in nitric oxide synthase: a molecular dynamics study, J.Inorg. Biochem. 153 (2015) 186–196.
[181] L. Chen, H. Zheng, W. Li, W. Li, Y. Miao, C. Feng, Role of a conserved tyrosine residue in the FMN–heme interdomain electron transfer in Inducible nitric oxide synthase, J. Phys. Chem. A 120 (2016) 7610–7616.
[182] M. Gu, H.P. Lu, Raman mode-selective spectroscopic imaging of coenzyme and enzyme redox states, J. Raman Spectrosc. 47 (2016) 801–807.
[183] A.L. Shen, T.D. Porter, T.E. Wilson, C.B. Kasper, Structural analysis of the FMN binding domain of NADPH-cytochrome P-450 oxidoreductase by site-directed mutagenesis, J. Biol. Chem. 264 (1989) 7584–7589.
[184] A. Persechini, O.K. Tran, D.J. Black, E.P. Gogol, Calmodulin-induced structural changes in endothelial nitric oxide synthase, FEBS Lett. 587 (2013) 297–301.
[185] U. Siddhanta, A. Presta, B. Fan, D. Wolan, D.L. Rousseau, D.J. Stuehr, Domain swapping in inducible nitric-oxide synthase. Electron transfer occurs between flavin and heme groups located on adjacent subunits in the dimer, J. Biol. Chem. 273 (1998) 18950–18958.
[186] R.T. Miller, P. Martasek, T. Omura, B.S. Siler Masters, Rapid kinetic studies of electron transfer in the three isoforms of nitric oxide synthase, Biochem. Biophys. Res. Commun. 265 (1999) 184–188.
[187] M.M. Haque, J. Tejero, M. Bayachou, C.T. Kenney, D.J. Stuehr, A cross-domain charge interaction governs the activity of NO synthase, J. Biol. Chem. 293 (2018) 4545–4554.
[188] Y.T. Gao, S.P. Panda, L.J. Roman, P. Martásek, Y. Ishimura, B.B. Masters, Oxygen metabolism by neuronal nitric-oxide synthase, J. Biol. Chem. 282 (2007) 7921–7929.
[189] Y.T. Gao, L.J. Roman, P. Martásek, S.P. Panda, Y. Ishimura, B.S.S. Masters, Oxygen metabolism by endothelial nitric-oxide synthase, J. Biol. Chem. 282 (2007) 28557–28565.
[190] V. Berka, W. Liu, G. Wu, A.L. Tsai, Comparison of oxygen-induced radical intermediates in iNOS oxygenase domain with those from nNOS and eNOS, J. Inorg. Biochem. 139 (2014) 93–105.
[191] A.V. Astashkin, Chapter ten—mapping the structure of metalloproteins with RIDME, Methods Enzymol. 563 (2015) 251–284.
[192] A.V. Astashkin, B.O. Elmore, W. Fan, J.C. Guillemette, C. Feng, Pulsed EPR determination of the distance between heme iron and FMN centers in a human inducible nitric oxide synthase, J. Am. Chem. Soc. 132 (2012) 12059–12067.
[193] A.V. Astashkin, L. Chen, X. Zhou, H. Li, T.L. Poulos, K.J. Liu, J.G. Guillemette, C. Feng, Pulsed electron paramagnetic resonance study of domain docking in neuronal nitric oxide synthase: the calmodulin and output state perspective, J. Phys. Chem. A 118 (2014) 6864–6872.
[194] N.S.E. Rigby, N.S. Scrutton, ELDOR spectroscopy reveals that energy landscapes in human methionine synthase reductase are extensively remodelled following ligand and partner protein binding, ChemBioChem 12 (2011) 863–867.
[195] Y. Dai, M.M. Haque, D.J. Stuehr, Restricting the conformational freedom of the neuronal nitric-oxide synthase flavoprotein domain reveals impact on electron transfer and catalysis, J. Biol. Chem. 292 (2017) 6753–6764.
[196] G.A. Ziegler, C. Vonrhein, I. Hanukoglu, G.E. Schulz, The structure of adrenodoxin reductase of mitochondrial P 450 systems: electron transfer for steroid biosynthesis, J. Mol. Biol. 289 (1999) 981–990.
[197] G.A. Ziegler, G.E. Schulz, Crystal structures of adrenodoxin reductase in complex with $NADP^+$ and NADPH suggesting a mechanism for the electron transfer of an enzyme family, Biochemistry 39 (2000) 10986–10995.
[198] J.J. Müller, A. Lapko, G. Bourenkov, K. Ruckpaul, U. Heinemann, Adrenodoxin reductase-adrenodoxin complex structure suggests electron transfer path in steroid biosynthesis, J. Biol. Chem. 276 (2001) 2786–2789.

[199] H. Sugimoto, Y. Shiro, Diversity and substrate specificity in the structures of steroidogenic cytochrome P450 enzymes, Biol. Pharm. Bull. 35 (2012) 818–823.
[200] J.D. Lambeth, D.R. McCaslin, H. Kamin, Adrenodoxin reductase-adrenodoxin complex, J. Biol. Chem. 251 (1976) 7545–7550.
[201] J.D. Lambeth, S.O. Pember, Cytochrome P-450scc-adrenodoxin complex. Reduction properties of the substrate-associated cytochrome and relation of the reduction states of heme and iron-sulfur centers to association of the proteins, J. Biol. Chem. 258(1983) 5596–5602.
[202] M. Tsubaki, A. Hiwatashi, Y. Ichikawa, Effects of cholesterol and adrenodoxin binding on the heme moiety of cytochrome P-450scc: a resonance Raman study, Biochemistry 25 (1986) 3563–3569.
[203] J.D. Lambeth, S. Kriengsiri, Cytochrome P-450scc-adrenodoxin interactions. Ionic effects on binding, and regulation of cytochrome reduction by bound steroid substrates, J. Biol. Chem. 260 (1985) 8810–8816.
[204] P.H.J. Keizers, B. Mersinli, W. Reinle, J. Donauer, Y. Hiruma, F. Hannemann, M. Overhand, R. Bernhardt, M. Ubbink, A solution model of the complex formed by adrenodoxin and adrenodoxin reductase determined by paramagnetic NMR spectroscopy, Biochemistry 49 (2010) 6846–6855.
[205] N. Strushkevich, F. MacKenzie, T. Cherkesova, I. Grabovec, S. Usanov, H.W. Park, Structural basis for pregnenolone biosynthesis by the mitochondrial monooxygenase system, Proc. Natl. Acad. Sci. U. S. A. 108 (2011) 10139–10143.
[206] J.D. Lambeth, H. Kamin, Adrenodoxin reductase and adrenodoxin. Mechanisms of reduction of ferricyanide and cytochrome *c*, J. Biol. Chem. 252 (1977) 2908–2917.
[207] K. Kobayashi, S. Miura, M. Miki, Y. Ichikawa, S. Tagawa, Interaction of NADPH-adrenodoxin reductase with $NADP^+$ as studied by pulse radiolysis, Biochemistry 34 (1995) 12932–12936.
[208] J. Shanklin, J.E. Guy, G. Mishra, Y. Lindqvist, Desaturases: emerging models for understanding functional diversification of diiron-containing enzymes, J. Biol. Chem. 284 (2009) 18559–18563.
[209] M. Ingelman, V. Bianchi, H. Eklund, The three-dimensional structure of flavodoxin reductase from *Escherichia coli* at 17 Å resolution, J. Mol. Biol. 268 (1997) 147–157.
[210] M.C. Bewley, C.C. Marohnic, M.J. Barber, The structure and biochemistry of NADH-dependent cytochrome *b*5 reductase are now consistent, Biochemistry 40 (2001) 13574–13582.
[211] A. Sánchez-Azqueta, M. Martínez-Júlvez, M. Hervás, J.A. Navarro, M. Medina, External loops at the ferredoxin-$NADP^+$ reductase protein–partner binding cavity contribute to substrates allocation, Biochim. Biophys. Acta Bioenerg. 1837 (2014) 296–305.
[212] K. Kobayashi, T. Iyanagi, H. Ohara, K. Hayashi, One-electron reduction of hepatic NADH-cytochrome *b*5 reductase as studied by pulse radiolysis, J. Biol. Chem. 263 (1988) 7493–7499.
[213] S. Kollipara, S. Tatireddy, T. Pathirathne, L.K. Rathnayake, S.H. Northrup, Contribution of electrostatics to the kinetics of electron transfer from NADH-cytochrome *b*5 reductase to Fe (III)-cytochrome *b*5, J. Phys. Chem. B 120 (2016) 8193–8207.
[214] K. Takaba, K. Takeda, M. Kosugi, T. Tamada, K. Miki, Distribution of valence electrons of the flavin cofactor in NADH-cytochrome *b*5 reductase, Sci. Rep. 7 (2017) 43162.
[215] S. Kimura, Y. Emi, S.I. Ikushiro, T. Iyanagi, Systematic mutations of highly conserved His 49 and carboxyl-terminal of recombinant porcine liver NADH-cytochrome *b*5 reductase solubilized domain, Biochim. Biophys. Acta Protein Struct. Mol. Enzymol. 1430 (1999) 290–301.
[216] J. Chalupsky, T.A. Rokob, Y. Kurashige, T. Yanai, E.I. Solomon, L. Rulisek, M. Srnec, Reactivity of the binuclear non-heme iron active site of Δ9 desaturase studied by large-scale multireference ab initio calculations, J. Am. Chem. Soc. 136 (2014) 15977–15991.
[217] H. Zhu, H. Qiu, H.W.P. Yoon, S. Huang, H.F. Bunn, Identification of a cytochrome *b*-type NAD (P) H oxidoreductase ubiquitously expressed in human cells, Proc. Natl. Acad. Sci. U. S. A. 96 (1999) 14742–14747.
[218] J. Xie, H. Zhu, K. Larade, A. Ladoux, A. Seguritan, M. Chu, S. Ito, R.T. Bronson, E.H. Leiter, C.Y. Zhang, E.D. Rosen, H.F. Bunn, Absence of a reductase, NCB5OR, causes insulin-deficient diabetes, Proc. Natl. Acad. Sci. U. S. A. 101 (2004) 10750–10755.
[219] C.E. Sparacino-Watkins, J. Tejero, B. Sun, M.C. Gauthier, J. Thomas, V. Ragireddy, B.A. Merchant, J. Wang, I. Azaro, P. Basu, M.T. Gladwin, Nitrite reductase and nitric-oxide synthase activity of the mitochondrial molybdopterin enzymes mARC1 and mARC2, J. Biol. Chem. 289 (2014) 10345–10358.
[220] M.B. Amdahl, C.E. Sparacino-Watkins, P. Corti, M.T. Gladwin, J. Tejero, Efficient reduction of vertebrate cytoglobins by the cytochrome b5/cytochrome b5 reductase/NADH system, Biochemistry 56 (2017) 3993–4004.
[221] X. Liu, M.A. El-Mahdy, J. Boslett, S. Varadharaj, C. Hemann, T.M. Abdelghany, R.S. Ismail, S.C. Little, D. Zhou, L.T. Thuy, N. Kawada, J.L. Zweier, Cytoglobin regulates blood pressure and vascular tone through nitric oxide metabolism in the vascular wall, Nat. Commun. 8 (2017) 14807.
[222] D. Leclerc, A. Wilson, R. Dumas, C. Gafuik, D. Song, D. Watkins, H.H. Heng, J.M. Rommens, S.W. Scherer, D.S. Rosenblatt, R.A. Gravel, Cloning and mapping of a cDNA for methionine synthase reductase, a flavoprotein defective in patients with homocystinuria, Proc. Natl. Acad. Sci. U. S. A. 95 (1998) 3059–3064.
[223] R.K. Wolthers, N.S. Scrutton, Electron transfer in human methionine synthase reductase studied by stopped-flow spectrophotometry, Biochemistry 43 (2004) 490–500.
[224] L. McIver, C. Leadbeater, D.J. Campopiano, R.L. Baxter, S.N. Daff, S.K. Chapman, A.W. Munro, Characterization of flavodoxin $NADP^+$ oxidoreductase and flavodoxin; key components of electron transfer in *Escherichia coli*, Eur. J. Biochem. 257 (1998) 577–585.
[225] H. Olteanu, K.R. Wolthers, A.W. Munro, N.S. Scrutton, R. Banerjee, Kinetic and thermodynamic characterization of the common polymorphic variants of human methionine synthase reductase, Biochemistry 43 (2004) (1988–1997).
[226] K.R. Wolthers, H.S. Toogood, T.A. Jowitt, K.R. Marshall, D. Leys, N.S. Scrutton, Crystal structure and solution characterization of the activation domain of human methionine synthase, FEBS J. 274 (2007) 738–750.
[227] D. Lexa, J.M. Saveant, The electrochemistry of vitamin-B12, J. Am. Chem. Soc. 16 (1983) 235–243.
[228] D.M. Hoover, J.T. Jarrett, R.H. Sands, W.R. Dunham, M.L. Ludwig, R.G. Matthews, Interaction of *Escherichia coli* cobalamin-dependent methionine synthase and its physiological partner flavodoxin: binding of flavodoxin leads to axial ligand dissociation from the cobalamin cofactor, Biochemistry 36 (1997) 127–138.
[229] T.A. Stich, N.R. Buan, J.C. Escalante-Semerena, T.C. Brunold, Spectroscopic and computational studies of the ATP: corrinoid adenosyltransferase (CobA) from *Salmonella enterica*: insights into the mechanism of adenosylcobalamin biosynthesis, J. Am. Chem. Soc. 127 (2005) 8710–8719.
[230] C.A. Orengo, J.M. Thornton, Protein families and their evolution — a structural perspective, Annu. Rev. Biochem. 74 (2005) 867–900.
[231] H. Raanan, D.H. Pike, E.K. Moore, P.G. Falkowski, V. Nanda, Modular origins of biological electron transfer chains, Proc. Natl. Acad. Sci. U. S. A. 2017 (2018) 14225.
[232] C. Ku, S. Nelson-Sathi, M. Roettger, F.L. Sousa, P.J. Lockhart, D. Bryant, E. Hazkani-Covo, J.O. McInerney, G. Landan, W.F. Martin, Endosymbiotic origin and differential loss of eukaryotic genes, Nature 524 (2015) 427–432.
[233] G.C. Smith, D.G. Tew, C.R. Wolf, Dissection of NADPH- cytochrome P450 oxidoreductase into distinct functional domains, Proc. Natl. Acad. Sci. U. S. A. 91 (1994) 8710–8714.
[234] N. Andreakis, S. D'Aniello, R. Albalat, F.P. Patti, J. Garcia-Fernàndez, G. Procaccini, P. Sordino, A. Palumbo, Evolution of the nitric oxide synthase family in metazoans, Mol. Biol. Evol. 28 (2010) 163–179.
[235] R.L. Wright, K. Harris, B. Solow, R.H. White, P.J. Kennelly, Cloning of a potential cytochrome P450 from the archaeon *Sulfolobus solfataricus*, FEBS Lett. 384 (1996) 235–239.
[236] I.F. Sevrioukova, H. Li, T.L. Poulos, Crystal structure of putidaredoxin reductase from Pseudomonas putida, the final structural component of the cytochrome P450cam monooxygenase, J. Mol. Biol. 336 (2004) 889–902.
[237] Y. Madrona, S.A. Hollingsworth, S. Tripathi, J.B. Fields, J.C.N. Rwigema, D.J. Tobias, T.L. Poulos, Crystal structure of cindoxin the P450cin redox partner, Biochemistry 53 (2014) 1435–1446.
[238] J.A. Houwman, C.P.M. van Mierlo, Folding of proteins with a flavodoxin-like architecture, FEBS J. 284 (2017) 3145–3167.
[239] E.A. Shephard, I.R. Phillips, I. Santisteban, C.N.A. Palmer, S. Povey, Cloning, expression and chromosomal localization of a member of the human cytochrome P450IIC gene sub-family, Ann. Hum. Genet. 53 (1989) 23–31.
[240] T.D. Porter, T.W. Beck, C.B. Kasper, NADPH-cytochrome P-450 oxidoreductase gene organization correlates with structural domains of the protein, Biochemistry 29 (1990) 9814–9818.
[241] D. Leclerc, M.H. Odièvre, Q. Wu, A. Wilson, J.J. Huizenga, R. Rozen, S.W. Scherer, R.A. Gravel, Molecular cloning, expression and physical mapping of the human methionine synthase reductase gene, Gene 240 (1999) 75–88.
[242] J.L. Parker, S. Newstead, Structural basis of nucleotide sugar transport across the Golgi membrane, Nature 551 (2017) 521–524.
[243] Z.Q. Wang, R.J. Lawson, M.R. Buddha, C.C. Wei, B.R. Crane, A.W. Munro, D.J. Stuehr, Bacterial flavodoxins support nitric oxide production by *Bacillus subtilis* nitric-oxide synthase, J. Biol. Chem. 282 (2007) 2196–2202.
[244] I. Gusarov, M. Starodubtseva, Z.Q. Wang, L. McQuade, S.J. Lippard, D.J. Stuehr, E. Nudler, Bacterial nitric-oxide synthases operate without a dedicated redox partner, J. Biol. Chem. 283 (2008) 13140–13147.
[245] L.M. Iyer, L. Aravind, S.L. Coon, D.C. Klein, E.V. Koonin, Evolution of cell–cell signaling in animals: did late horizontal gene transfer from bacteria have a role? Trends Genet. 20 (2004) 292–299.
[246] N. Andreakis, S. D'Aniello, R. Albalat, F.P. Patti, J. Garcia-Fernàndez, G. Procaccini, P. Sordino, A. Palumbo, Evolution of the nitric oxide synthase family in metazoans, Mol. Biol. Evol. 28 (2011) 163–179.
[247] B.S.S. Masters, The journey from NADPH-cytochrome P450 oxidoreductase to nitric oxide synthases, Biochem. Biophys. Res. Commun. 338 (2005) 507–519.
[248] D.F.V. Lewis, E. Watson, B.G. Lake, Evolution of the cytochrome P450 superfamily: sequence alignments and pharmacogenetics, Mutat. Res. Rev. Mutat. Res. 410 (1998) 245–270.
[249] L.E. Bird, J. Ren, J. Zhang, N. Foxwell, A.R. Hawkins, I.G. Charles, D.K. Stammers, Crystal structure of saNOS, a bacterial nitric oxide synthase oxygenase protein from *Staphylococcus aureus*, Structure 10 (2002) 1687–1696.
[250] R.T. Ruettinger, L.P. Wen, A.J. Fulco, Coding nucleotide, 5′ regulatory, and deduced amino acid sequences of P-450BM-3, a single peptide cytochrome P-450: NADPH-P-450 reductase from *Bacillus megaterium*, J. Biol. Chem. 264 (1989) 10987–10995.
[251] S. Jeandroz, D. Wipf, D.J. Stuehr, L. Lamattina, M. Melkonian, Z. Tian, E.J. Carpenter, G.K.-S. Wong, D. Wendehenne, Occurrence, structure, and evolution of nitric oxide synthase-like proteins in the plant kingdom, Sci. Signal. 9 (2016) re2.
[252] G. Lu, Y. Lindqvist, G. Schneider, U. Dwivedi, W. Campbell, Structural studies on corn nitrate reductase: refined structure of the cytochrome b reductase fragment at 2.5 Å, its ADP complex and an active-site mutant and modeling of the cytochrome b domain, J. Mol. Biol. 248 (1995) 931–948.
[253] H. Yamasaki, Y. Sakihama, Simultaneous production of nitric oxide and peroxynitrite by plant nitrate reductase: in vitro evidence for the NR-dependent

formation of active nitrogen species, FEBS Lett. 468 (2000) 89–92.
[254] T.D. Porter, New insights into the role of cytochrome P450 reductase (POR) in microsomal redox biology, Acta Pharm. Sin. B 2 (2012) 102–106.
[255] T. Omura, O. Gotoh, Evolutionary origin of mitochondrial cytochrome P450, J. Biochem. 161 (2017) 399–407.
[256] F. Elahian, Z. Sepehrizadeh, B. Moghimi, S.A. Mirzaei, Human cytochrome *b*5 reductase: structure, function, and potential applications, Crit. Rev. Biotechnol. 34 (2014) 134–143.
[257] R.P. Goodman, S. Calvo, V.K. Mootha, Spatiotemporal compartmentalization of hepatic NADH and NADPH metabolism, J. Biol. Chem. 293 (2018) 7508–7516.
[258] A. Wagner, Arrival of the fittest: solving evolution's greatest puzzle, 1st ed. London: Oneworld Public.
[259] F.H. Arnold, Directed laboratory evolution: bringing new chemistry to life, Angew. Chem. Int. Ed. 57 (2018) 4143–4148.